UCLouvain

École polytechnique de Louvain

Design and realization of traction machine bits adapted to tendons for orthopedic surgery

Author: **Walid HADJ**
Supervisors: **Vincent LEGAT, Olivier CORNU**
Readers: **Greet KERCKHOFS, Robin EVRARD, Alexandre ENGLEBERT**
Academic year 2022–2023
Master [120] in Biomedical Engineering

Contents

Acknowledgment . . . 9
Abstract . . . 10
Introduction . . . 11

1 Overview of graft techniques and their indications **12**
1.1 Properties of the tendons . . . 12
1.1.1 Histology of the tendon . . . 12
1.1.2 Biological response to mechanical stimulation . . . 13
1.1.3 Description of the two junction tissues . . . 14
1.1.4 Mechanical properties of the tendons . . . 14
1.2 Overview of the various types of tendons and ligaments found in the human body . 15
1.2.1 Description of the knee ligaments . . . 15
1.2.2 Achilles tendon structure . . . 17
1.2.3 Joining tendons to the knee . . . 17
1.2.4 The hamstring tendon . . . 17
1.3 Tendons injuries . . . 18
1.3.1 Healing process . . . 18
1.3.2 Achilles rupture . . . 18
1.3.3 Anterior cruciate ligament rupture . . . 19
1.3.4 Quadriceps tendon rupture . . . 20
1.3.5 Patellar tendon rupture . . . 22
1.4 Treating Injuries: Available Methods . . . 24
1.4.1 Autograft for tissue replacement . . . 24
1.4.2 Allograft for tissue replacement . . . 24
1.4.3 Xenograft and synthetic materials : an alternative option . . . 25
1.5 Accessing transplants: methods and barriers . . . 25
1.5.1 Tissue bank as a guaranty of safe allografts . . . 25
1.5.2 Criteria for tendon taking . . . 25
1.6 Decontamination techniques to ensure safe allograft delivery . . . 26
1.6.1 Chemical treatments . . . 26
1.6.2 Gamma irradiation process . . . 27
1.6.3 Electron Beam irradiation . . . 27
1.6.4 Ethylene oxide application . . . 27
1.6.5 Sterilization by autoclave . . . 28
1.7 Concerns surrounding tendon allografts . . . 28
1.8 Possible solutions . . . 30
1.9 Conclusion . . . 30

2 Mechanical properties of biological tissues : State of the art **31**
2.1 Overview of classical traction tests on metallic samples . . . 31
2.1.1 Load to failure tests . . . 31
Definition and setup . . . 31
Stress-strain curve and mechanical properties . . . 33
2.1.2 Cycling loading tests . . . 34
Fatigue phenomenon : Definition and characterization . . . 34
Fatigue life and Wöhler curve . . . 35
2.2 Traction tests in the textile sector : a comparison base with tendons in an universal way 37
2.3 Biaxial testing of biological soft tissues . . . 38
2.4 Mechanical tests on human tendons to extract their mechanical properties . . . 39
2.4.1 Characterization of Achilles human tendon . . . 39
2.4.2 Fatigue loading investigations . . . 41
2.4.3 In vivo-testing with ultrasound imaging . . . 43
Measuring challenges in vivo . . . 44
Challenges for signal processing and calculation to measure the force on the tendon . . . 45
Limitation of this technique . . . 46
2.5 Impact of treatments . . . 46
2.5.1 Overview of mechanical properties variation due to sterilization processes . 46
2.5.2 Impact on tendon after Gamma irradiation exposure . . . 47
Altered mechanical properties after high dose exposure in dry conditions . 47
Low dose exposure as pre-treatment . . . 47
2.5.3 Limited impact of Electron Beam exposure . . . 48
2.5.4 Long-term impact of peracetic acid treatment . . . 48
2.5.5 Ropivacaine administration as a impacting factor . . . 49
2.5.6 Mechanical properties of periosteum : a driver for graft stability . . . 50
2.6 Overview of the different bits used for *in vitro* studies . . . 51
2.7 Conclusion . . . 53

3 Mechanical design of the bits **54**
3.1 Specifications of the system . . . 54
3.2 Attachment by drilling . . . 55
3.2.1 Invalidation through Finite Element methods . . . 55
3.3 Attachment by compressing . . . 57
3.3.1 Cylindrical arrangement with frozen-water . . . 57
3.3.2 Cylinder arrangement by compression with two plates . . . 58
3.3.3 System to lock the cylinder . . . 59
Connecting rod-crank system . . . 59
Friction screws . . . 60
Dowel pin . . . 61
Shaft support with hose clamp . . . 62
3.4 Added grippers to bone extremity . . . 63
3.4.1 Type of bone insertion to consider . . . 63
3.4.2 Adapting gripper configuration . . . 64
3.5 Two merged systems outcome . . . 66
3.6 Prototyping with a 3D-printed model . . . 67
3.6.1 First trials with low scales . . . 68
3.6.2 Scaled-up trial . . . 70

3.6.3 Design features outcome . . . 71
3.7 Material of the bits . . . 71
3.8 Adjustment of the model for the machining process . . . 72
3.8.1 Cylinder assembly . . . 72
3.8.2 Grippers assembly . . . 73
3.9 Analytical study of the dynamic . . . 75
3.9.1 Analyze of the flexion of the cylinder . . . 75
3.9.2 Analyze of the torsion of the cylinder . . . 79
3.10 Finite Element method to simulate the efforts . . . 80
3.10.1 Simulation of the efforts born by the cylinder . . . 80
Flexion study . . . 80
Torsion study . . . 81
3.10.2 Simulation of the efforts born by the grippers . . . 82
3.11 Validation of the design . . . 83
3.12 Final dimensions based on allograft data and the external pieces . . . 86
3.13 Technique used for machining . . . 88

4 Tensile tests **90**
4.1 Fabric samples to validate the model . . . 90
4.1.1 Samples preparation and methods . . . 90
Free-ended samples . . . 90
Rigid block ended sample . . . 91
4.1.2 Results . . . 93
4.2 Validation with biological material . . . 100
4.2.1 Overview of the animal models . . . 100
4.2.2 *In vitro* testing with tendons of pigs . . . 101
4.2.3 Samples preparation and origin . . . 101
4.2.4 First results : Slipping problem . . . 101
4.2.5 Alternatives to avoid slipping . . . 102
4.2.6 Results . . . 103
4.3 Tests with human tendons . . . 106
4.4 Conclusion . . . 106

5 Discussion and conclusion **107**
5.1 Areas of improvement . . . 107
5.2 Outlooks . . . 107
5.3 Conclusion . . . 108

Bibliography **117**

List of Figures

1.1 Multi-unit hierarchical structure of the tendon [1] . . . 13
1.2 Qualitative description of the stress-strain curve of tendons . . . 15

1.3 Schematic view of the ligaments present inside the knee . . . 16
1.4 Illustration of the anatomical plan of the human body [2] . . . 16
1.5 Schematic view of Achilles tendon in human adult body [3] . . . 18
1.6 Diagnosis tests of Achilles tendon injury . . . 19
1.7 Representation of the Passing of the tendon through the tunnel during ACL reconstruction surgery [4] . . . 20
1.8 Illustration of a complete rupture of quadriceps tendon . . . 21
1.9 X-rays imaging of the knee. The kneecap is displaced because of a torn quadriceps tendon. The keencap is pulled downward by the patellar tendon . . . 21
1.10 Illustration of the surgery process for reattaching the quadriceps tendon . . . 22
1.11 Illustration of complete patellar tendon rupture. Reinforcement can be performed by using tendon graft, non-resorbable steel wire or resorbable nylon wire running at the upper tibial end, near the anterior tibial tuberosity and wrapped around the patellar tendon . . . 23
1.12 Illustration of the suturing process for reattaching the patellar tendon . . . 24
1.13 Data of the tissue bank of Saint Luc Hospital . . . 28
1.14 The evolution of the number of donors over years . . . 29
1.15 Data of population mean age from the tissue bank of Saint-Luc hospital (left) and European Union (right) . . . 29

2.1 Illustration of the experimental set up of load to failure tests [5] . . . 31
2.2 Classical tensile test machine or uniaxial load to failure tests [6] . . . 32
2.3 Type of specimen shape used to induce the failure at a specific location [7] . . . 33
2.4 Typical force-strain curve (a) and the corresponding stress-strain curve (b) obtained by an uniaxial load to failure test [7] . . . 33
2.5 Typical cycling loading tests performed on materials . . . 34
2.6 Elastic domain of the stress-strain curve of a given material. The area bounded by the arrows is referred to the hysteresis . . . 35
2.7 Typical Wöhler curve showing the fatigue life of a given material . . . 36

2.8 Example of devices used for tensile tests on textile sector . . . 37
2.9 Schematic representation of the different methods for gripping samples in biaxial testing. . . . 38
2.10 Illustration of classical biaxial machine . . . 39
2.11 Force-strain relationship for the load-to-failure tests . . . 40
2.12 Evolution of cracks in bovine extensor tendons over the cycles . . . 42
2.13 Experimental set-up of controlled *in vivo* testing to induce fatigue phenomenon . . . 43
2.14 *in vivo* force-elongation relationship measurement of the patellar tendon during knee motion. The quadriceps is stimulated to provoke isomeric contraction. An ultrasound scan is performed to measure the elongation coupled to the electromyographic activity 44
2.15 Illustration of the shift between the tibia body (solid line) and the axis of the patella apex (dashed line) during quadriceps contraction . . . 45
2.16 Stress-strain relationship of the harvested calcaneal periosteum during load to failure tests . . . 50
2.17 Clamp systems to lock the free-end tendon . . . 51
2.18 PMMA system that embeds the bone block attached to the tendon sample . . . 52

3.1 Drilling solution . . . 55
3.2 3D scan of a leg tendon from the tissue bank of Saint Luc Hospital . . . 56
3.3 Simulation of tensile test applied on the Achilles tendon drilled by the device . . . 56
3.4 Cylindrical configuration with frozen nitrogen . . . 57
3.5 3D-view of the proposed design with cylinder sliced at the center for clamping the sample . . . 59
3.6 Design of the complex rod-crank system that locks the rotation . . . 60
3.7 Example of friction screw used to lock the rotational movement of the cylinder, all designed with SolidWorks . . . 61
3.8 Example of Dowel pins used in the industry . . . 62
3.9 Example of shaft support with hose clamp equipped with a clamping lever proposed by Misumi . . . 63
3.10 tendon-to-bone insertion configurations . . . 64
3.11 Design of the grippers configurations . . . 64
3.12 3D view of the designed grippers. The intermediate piece is aligned with both grippers and enables both configurations . . . 65
3.13 3D-view of the merged model of bit. 1: Semi-cylinder that clamps the free-end of the tendon before coiling. 2 : Detachable hybrid piece with flat face and cavity on the other side. 3 : Hybrid gripper assemblage. 4 : Pillars holding the rotating cylinder. 5 : Groove for the fixation site of the grippers. 6 : Simple model of gripper with cavity. 7 : Handle to facilitate the manual rotation of the cylinder. 8 : Through holes for the dowel pins fixating the grippers to the support. 9 : Main cylinder with a flat surface at the center for the clamping site. 10 : Through holes for the dowel pins immobilizing the cylinder during the test. 11 : Main support attached to the traction machine. . . . 66

3.14 Illustration of the principle of the MLSA 3D-printing technique used for prototyping 67
3.15 Properties of the SuperPP resin 68
3.16 3D view of the designed system with adaptation to the 3D-printing process 69
3.17 First 3D-printed prototypes 69
3.18 Corrected trial of the 0.3 scaled model 70
3.19 Scaled-up 3D printed prototype with corrections on the grippers 70
3.20 Revisited version of the clamping cylinder and its cover 73
3.21 top sectional view of the gripper insertion to the support 74
3.22 Final version of the grippers 75
3.23 2D problem of the cylinder-beam flexion 76
3.24 Values of the radius with respect to the maximum tolerated stress 77
3.25 Traction machine Zwick and Roll that will be used for the tests 78
3.26 Bended cylinder-beam at maximum constraint vs straight beam 78
3.27 Illustration of the torsion problem during tensile tests 79
3.28 Results of the simulation of the flexion effort born by the cylinder with the drilled version 80
3.29 Simulation of the constraints across the whole component for the configuration without the dowel pins 81
3.30 Results of the simulation of the torsion effort born by the cylinder with the drilled version 82
3.31 Results of the simulation of the traction effort born by the gripper 82
3.32 Sectional view of the cylinder assembly. 1 : Enlargement of the section of the cylinder to make a stop to the bearing housing. 2 : Bearing housing on one end of the cylinder. 3 : Ring separating the knurled handwheel from the bearing housing 4 : Clamping cylinder inserted across the additional components. 5 : Knurled handwheel 83
3.33 Final design of the cylinder assembly adapted to the metallic version. 1 : Support shaft with hose clamp that lock the rotational motion of the clamping cylinder. 2 : Clamping cylinder-cover assembly. 3 : Bearing housing. 4 : Knurled handwheel . . 84
3.34 Final design of the grippers assembly adapted to the metallic version 85
3.35 Support shaft attaching the bit to the traction machine 85
3.36 Schematic Top view of the block bone insertion into the system. a : One paired gripper with cavity. b : Bone block of a sample. c : Contact edge of the gripper along which the sample lie during the test. d : Tendon insertion to the bone block. 88
3.37 Pictures of the machining processes used : Grinding (a) and Turning (b) 89

4.1 Picture of the sample fine positioning on the clamping cylinder. The traversal and longitudinal position was set before clamping 91

4.2 Experimental set up of polypropylene-resin block complex. a: The center of each mold cube has been drawn on the upper template. b : a hole has been drilled at those centers using a soft drilling machine. c : The extremity of the rope has been burnt to pass through the hole. d : the epoxy resin and the hardener has been mixed thoroughly. e : The mixture has been poured using a syringe for fine dosage (30ml). f : The ropes has been stretched and immobilized by pins lying on the top template . 92

4.3 Final product of the polypropylene-epoxy sample 92

4.4 Typical load force-strain relationship for each group 93

4.5 Linear regression performed on the polyester (a), polypropylene (b) and polypropylene-epoxy complex samples (c) 95

4.6 Plot of the linear regression performed on the maximum loading force (a) and the strain at failure (b) data for the polypropylene ropes 97

4.7 Linear regression performed on the free-ended samples (a) and bloc-ended samples (b) 100

4.8 Picture of the tendon harvest on one pig. 101

4.9 Pictures of the solutions that have been considered to prevent slipping. a : The sample is sandwiched between the two pieces of scratch and they are both clamped. b : The sample is wrapped around a piece of pad and then clamped. c : A piece of grip tape is stick to the clamping surface and is in contact with the clamped tendon 102

4.10 Pictures of the damages on the extremities of the tendons using a piece of grip tape. Five samples of pigs (a) and one bull Achilles tendon (b) were tested 103

4.11 Typical Stress-strain relationship of a pig tendon from the upper limb 104

List of Tables

2.1 Reported mean mechanical properties of human Achilles tendon-bone complex during *in vitro* tensile tests for $1mms^{-1}$ and $10mms^{-1}$ 40

3.1 Parameters of the printer for the two first prototypes 68
3.2 Mechanical properties of interest for the two stainless steel grade considered 72
3.3 Dimension of the free-ended tendon 86
3.4 Dimension of the bone-block attached to the tendon 87

4.1 Statistics on the failure location of the polyester ropes 93
4.2 Location of failure of the polyester ropes 94
4.3 Force data during the tensile tests on the polyester samples 96
4.4 Location of failure of the polypropylene ropes 98
4.5 Force data during the tensile tests on the polypropylene samples without resin bloc 99
4.6 Location of failure of the resin polypropylene complex samples (from the bottom bit) 99
4.7 Paired samples from limb 1 and limb 2 with pig 3 and 4 105
4.8 References of the human samples 106

Acknowledgment

I would like to express my deepest gratitude to my supervisors, Mr Olivier Cornu and Vincent Legat, for their guidance and constant support throughout the course of this research project. Their expertise and dedication have been instrumental in shaping my academic journey.

I extend my heartfelt appreciation to my friend, my parents and my siblings Sarah and Malik, for their valuable support from the beginning of my studies. They have been always present to guide me and brought me encourage during my academic journey.

My sincere thanks go to the team in Tissue Bank of St Luc Hospital, including Alix de Pierpont, Bernard Godts and Xavier Merny for their generous assistance and encouragement, and for the proposition of this master thesis. Their continuous support and belief in my abilities have been a constant source of motivation. I am also grateful for their willingness to offer their time and resources to help me overcome challenges.

I would like to acknowledge the support of the CHEX institute, more particularly Lies Fievé, Robin Evrard, Alexandre Englebert and Gwen Geaurin whose valuable contributions and collaboration have played a pivotal role in the success of this project. Their help in tendon harvesting and 3D-printing process has broadened my perspective and enriched the outcomes of my research.

I am deeply grateful to Benoit Herman, Vincent Musette and Hervé Laurent for their unwavering support and encouragement throughout the design process and the machining. Their expertise in mechanics and the time that they used to help me have been immensely valuable. T

I wish to express my gratitude to Cathrine Doneux and Quentin Mestrez for their technical assistance and expertise in tensile testing stage. Their willingness to share their knowledge, offer guidance, and provide valuable resources have been instrumental in overcoming obstacles and achieving the desired outcomes.

I would like to acknowledge the contributions of my Tant Bacia and my Uncle Farid for their help to improve the quality of the writing and their valuable support. Their meticulous attention to detail and collaborative spirit, have significantly contributed to the accuracy and reliability of the findings presented in this work.

Last but certainly not least, I would like to pay tribute to my pay tribute to my dear grandmother who would have been proud of me with the thesis I worked on.

Abstract

The mechanical properties of the tendons are not systematically measured yet. The demand of allograft is growing and the population is aging. Shortages can thus happen. A solution for this problem could be the reduction of the tendon allografts wastes by developing new safety treatments. But the mechanical properties need to be thoroughly assessed to validate the treatment. To provide relevant information on the behavior of the tendon in traction, a proper model of bit has to emerge to correctly assess the properties of the tendons. For this purpose, this thesis aims to provide a reliable model that can be fixed to a classical tensile test machine. Fabric samples and tendons will be tested to assess the efficiency of the device.

Introduction

Tendons and ligaments are crucial tissues that ensure bone holding and force transmission from muscles to bone to carry a motion. Therefore, tissue reconstruction is essential if there is a loss of function or stability, which requires either autograft, allograft, xenograft or synthetic replacement to implant a new tendon or replace a ligament. For those, strict procedures are followed in order to assess the quality of the graft. In fact, sterility and mechanical strength among others have to be strictly ensured to avoid any virus or bacteria transmission, diseases development and a re-rupture. Therefore, the choice of the tendon and the sterilization process will be decisive for the well-being of the patient.

However, the mechanical properties of tendons can be highly variable and may depend on various factors such as the temperature and humidity of the surrounding environment, the duration of time since harvesting, and the age of the donor. Those elements may negatively impact the mechanical strength of the tendons which can lead to rupture if the whole process of implantation is not well designed. Additionally, donors are typically individuals who have passed away and expressed their desire to donate their body for medical purposes. Those donors are likely to belong to the older age category. As a result, the tendons obtained from such donors should potentially have reduced mechanical strength, and this issue may become increasingly prevalent as the global population continues to age, as per the statistics provided by the European Union [8]. In fact, the proportion of people of more than 64 years or older increased from 10% to 15% between 2001 and today, and it is expected to double in 2050 according to the predictions. This rapid pace is also confirmed by the World Health Organization [9]. As a consequence, surgeons get samples that present higher risks to be weak. Mechanical properties are very difficult to assess without conducting tensile tests and because of the aforementioned trend, it is important to start to evaluate them in the scope of more extensive clinical studies.

Tensile tests have been widely carried to assess mechanical properties of the tendons and determine the impact of secure treatments. However, those tests were specifically designed for a certain type of tendon with a certain resistance. The exploration of new solutions for tendon allograft transplantation requires a universal model that can be used by non-trained staff. For this purpose, this thesis aims to design, test and validate a model of bits that fix tendons for traction tests. Classical in vitro tensile tests in standard conditions will be performed. This model will come up after a deep analysis of the constraints and specifications of the problem, as well as the possible design options.

Chapter 1

Overview of graft techniques and their indications

Before looking into the design of such a device, it is important to have an overview of the tendon properties and what is it composed of. Tendon graft uses and their sterilization process also need to be understood.

1.1 Properties of the tendons

1.1.1 Histology of the tendon

Tendon is a connective fibro-elastic tissue of white color that is constituted of 70% of water and 30% of extracellular matrix (ECM). 60% of this structure is made up of collagen of two types : 95% of collagen of type I and 5% of collagen of type III [10]. The rest is made up of other proteins such as proteoglycan, glycoprotein and elastin, but also minerals : calcium, magnesium, cadmium and cobalt. Those minerals are involved in metabolism and tissue growth during childhood. The mechanical behavior of the tendon is primarily driven by the ECM, particularly by the elastin, conferring its elastic characteristic. [11]

Living cells lie in the ECM and account for about 20% of the total volume of the tendons. Between 90 and 95% of them are tenocytes and tenoblasts and the rest are endothelial, synovial and endothelial cells. Tenoblasts are immature cells with a metabolic activity that is high, before becoming tenocytes, which are responsible of ECM synthesis.

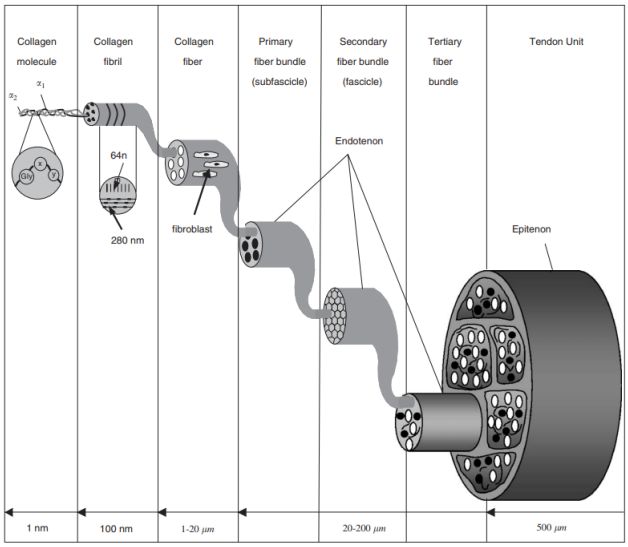


Figure 1.1: Multi-unit hierarchical structure of the tendon [1]

Figure 1.1 shows the hierarchical structure of the tendon with all its different sub-units. Collagen is assembled in microfibrils that give together the fibrils, which is the smallest structural unit of the tendon. Collagen fibrils are assembled and bounded together with endotenons to give the fibers. Endotenons contain blood vessels, nerves and lymphatics. Primary, secondary and tertiary fiber bundle are the next structures that enclose the fiber. The secondary fiber bundle contains a connective tissue sheath called epitenon and incorporate the blood, lymphatic and nerve supply of the tendon. Paratenon is another connective tissue that surrounds the tendon and form the peritendon together with epitenon whose role is to reduce friction between the tendon and the surrounding tissues. The resistance to traction is determined by the fact that most of the fibers have a longitudinal orientation. [1]

Nerves that innervate the tendon come from the muscles, skin or peritendon are mainly sensitive, i.e allow to sense the pain and pressure variations thanks to mechanoreceptor in myelinated fibers. Tendons are vascularized by three circuits : two for the extremities and one that vascularizes the main body of the tendon from the paratenon or the synovial sheath. Vascularization become poorer with age and physical efforts, especially at the junction and at the areas where physical solicitations are applied. [11]

The function of the tendon is to transmit the force developed by the muscles to the bones, which allows to perform movements and to maintain the body posture. It is a very stiff structure that can support large loads in traction [12]. This ability is highly dependent on the structure of the tendon, as well as its physiological state.

1.1.2 Biological response to mechanical stimulation

Cells are involved in the mechanical response for the tendons. Inside the cells, cytoskeleton is responsible of organizing and locating signaling molecules that relays the information in the cells, thereby responding to external forces. This organelle is composed of actin polymers that bind with many types of proteins, and is able to form intra-cellular connection with the different structures inside the cells. Its structure changes with extracellular loading which can induce signal transduction cascade with the activation of G protein receptors and integrins. These are transmembrane proteins whose ECM domain binds to substrates, serving as a signaling bridge between the ECM and the cell. Signals propagate through ligand-integrins binding affinity and is mediated by the activation pf

G-proteins, which results in cytoskeleton reorganization, cell differentiation, gene expression and protein production. [1]

The structure and the composition of the tendon evolve in function of mechanical loading. Some studies reported a change in collagen I expression by the fibroblasts in response to altered mechanical constraints [13]. Moreover, some studies using in vitro models reported a high concentration of prostaglandin E2 and leukotriene B4 that enhance protein production, strengthening the biological tissue [14]. Growth factors are also more present during cyclic loading and the concentration of them increases with the magnitude of the effort. In the cellular scale, it has been observed that cytoskeletal actin filaments of fibroblasts tends to align to the direction of the mechanical strain during cycling loading [15]. In the long term, gene expression is also adapted to the mechanical effort borne by the tendon and influence proteins and growth factors production. Those cells reactions are essential for the tissue to maintain its integrity and to fulfill its function. [1]

1.1.3 Description of the two junction tissues

The junction with the bone and the one with the muscle are two completely different structures. The tendon-muscle junction is weak compared to the enthesis but it ensures a lower tension on this zone while transmitting the force from the muscle to the tendon during contraction. This is due to the deep embedding of collagen fibers between myocytes.[11]

The enthesis is the junction tissue between tendon and bone. Two types of enthesis exist : fibrous enthesis and the fibrocartilaginous enthesis. For the first, the tendon is directly attached to the bone from adulthood, and for the second, both tissues are separated by a transitional zone composed of hyaline fibrocartilage. The enthesis can also bear tensile and shear stress but, as opposed to tendons, can also bear compressive stress. Those stresses have a strong influence on histopathological state of fibrocartilage and, hence, on the appearance of pathology affecting the enthesis. [1]

On the microscopic scale, there are three sections that compose the tissue : a mineralized one next to the bone, an unmineralized one next to the tendon body and a gradient of minerals in between. This gradient is likely to minimize stress concentration during solicitation. This can often arise with two different materials with different mechanical properties and a tiny interface in between, which increases the risk of crack propagation and rupture. The mechanical behavior of the enthesis during tension loading in physiological condition is not well understood. To fill this gap, Deymier et al. [16] carried out a mechanical study of enthesis in mice and hedgehogs. The method will be detailed in the state of the art but it has been shown that the mechanical characteristics, essentially Young Modulus and failure stress, are dependent of the local composition of the tissue. The mineral content was not a determining factor, but this study identified a high-compliance zone (i.e a highly deformable zone) within the enthesis. This region acted as an energy-absorbing component and is localized to the mineralized gradient of the tissue.

1.1.4 Mechanical properties of the tendons

This section gives an overview of the mechanical properties [1] of the tendons. As we will see further, mechanical behavior of such a tissue can significantly differ from one sample to another. Nonetheless, a qualitative analysis of those properties can be done to describe the type of material and general properties of the tendons.

This tissue is viscoelastic similarly to soft tissues like skin. This is due to the high content of water, collagen and proteins interactions which explains why tendons deforms at very low strain rates, enabling it to store energy. At high strain rates, tendons deforms less but are able to transfer important loads. This is very practical in the physiological conditions, since the tendons have to transfer forces but also bear some stress.

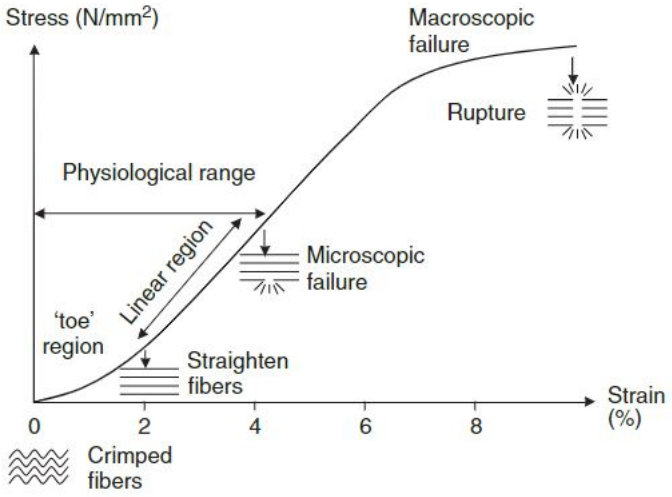


Figure 1.2: Qualitative description of the stress-strain curve of tendons

Figure 1.2 shows a typical stress-strain curve that is observed during tensile tests. The section 3.1.1 will detail this type of test. After a toe region where the fiber is stretched-out, a linear region is observed. In this region, where the slope of the curve is equal to the Young Modulus, tendons are reversibly deformed until the Ultimate Elastic Modulus. This linear region is very large but the physiological conditions do normally not require such high constraints. After this ultimate elastic Modulus, macroscopic tears appears and deformations are irreversible.

1.2 Overview of the various types of tendons and ligaments found in the human body

The main mechanical properties and the composition of the tendon have been explained in the previous section. In this section, the main tendons in the human body that are subject to injuries are detailed.

1.2.1 Description of the knee ligaments

The knee is one of the most complex joint in the body. Figure 1.3 shows the main ligaments present the knee : Anterior Cruciate Ligament (ACL), Posterior Cruciate Ligament (PCL), Medial collateral ligament (MCL), Lateral collateral ligament (LCL) and the patellar tendon. This tendon is also known as the patellar ligament, and will be covered further bellow. The arcuate and oblique popliteal ligaments are also located inside. Inserted in the tibia, the ACL and the PCL initiates forward, backward and rotation of this bone with respect to the knee. The ACL is located on the anterior intercondylar area of the tibia and expands in an oblique proximo-dorso-lateral direction toward the dorsal part of the lateral condyle of the femur. The ACL is weaker than the PCL due

to the fact that it is less vascularized and less robust, which is the reason why it breaks more often. [11]

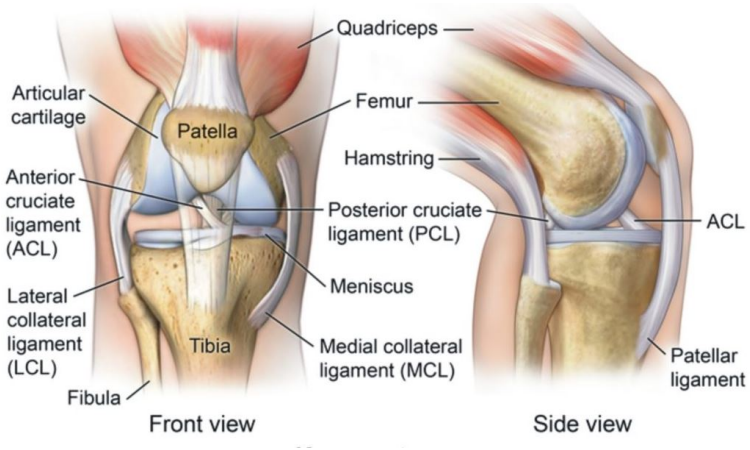


Figure 1.3: Schematic view of the ligaments present inside the knee

For each position of the knee, at least one of those ligaments is partially or completely in tension. The ACL prevents the joint from moving in the sagittal plan as defined in figure 1.4, which is the reason why the knee moves toward in a way similar to a drawer on this plan when the ACL is broken. The posterior movement of the knee is prevented by the PCL. [11]

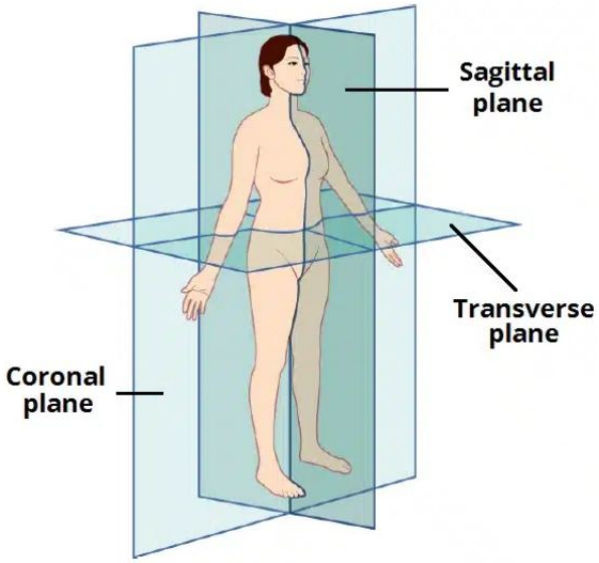


Figure 1.4: Illustration of the anatomical plan of the human body [2]

Although the MCL and the LCL are less well-known, they are essential to reduce the stress on the knee during a motion. The MCL is attached at the medial epicondyle of the femur and expands toward the medial condyle of the tibia while the LCL is fixed on one end at the lateral epicondyle of the femur and the head of the fibula on the other end. They also play a role for stabilization and friction reduction on the articulation. [17]

Regarding blood supply and innervation, the whole knee receives blood through branches from the popliteal artery and femoral artery that come across the knee joint. More specifically for the ACL and the popliteal ligament, vascularization partially comes from the synovial lining that coats those tissues. The synovial lining The femoral nerve innervates the flexor muscle and the structure of the

knee while the sciatic nerve innervates the extensor muscles, and the popliteal lymph nodes inside the popliteal fossa are responsible of the lymphatic drainage in the knee. [17]

1.2.2 Achilles tendon structure

Achilles tendon is the strongest tendon of the body and bears the highest mechanical stress. It measures usually 15 cm. The musculotendinous end is attached to the gastrocnemius muscle, and is bounded to middle of the calf. The tendon is rounded at about 4 cm from its insertion to the muscle where it is flattened. It then widens to become cartilaginous and inserts into an area located in the middle of the lower part of the posterior surface of the calcaneus bone. Because of the fact that it is mostly avascular, the tendon is white. [18]

The Achilles tendon is supplied with blood from three different region : the musculotendinous junction, the middle of the tendon, and at the junction to the bone. The vessels come from the perimysium (tissue surrounding the muscle), the periosteum (tissue surrounding the bone), the paratenon (tissue surrounding the tendon) and mesotenon. Regarding innervation, the tibial nerve and its branches innervate the tendon to provide sensory feedback to brain. [18]

1.2.3 Joining tendons to the knee

The patellar tendon and the Quadriceps tendon are the two tendons that connect the knee to the Quadriceps at the top part and to the tibia at the bottom parts.

The patellar tendon is the only tendon with two bone insertions. On the upper part, it is attached to the patella on its distal two-thirds of the anterior part, and to the frontal part of the tibia on the lower part [19]. This forms a continuity between the quadriceps and the tibia, and participates to the extension of the bone and to the patella stabilization [20]. The length of this tendon is ranged between 38 and 49 mm. The infrapatellar branch of the saphenous nerve runs through the sartorius muscle and innervates the patellar tendon. Branches of genicular arteries supply the tendon with blood [21].

The Quadriceps tendon is composed of three layers : the superficial layer, the middle layer containing two sub-layers and the deep layer. They follow the same layer-arrangement of the four muscles forming the quadriceps and bind them to the patella [22]. The blood supply is split into two sources. The lateral femoral circumflex artery provides blood to the rectus femoris, vastus intermedius, and vastus lateralis muscles and, by extension, the layer-arrangements of the tendon in contact with them. The femoral artery, one branch of the popliteal artery and the profunda femoris artery supply the vastus medialis on the other hand. the femoral nerve provides afferant connexion to the quadriceps tendon and is responsible for pain feeling. [23]

1.2.4 The hamstring tendon

On the other side of the leg, the hamstring tendon connects the hamstring muscles (the biceps femoris, semitendinosus, and semimembranosus) to the back of the patella. The semitendinosus muscle is so called because of the high length of its tendon located in the popliteal fossa. This tendon curves around the tibia and runs over the medial collateral ligament of the knee. Two branches of the tibial nerve innervate the tendon and the muscle, and the popliteal vessels supply the tissues with blood. On the top laterally of the biceps femoris and semitendinosus muscles lies the semimembranosus tendon. It runs medially to the anterior part of the other hamstring tendons [24]. Those tendon measure between 19 and 22 cm approximately [25] and are often harvested for ACL reconstruction if an autograft is required because of a better surgical recovery compared to other tendons [26].

1.3 Tendons injuries

In the United States, muscular disorders costed 213 billion US dollars in 2011 [27]. Half of those disorders are due to tendons or ligament. Tendinopathy and tendon rupture are the two type of injuries that occur. It can be caused by hyperpronation (that leads to inflammation), excessive loading, and trauma due to an accident.

1.3.1 Healing process

Four phases compose the healing process of such tissue. The inflammatory phase is the first and is characterized by the recruiting of red blood cells, neutrophils, monocytes and macrophages that stimulate among others tenocyte proliferation and synthesis of collagen type III. Then, proliferation phase arises when fibroblasts, responsible for the synthesis of collagen and proteoglycan, are recruited and proliferate. After, remodeling phase starts when more collagen III is sythetised. Finally, modeling phase starts and lasts for several weeks with the reshape and the resized of the healed tissues. [28]

All those phases play a crucial role in the healing process and mechanical properties recovery. In fact, some studies report that all mechanical properties of the healed tendons (stiffness, Young modulus, stress and strength) are negatively affected, which increase the risk of re-rupture. This has been proved with human Achilles tendons from healed people compared to normal group thanks to ultrasound testing during elongation of the tendon [29]. Hence, mechanical properties of the tendons are highly variable and dependent on a lot factors that have to be taken into account for care prescriptions.

1.3.2 Achilles rupture



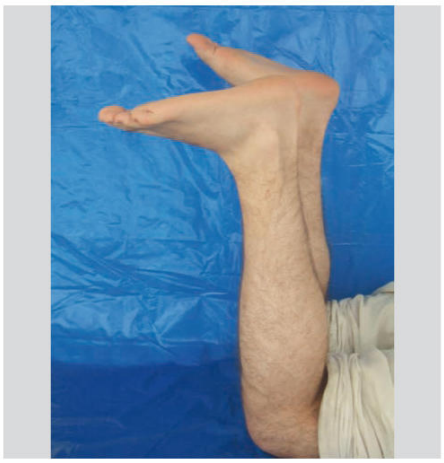
Figure 1.5: Schematic view of Achilles tendon in human adult body [3]

Although it is the strongest tendon in the body, Achilles tendon is one of the most often ruptured or injured. In most cases, the rupture occurs during a sport activity, more specifically in case of intense effort. But it can also happen in case of corticoids dose taking or systemic diseases. A rate of 18 per 100,000 people suffering from Achilles rupture is reported every year only in Europe, and men are 6 times more involved than women. The rupture often occurs between 2 and 8 cm from the ankle bone, which corresponds to the weakest region of the tendon, as seen in figure 1.5. This area is the thinner region of the tendon which is the reason why the rupture occurs more likely here. Patients immediately feel a severe pain when the tendon breaks, and a hematoma can appear. For the diagnosis shown in figure 1.6, patients can also feel pain during the palpation by the practitioner

(Figure 1.6b), and a spontaneous bending of the foot is more important than a healthy individual (figure 1.6a). A radiography can be done to differentiate the rupture from a bone tear, MRI and ultrasound tests may also be prescribed. [30]



(a) Palpation on the rupture location during diagnosis



(b) Increased spontaneous bending of the foot during tests for diagnosis

Figure 1.6: Diagnosis tests of Achilles tendon injury

There are several treatment options available for this type of injury. If the tears are not severe, immobilization in plantar flexion is the one commonly used to reduce the diastasis (tissue separation) at the ends of the tendon and promote healing. To enhance tissue curing, suture of the extremities can be performed, for some cases with reinforcement by a tendon graft such as autologous small plantar tendon. In case of complication such as infection requiring partial resection that creates a large gap, the replacement of the broken tendon by a healthy tendon graft can be done by applying the Bosworth technique. It consists in the muscular fascia reverseplasty to implant the tendon tissue [31]. The healthy graft may come from a peroneal tendon or Achilles tendon, or even from the fascia lata. Some studies reported the use of Peroneus brevis tendon allograft [32] to fill the gap but reliable positive outcomes is lacking. It can be replaced by a tendon from the patient (autograft) or one from a donor (allograft). For the latter, the new tendon can be delivered with a calcaneal bone block and in that case, this block is screwed into the ankle, while the other end is sutured. Although complications are possible, particularly with the use of donor transplantation, it remains one of the most effective techniques available. [33]

1.3.3 Anterior cruciate ligament rupture

ACL tears is another type of very common injury that arises especially in football and gymnastics practice. The patient may have a knee lesion, ranging from a stretch to a partial or total ligament tear. This may results from a hit to the knee, knee torsion including a poor landing after a jump or a body twist while the foot is anchored to the ground as it can happen during ski practice. [11]

At the time of the trauma, pain with a cracking sound is felt by the patient. Hemarthrosis (bleeding in the joint) may also happen, and patient will have trouble to walk or to keep stable. To diagnoses the injury, the doctor can perform several knee leg tests such as Lever Sign Test or Lachman Test [34]. In those tests, he or she will feel a soft, delayed stop of the shinbone instead of a hard stop. They will be accompanied by a radiography or an MRI to detect a possible lesion or fracture around. If the patient feels an instability or practices high level sport, such an injury requires a surgery. But before that, the patient has to immobilize and cool his/her knee, and take painkillers. Figure 1.7 shows the

needed surgery called a ligamentoplasty under arthroscopy, where a small incision is made to pass the instruments and the camera. This limits blood loss and decreases postoperative recovery time. The broken ACL is prepared and partially cleaned if the knee integrity is ensured. The surgeon then uses a compass to place a pin in the natural insertion of the ACL on the femur in order to create a femoral tunnel. The same process is done on the tibia for the tibial insertion of the ACL. The surgeon will then pass a tendon through the tunnels, which will then be fixed with screws. [11]

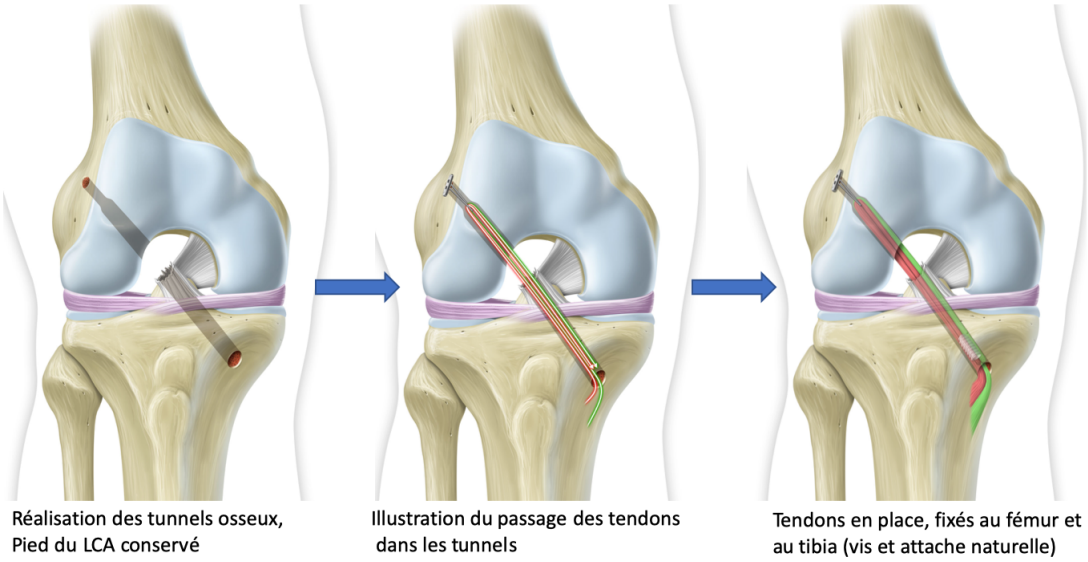


Figure 1.7: Representation of the Passing of the tendon through the tunnel during ACL reconstruction surgery [4]

The patient may have to be hospitalized for two days after such a surgery. Pain, blockages and unpleasant sensations rapidly disappear, but the rehabilitation lasts between 3 and 6 months. He or she must have physiotherapy sessions to regain the flexibility and mobility of his knee, but also to get muscular reinforcement due to the loss of muscle mass during immobilization. Patients will gradually regain their activities but the sport practice cannot be possible after 6 to 8 months. At the professional level, 35% of the athletes do not recover their preinjury level [35].

Sometimes, complications may occur after the surgery. Articular stiffness, that manifests itself as a loss of motion, is a possible post-injury inconvenience, especially when the physiotherapy did not go well. Hemarthrosis can also happen even after surgery, which requires a drainage, washing and antibiotics and sometimes surgical revision. The patient will have to take a preventive anticoagulant treatment to avoid venous thrombosis and will have to postpone returning to sport. Patients may have inflammatory reactions that arise more likely if they received an allograft, which results in localised pains. [11]

1.3.4 Quadriceps tendon rupture

Tears on Quadriceps tendon are not common but may occurs during running or jumping practice, when the knee is partially bent and bears a heavy load. Rupture can be partial, with the appearance of small tears in the tendon, or complete, as illustrated in figure 1.8. In that case, the knee cannot straighten during quadriceps contraction because those muscles are not connected with it anymore. Some factors increase the risk of rupture, such as tendinitis or chronic diseases that disturb blood supply, such as chronic renal failure or hyperparathyroidism, steroid or fluoroquinolones use, or a lack of physical activity can also lead to tendon weakness and increase the risk of injury. [36]

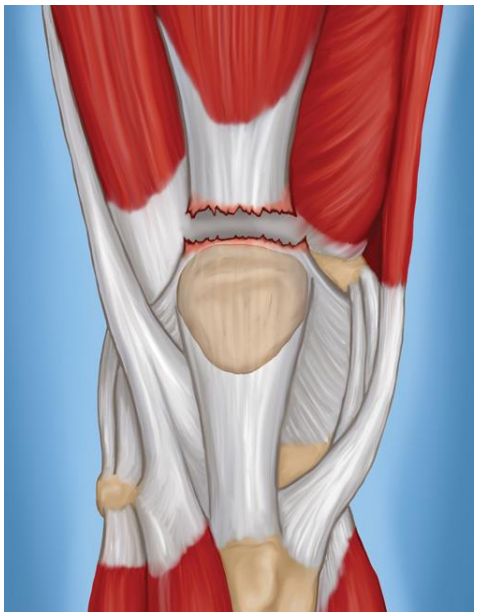


Figure 1.8: Illustration of a complete rupture of quadriceps tendon

Some symptoms associated to tendon rupture are the same with other tendons injury. Bruising, cramping or tenderness are the most common. More specifically for this tendon, skin deformation, or indentation, at the top of the knee, or droop, are the symptoms that may be felt by the patient. As for Achilles or ACL, doctors may carry touch tests to diagnose the rupture, to check how the knee can be straightened. MRI or X-rays scan can be done to clearly see the injury, as shown in figure 1.9. The kneecap is not normally localized as it has been pulled by the patellar tendon since the quadriceps tendon is torn. Soft tissues are more visible with an MRI scan that enables practitioners to quantify the amount of torn tendon and localize the tears. [36]



Figure 1.9: X-rays imaging of the knee. The kneecap is displaced because of a torn quadriceps tendon. The keencap is pulled downward by the patellar tendon

Depending on the age and the severity of the injury, the treatments can differ. Sometimes, the

knee will heal by itself if the doctor immobilize it for 3 to 6 weeks with a brace to keep it straight. Physical therapy will be then needed to restore the strength of the knee and the range of motion. For more severe injuries, a surgery is required. The doctors will reattach the injured tendon to the top of the knee usually by suturing, as shown in figure 1.10. Sutures are threaded through holes that are drilled into the knee. They are then tied to ensure a good position and tension of the tendon. Sometimes, metallic anchors can be alternatively required to ensure the fixation to the bone. If the knee is not stable, surgeons may need to use cables to hold it, and have to be removed for a later surgery. [36]

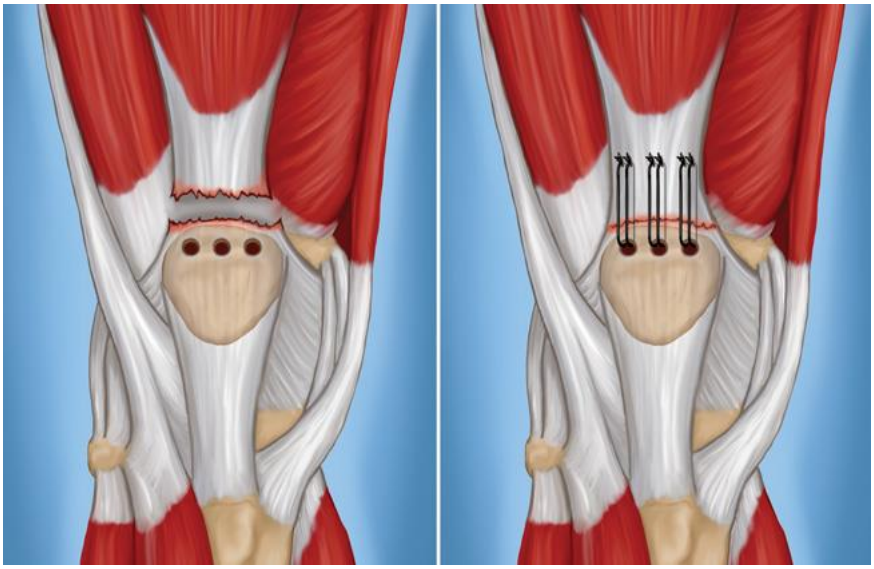


Figure 1.10: Illustration of the surgery process for reattaching the quadriceps tendon

As for any surgery, complications may happen. In this case, weakness and loss of knee motion are sometimes observed. Re-rupture can also be possible. Complications related to anesthesia, blood clot, infection or wound breakdown, which is common for any type of surgery, are also included to the possible complications, although this is quite uncommon. Rehabilitation plan is customized by the doctors and physiotherapists, taking into account the time, the types of exercises or the frequency of the sessions. Complete recovery may last between 4 and 12 months, and a return to previous activities is most of the time ensured. [36]

1.3.5 Patellar tendon rupture

As for the other tendons, Patellar may also partially or completely break (figure 1.11). In that case, the knee is not able to straighten anymore. The rupture is often localized at the bone insertion, which can also sometimes break off, but can also happen at the middle of the tendon. This may be due to falls directly on the knee or a bad landing after a jump where the knee is bent and the foot is anchored to the floor. The risk of tears is enhanced when the tendon is weakened because of some factors such as tendinitis, occurring after cyclic heavy loading during jump or run, corticosteroid or steroid use, or chronic diseases such as kidney failure, diabetes or high cholesterol. Previous surgical intervention such as for ACL reconstruction may move the knee putting the patellar in non usual tension which can also weaken it. [37]

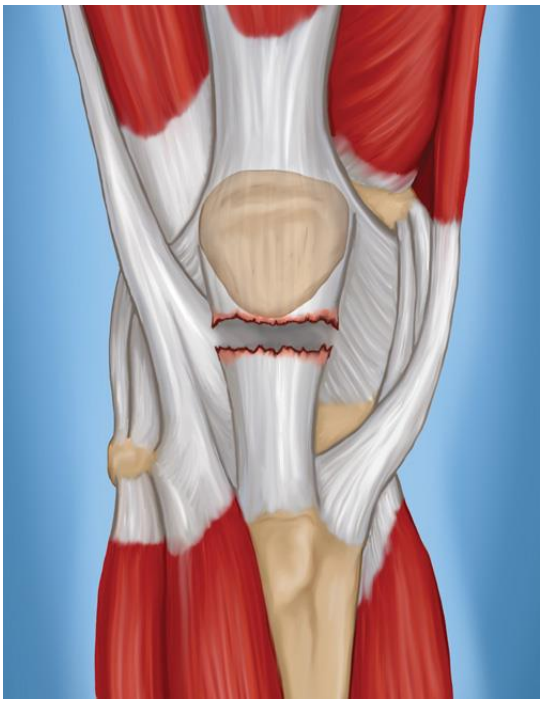


Figure 1.11: Illustration of complete patellar tendon rupture. Reinforcement can be performed by using tendon graft, non-resorbable steel wire or resorbable nylon wire running at the upper tibial end, near the anterior tibial tuberosity and wrapped around the patellar tendon

Similarly to other tendons rupture, the patient may have bruising tenderness or cramping due to this injury. The knee can also move up as with quadriceps tendon rupture because the knee is not anchored anymore, which results in pain and difficulty to walk. Knee touch tests and X-rays or MRI scan will be conducted to diagnosis the injury, which gives similar image as obtained in figure 1.8. [37]

Immobilization and physical therapy are also prevalent for partial tears. Similarly for the quadriceps tendon, those two options will depend on the gravity of the injury and will be customized based on the patient. For complete rupture, the same process as for Quadriceps tendon is carried to fix the patellar tendon (figure 1.12). Ice and medication are needed after the surgery to reduce pain, and a rehabilitation procedure starts as well to fully recover after 6 to 12 months. A loss of up to 15% of the leg strength compared to the healthy leg is always observed and has to be overcome by physical exercises. This always happens for any injury in the limbs, since immobilization and inactivity are required to help the tissue to heal properly. [37]

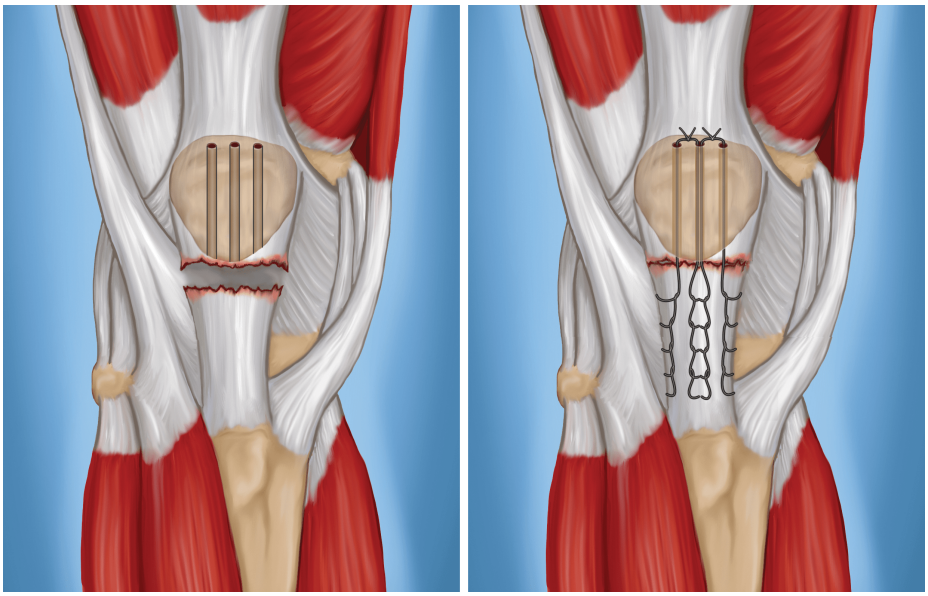


Figure 1.12: Illustration of the suturing process for reattaching the patellar tendon

1.4 Treating Injuries: Available Methods

In case of severe injury that interferes tendons stability, a surgery is required. This is very often the case. In fact, more than 300,000 people undergo a surgery to repair a broken tendon in the United State [28]. When a ligament or tendon needs to be replaced, there are typically two methods that can be used: allograft and autograft. Those methods are elaborated in this section.

1.4.1 Autograft for tissue replacement

Autograft consists in harvesting a tissue directly from the body of the patient, usually in a unaffected area, to replace the damaged tissue. This technique offers a notable advantage of reducing significantly the risk of rejection since the replacement tissue comes from the same body. Moreover, there are no concerns regarding diseases transmission. However, the drawback is the limited choice of the appropriate tendon, which has also to be strong enough to withstand the new constraints of a different region from its former place. Pain can also be associated to the region where the healthy tendon has been harvested, and rehabilitation time as well as surgery duration could be longer. [38]

1.4.2 Allograft for tissue replacement

Allograft, which consists in implanting a biological tissue from a donor to another patient, is one of the care method widely used especially in orthopedic surgery and sports medicine, because of the availability of the tissues and the reliability of the process [39]. The first allograft was experimented by Pierre Flourens in 1847 and has been common for 50 years now. As seen later in section 2.5.1, strict rules and thorough tests are realized. If they are positive, the grafts are discarded. Other donors that presents the risk of transmitting any diseases are also removed out, which results in a high amount of tissues that are rejected. In fact, in the United States, for 21,371 donors in 2022, 9,429 have been discarded according to the Organ Procurement and Transplantation Network [40]. This drawback poses a significant problem for graft availability. One solution to reduce the wastes while ensuring the quality of the tissue is to develop different sterilization methods to eliminate more markers of infectiousness, but the impact on the biological and mechanical properties is very difficult to predict. [41]

1.4.3 Xenograft and synthetic materials : an alternative option

Sometimes, surgeons do not use allograft or autograft to care for a tendon rupture. In those cases, they may use a xenograft, which involves the harvesting of animal tissue for transplantation into the patient, or synthetic materials as a substitute of the human tendons. Xenografts usually come from pig or bovine because of the physiological and anatomical similarities with human tendons, and offer the advantage of low cost procuring and high availability. But the patients can present immunization reactions to the graft. Additionally, several processes must be carried to reduce those complications which weaken the sample and involve higher costs. Synthetic material is an alternative that has been used by pharmaceutical firms to develop a tissue whose mechanical properties are compatible with those of the human tendon. High availability is also an advantage of this solution but this requires also high costs, which is the reason why this is not widespread. [11]

1.5 Accessing transplants: methods and barriers

Because of their advantages mentioned before, allograft is a reliable option for surgeons for tendon or ligament repair. The source of the tissues is extremely controlled to ensure very low risk of complication for the patients. In Belgium, some institutions such as the Belgian Transplantation Society (BTS) are responsible for the safety of the grafts and follow the European regulations.

1.5.1 Tissue bank as a guaranty of safe allografts

Tissue banks are the institution complementary to hospitals that handle human allografts including tendons, from harvest to delivery. They ensure to provide allografts that are compliant with the safety regulations as detailed in the next section, for educative, clinical research or transplantation purposes. In 1982, St-Luc Hospital in Brussels founded its tissue bank that also collaborates with the UCLouvain. Open at any time, this institution can handle any potential new grafts as soon as a potential donor is identified. At St-Luc, 20.5 tendons are harvested every year on average, on donors having a mean age of 48 years old. Depending on the donor, the harvest can be spongy, i.e. its fascia lata and its bones only are exploitable because mechanical properties of the native tissue are not ensured, or complete if the donor is younger. For the latter, tendons can be extracted. [11]

1.5.2 Criteria for tendon taking

The 9^{th} October 1997 and 24^{th} May decrees defined the criteria and safety rules for a donor to be eligible. Strict rules are written to ensure the quality of the tissue by carrying out a complete evaluation of the donor. As a matter of fact, some markers of infectiousness are systematically searched, such as for viruses like human immunodeficiency virus (HIV), syphilis and hepatitis B and C. The surgeon has to take note himself/herself of the microbiological tests results and to inform the patient whether the allograft can be transplanted or not. All donors who accepted the donation have to undergo those tests as well as a medical check-up and medical history investigation. Many exclusion criteria prevent the donor to be eligible such as hepatitis or nervous diseases history, HIV infection or surgical intervention for an allograft transplantation. Growth hormone treatments, use of corticosteroids or unknown death causes are also included in the exclusion criteria. [41]

The risk of diseases transmission is low if the presence of such disease within the population is not significant and if antibody trace are not found inside the body. For instance, HIV transmission by blood transfusion is estimated to be ranged between 1 and 5 over 1 million, and 6 over 1 million

by tissue transplantation. Virus detection, quarantine and the application of validated contaminant inactivation treatment are some ways to further reduce the risks. [41]

Tendon extraction is carried out by a crew of three to four professionals among which at least one is an orthopedic surgeon. Tissues are sterilely taken and frozen at -80°C on site to keep their mechanical strength. They can also be conserved by freeze-drying although this technique is not usually used for tendons. In fact, the exposure to the environment, leading to a risk of bacteria contamination, after closed package breaking requires additional sterilization processes application that can potentially affect the mechanical properties. It consists in setting up the conditions for having the water triple point, enabling to get gas water directly from solid without damaging the sample. It has to be vacuum-packed and can be stored for up to 5 years as established by the European Union. [41]

For delivery, the tendon is defrosted in physiological serum at a temperature of 37°C to 40°C to avoid any irreversible damage on the tissue, and is then dip in half liter of an antibiotic solution. For transplantation, those procedures have to be strictly followed and the patient must be aware of the origin of the allograft. [41]

1.6 Decontamination techniques to ensure safe allograft delivery

As explained before, the allograft must be totally secure. If it cannot be totally ensured, an additional treatment can be applied to remain compliant with the regulations. Several methods exist and are valid only if they reduces the contamination risks to less than one per million. Yet, there are no norms that frame the use of those processes, and the mechanical and biological properties can be affected. Nevertheless , they remain efficient to avoid any transmission diseases.

1.6.1 Chemical treatments

Chemical treatments can be used to removed out cells from the tissue or to kill bacteria. For this aim, antiseptics and antibiotics are the main products that compose the solution in which the graft is immersed, while solvent-detergent products such as ethanol, acetone or ether are used to wash away cells. Those involve proteins coagulation, degradation of the cell membrane and precipitation of nucleic acids which leads to cell death. 15 hours after exposure, no germ traces can be found. [41]

This methods has been proved to be effective against HIV and hepatitis B. Regarding tendons, the World Health Organization considers them to have little or no risk of infection by a rare contaminant. Yet, it will be constantly reviewed in light of the emergence of new variants as for the Creutzfeldt-Jakob disease. [41]

Some other techniques are in development to further improve the decontamination process without affecting the mechanical and biological properties. Cartmel et al. [42] showed the efficiency of the phenoxypolyethoxyethanol, tri(n-butyl)phosphate and sodium dodecyl sulfate to remove cells while ensuring integrity in terms of mechanical properties and structure. Tensile stress and histological analysis were carried out to look in details the cellularity, the nativity and the structure of the tendon samples. Further studies can be carried out to develop an effective treatment and a suitable protocol based on those products.

Several chemical treatments showed however altered mechanical properties on the tendons after application. Zhang et al. [43] showed that peracetic acid-ethanol affects mechanical parameters such as the elongation and the strain of the tendon during load to failure tests. However, they concluded that this is not sufficient to seriously jeopardize the integrity of a graft, and suggest further in vivo and in vitro studies. This shows the difficulty to predict the impact for transplantation.

1.6.2 Gamma irradiation process

The irradiation process is one effective but aggressive way to sterilize the tissues. The cobalt 60 emitting gamma rays and particle accelerator emitting beta rays are the two methods for this process. Both provoke ionization of matter by photoelectric effect when the rays interact locally with it. This affects the nucleic acids structure and other molecules which lead to degeneration of viruses or bacteria. A dose of 25 kGy is proved to be sufficient to ensure bacteria removal, but a limiting exposure to potential contamination during manipulation prior the treatment is preferred. [41]

Although the efficiency against bacteria is proved, the sterilization against viruses is more difficult to ensure whereas the HIV markers are inactivated by the irradiation according to some studies [44]. Therefore, it has been suggested that a dose of 35 kGy is necessary to sterilize a contaminated tissue [45]. Nevertheless, the contaminant agents that do not have nucleic acids, such as prions, which are a specific type of proteins, seem to be resistant. [41]

Regarding the integrity of the tendon, it seems to be that there is an optimal dose of gamma rays that ensures decontamination while preserving mechanical properties of the grafts. However, a higher dose can impact the mechanical strength, and this is true also for other type of tissues. Vettese et al. [46] showed that collage cross-linking anomalies are also occurring following gamma irradiation exposure but also chemical treatments, enhancing protein denaturation. This will be more detailed in the next chapter.

1.6.3 Electron Beam irradiation

An alternative of the gamma and beta rays also used for sterilization is the Electron Beam.This consists in a exposure of a continuous flow of electrons that hit the DNA of the micro-organisms. Similarly, it breaks the strands, leading to cell death. The advantage of this technique is the effectiveness of the sterilization process and the controlled harmful effects on the users compared to the gamma irradiation.
[47]

It has been proved that this technique is efficient to sterilize tendon allografts without affecting the mechanical properties. For ACL repair, it provides very good clinical results according to some studies. [48]

1.6.4 Ethylene oxide application

Ethylene oxide is an alkylating gas widely used mostly for the sterilization of bone grafts but is still effective for tendons. The whole process lasts about 180 minutes, from gas introduction to the complete exposure. A long aeration time (about 8 to 12 hours) at 50 to 60°C is require to ensure complete gas evacuation. This gas inactivates all microorganisms but some bacteria can be resistant to it. Some factors, such as salt and organic materials, can decrease the efficiency of the process. [49]

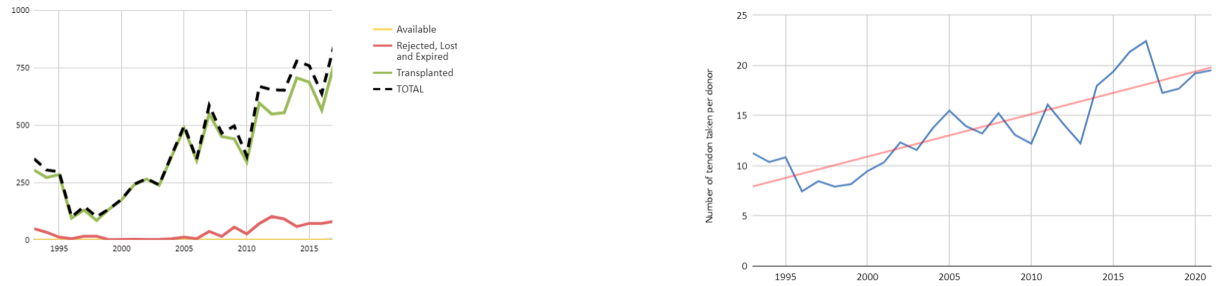
This technique is not used anymore in the hospital because it can cause severe hazards to staff and patients (irritation and neurological dysfunction notably). Cost is also a limiting factor of this technique. Regarding the mechanical properties, some studies [50] revealed that the failure load and Young modulus of elasticity are not affected but it can be sometime responsible for inflammatory response, leading to failure. This is the reason why the tissue must have no more contact with ethylene oxide molecules for transplantation. [51]

1.6.5 Sterilization by autoclave

Autoclave is a technique based on heat exposure to heat and steam. This does not require heavy infrastructure and is relatively cheap. The principle is the exposure of the graft to a hot steam at 120°C for 15 minutes in accordance with the European regulations, but the duration and the temperature can vary for some specific cases. Proteins present is bacteria are denatured, which lead to their death. However, toxins can be more resistant to this technique, as well as other high resistant bacteria or virus, which requires higher temperature. [41]

1.7 Concerns surrounding tendon allografts

As explained in previous section, allograft transplantation is very convenient for healing injuries with tendon rupture. As a consequence, this has been widely used by surgeons in the last decades, as shown in figure 1.13a. The number of transplanted allografts (green curve) has more than doubled from 1995 to nowadays. Although this technique offers a large spectrum of possible implants, surgeons are not able to bet all the cares on it. In fact, it can be seen that the stock of available graft is depleted each year, as indicated by the yellow curve. At the end of the year, all received grafts by the tissue bank have been transplanted or rejected (red curve) which highlights the existence of a waiting list for additional patients.



(a) Graft status of the tissue bank in Saint-Luc Hospital

(b) Number of tendons harvested per donor over years

Figure 1.13: Data of the tissue bank of Saint Luc Hospital

To overcome this, awareness-raising campaigns have been done to encourage people to register in the donor lists. This had a positive effect on the incoming grafts, as shown in figure 1.14. Despite some fluctuations, a positive trend of the number of donors can be drawn until today. However, those donors do not ensure acceptable tendon grafts. Some donors have contraindication preventing tendon harvest, such as the ones discussed before.

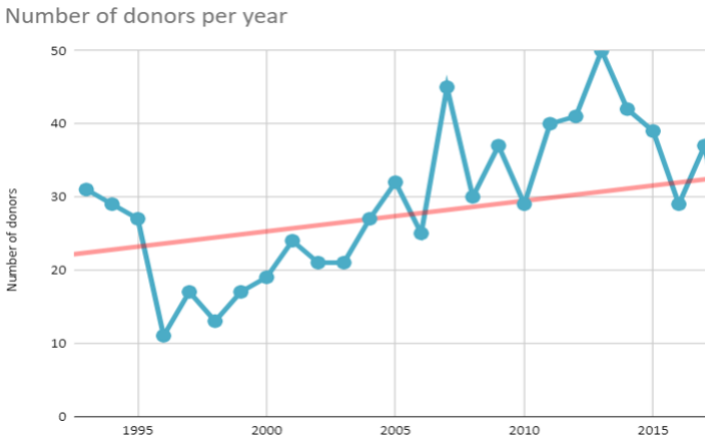
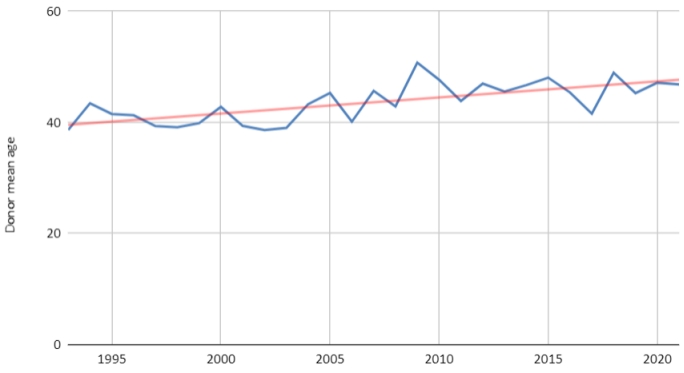
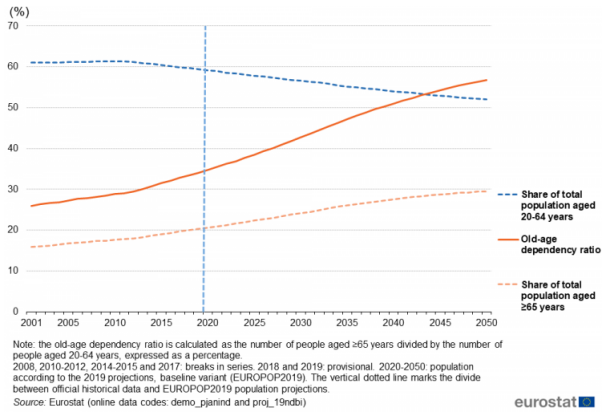


Figure 1.14: The evolution of the number of donors over years

Another reason why some donors cannot provide grafts is the age. Surgeons cannot use the tendons of people that are too old (more than 60-65 years old) since theirs tendons are weaker and risk to break if they are transplanted to a younger patient that provokes higher loads. This refusing factor is going to be faced more often according to the data of the tissue bank of Saint-Luc hospital shown in figure 1.15a that plots the mean age of donors providing tendons for transplantation. The mean age shows a rise of roughly 12.5% slightly before 1995 and until today, increasing from 40 to 45 years old in 2020. According to the prediction of European Union [8], The tissue bank will observe a continuous rise over years if we observe the data of the proportion of people older than 65 years (figure 1.15b). The orange dashed curve represents this proportion, and a trend of increase can be observed from the beginning of the century and goes beyond today according to the predictions.



(a) Mean age of procured tendon donors over years



(b) Proportion of population of 65 years or older vs 24-65 years old over the 21st century

Figure 1.15: Data of population mean age from the tissue bank of Saint-Luc hospital (left) and European Union (right)

Since it is expected to double within a half-decade, two problems will be posed : first, the aging of the population increases the risk of tendon rupture, which will lead to a higher number of patients requiring allografts. Second, tendons from donors will likely be of lower quality as the mean age of the deceased population increases. Therefore, it is imperative for the scientific community to address this issue and find solutions.

1.8 Possible solutions

To address the shortage, the tissue banks in all hospital can even further encourage people to donate tendons but this solution cannot give short-term outcomes and these are not guaranteed. Another more interesting solution could be to maximize the number of taken tendons of the donors. This opens the door to the exploration of new types of tendons for a specific context, such as the tendon of the forearms. However, those tendons are much smaller and thinner than those that we find in the lower limbs, which limits the ability to fulfill the function of Achilles tendon for example.

Since population is aging, older donors can be considered. While investigations can be performed to address the increased risk of rupture in older donors, convincing results are not guaranteed. But, the problem could be then tackled from another point of view. In fact, strict procedures force tissue banks to discard several grafts every years as explained before. To reduce those wastes, existing decontamination processes can be improved, or new ones can be developed to eliminate specific virus or diseases. This could clearly help the healthcare system to remove patients from the waiting lists, but the serological check-up of the grafts is not sufficient to perfectly assess the efficiency of a specific decontamination process. Indeed, the impact on the mechanical properties should potentially be significant and this has to be quantified properly. Older donors can also be considered to provide tendons for more aged people. Currently, regulations forbid transplantation from 60 years-aged donors but mechanical studies can be carried to provide significant results on border line tendons that are discarded, in order to expand the possibilities of grafts.

1.9 Conclusion

As discussed in earlier sections, there is a growing focus on the mechanical properties of tendons. This is a significant concern for surgeons as the decreasing reliability of grafts is directly linked to the mechanical properties of tendons. Even more seriously, re-rupture of the tendons after implantation occurs for between 5.6 and 6.9% of cases [52]. Expanding the pool of available donors to increase the variety of tissues is a challenging task, but limiting the extent of graft wastes is a feasible approach. Indeed, new sterilization processes can be developed to eliminate the markers of infectiousness of viruses. However, there is a risk of affecting the biological properties of the tissues, which can hence affect negatively the mechanical properties, as will be discussed in more detail bellow.

Therefore, tensile tests become more and more important to help healthcare staff to address the shortage. For this purpose, surgeons need a traction machine to assess accurately the mechanical properties of the processed tendons. But the major challenge of such a machine is designing the bits that fix the tendon to the machine. In fact, tendon is a weak tissue compared to metal samples classically used for such tests, it can indeed break if it is compressed which invalidates the results if the rupture is localized at the area where it is hold.

The objective of this thesis is thus to design the appropriate bits, assess their efficiency and validate the model through tensile tests. Some studies have been carried out to assess the mechanical properties of the tendons as will be seen in the next chapters, but they have certain limitations associated with them.

Chapter 2

Mechanical properties of biological tissues : State of the art

Tensile stress on tendons have been performed to quantify relevant mechanical properties of tendons and to describe the stress-strain curve of many types of tendons. This has been useful to link those properties with the structure of the tissues and to understand their behavior under physiological constraints. This chapter covers the main mechanical tests that have been performed, using different methods and types of samples. The type of the bit will be specifically highlighted to give relevant elements for the mechanical design of the coming system, and a comparison with the tests performed in other sectors will be made.

2.1 Overview of classical traction tests on metallic samples

Before covering the tensile tests of tendons, classical traction tests are here describe to highlight the different parameters of such experiments, and some features and interest of this kind of tests.

2.1.1 Load to failure tests

Definition and setup

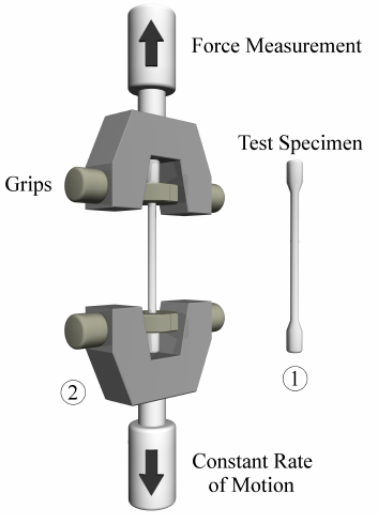


Figure 2.1: Illustration of the experimental set up of load to failure tests [5]

The load-to-failure test is a mechanical test "*that applies force to a material specimen in order to measure the material's response to tensile (or pulling) stress*" as defined by Instron, a well-known firm in the materials testing industry [53]. It "*provides information about the tensile strength, yield strength, and ductility of the metallic material*" (Saba et al.) [54] and enables to record the force necessary to stretch a material until failure. The tensile tests can be either biaxial or uniaxial. For the latter, the extremities of the sample are gripped and a traction force is applied aligned with the axis of the sample, as illustrated in figure 2.1. It is thereby stretched as a response of the constraint, and the values of force recorded by a sensor (figure 2.2) are retrieved in function of the elongation. The rate at which the sample is stretched can be controlled either by a constant displacement rate of the crosshead beam of the machine or by applying a constant increase of the force.

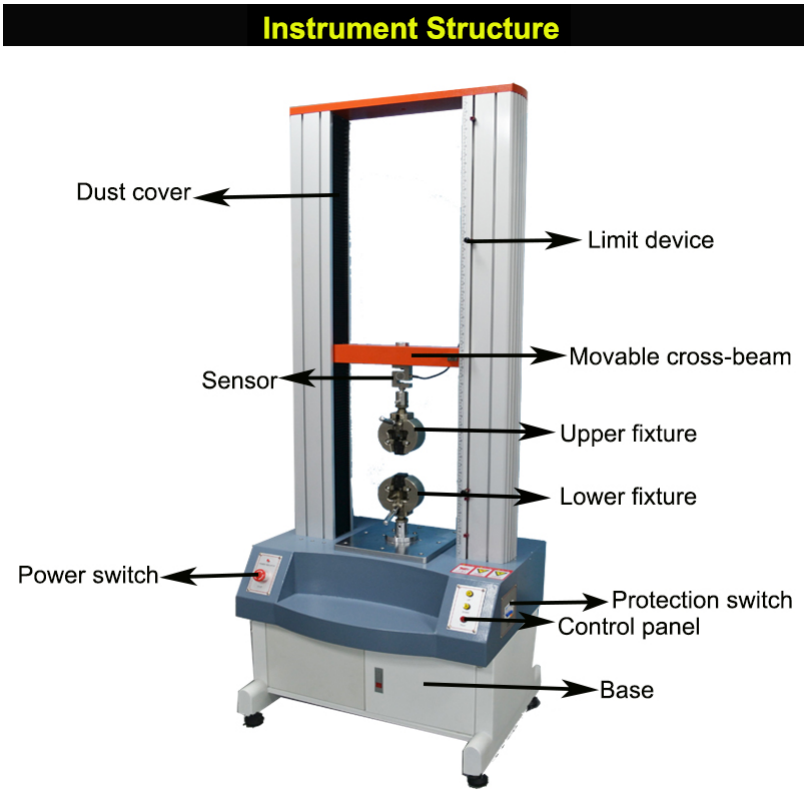


Figure 2.2: Classical tensile test machine or uniaxial load to failure tests [6]

These kind of tests are performed in the scope of the development of new materials or fabrication processes. Moreover, the choice of a material for a specific application requires some guarantees regarding its strength. To assess it, engineers carry out such tests to analyze the behavior of the material under stress. The types of tested material are most of the time metallic or made up of polymers, composites of ceramics, but the materials can also include textile and, more recently, biological tissues. Except for the latter, those samples are relatively homogeneous in terms of structure and composition. For this reason, the failure location is difficult to predict and can occur randomly. Therefore, it is common to purposely reduce the section of the sample as illustrated in figure 2.3. This reduction will weaken the sample at this particular area which will predispose the rupture location. To avoid adverse effects at the extremities (shoulders), it has been recommended to set the length of the reduced section at four times its diameter, and the transition section length at minimum this same diameter. [7]

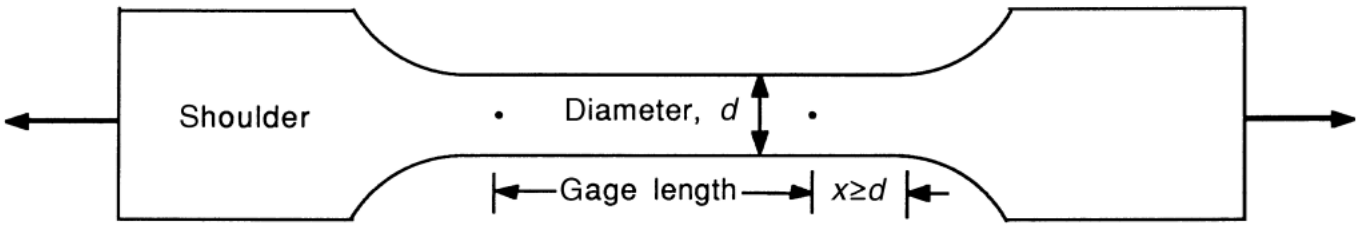


Figure 2.3: Type of specimen shape used to induce the failure at a specific location [7]

Stress-strain curve and mechanical properties

Uniaxial load to failure tests provide several data regarding the mechanical behavior of the samples during such solicitations. Figure 2.4 shows the typical curve obtained by conduction a load to failure stress. It displays either the force or the stress in function of the elongation. The elongation and the stress are defined as :

$$\begin{cases} \epsilon = \dfrac{L - L_0}{L_0} \\ \sigma = \dfrac{F}{S} \end{cases} \tag{2.1}$$

where L_0 is defined as the length reference, i.e. the distance between two aligned reference points before testing, L as the distance between those two points at a certain moment of the test, F as the traction force applied at a certain time and S the section of the sample. The reference length is defined on the sample between the grips and the bounds displacement are recorded in the L variable.

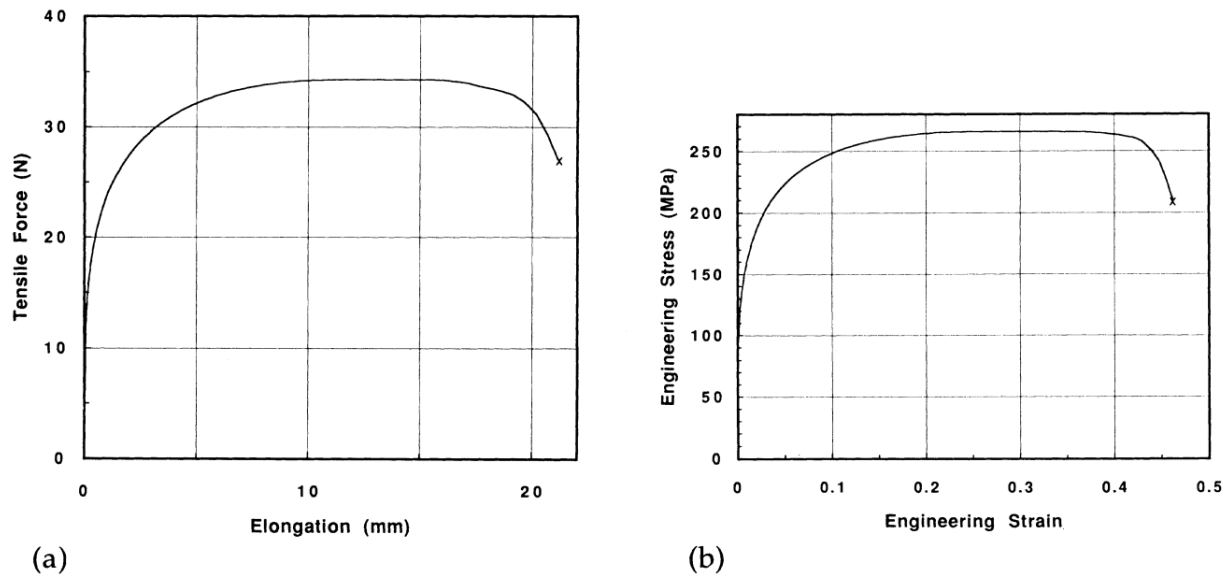


Figure 2.4: Typical force-strain curve (a) and the corresponding stress-strain curve (b) obtained by an uniaxial load to failure test [7]

Three regions can be featured on this graph : An elastic region, a plastic region and the failure. The elastic region is a linear curve whose range corresponds reversible deformation. It means that

the sample returns to its initial shape when the stress is released. The slope corresponds to the Young modulus of the materials and gives information about the stiffness of the material ; a high value corresponds to a rigid material that hardly deforms while a low value corresponds to a soft material that deforms easily. The range of this part of the curve depends on the materials. The plastic region is a non-linear curve that corresponds to non-reversible deformations. In fact, the material remains deformed after the release of the stress if it is inside the range of the plastic region. The curve shape depends also on the material, and the transition point between both regions is called the ultimate tensile strength. This critical value is very important for engineering design as the solicitations for a specific application cannot reach this value, otherwise adverse effects will occur. Finally, the curve reaches the end of the test that corresponds to the failure point from which the maximum strain can be retrieved. Those properties are important to assess the quality of a material in terms of mechanical resistance for specific applications such as in construction to study the deformation of steels used for buildings, or in biomedical engineering for the development of a medical product [55].

2.1.2 Cycling loading tests

Cycling loading test is a non-destructive test defined by Hoeppner as "*the application of repeated or fluctuating stresses, strains, or stress intensities to locations on structural components*", locations at which *The degradation that may occur is referred to as fatigue degradation*" [56]. Those tests are crucial for the selection of a material for a specific application, but also for the design of its shape and its micro-structural features. They are performed in sectors where the mechanical components are subject to regular loading such as the fans inside the turbine of planes, components of bridges or implants designed in the biomedical sector. Figure 2.5 shows how the load is applied over time during cycling tests in order to observe fatigue. The load is applied and released several times, and the maximum load is controlled in order to prevent the sample to break at the early stages.

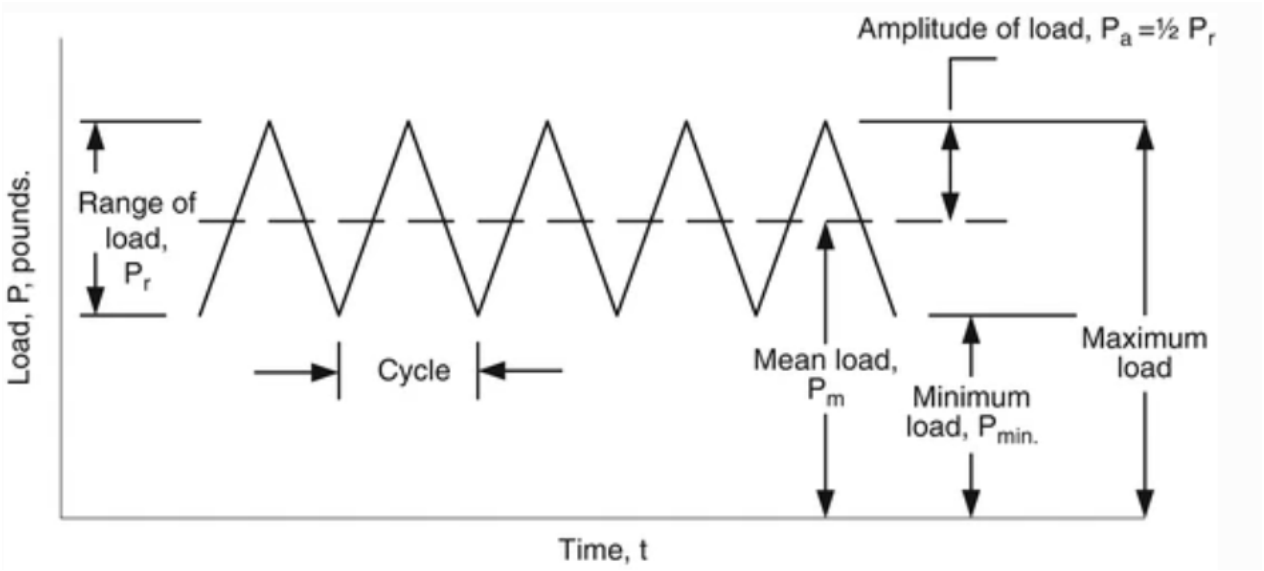


Figure 2.5: Typical cycling loading tests performed on materials

Fatigue phenomenon : Definition and characterization

Fatigue is the result of cumulative loading that involves the apparition of cracks that can lead to failure if the process is sufficiently repeated. Three steps of fatigue occur during cycling load : The first one is the crack initiation. This is the apparition of the first crack that occurs at the locations

where the stress concentration is the highest which is usually referred to some regions such as pores or discontinuous areas. Then starts the second step called the crack propagation that implies the growth of the crack along the plane at the highest stress concentration to end up with the last step : final fracture of the material. [57]

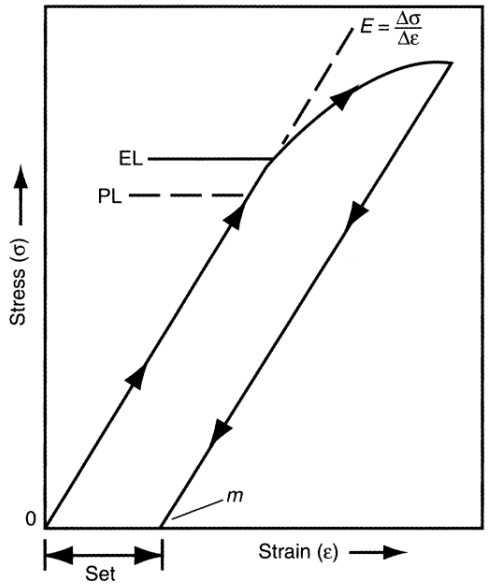


Figure 2.6: Elastic domain of the stress-strain curve of a given material. The area bounded by the arrows is referred to the hysteresis

The stress applied during the cycling load tests can be ranged within the elastic region of the stress-strain curve described in the previous section. As explained before, such a constraint induces non-permanent deformation, but a cycling loading can provoke the fatigue of the material as shown in figure 2.6. When the load is released, the deformation remains permanent at zero stress before disappearing. The area encompassed by the cycle is called hysteresis. When the sample is subject to fatigue, the deformation remains and becomes even greater after repetitive loading cycles.

Fatigue life and Wöhler curve

The loading tests described above enables to characterize the fatigue phenomenon. For a specific application, engineers have to know the range at which the cycling loading can be applied without breaking a mechanical component. To this end, a German engineer called August Wöhler came up with the idea to represent the fatigue life in a diagram as plotted in figure 2.7. He proposed a curve describing the total strain amplitude as a function of the number of cycles required to initiate a crack. The area encompassed inside the curve is representative of the so-called fatigue life, which is the range where engineers can allow the solicitations. The information extracted from this typical curve have to be taken with cautious. In fact, the curve does not take into account some factors that influence the crack initiation, such as the micro-structure of the material, the temperature or the chemical environment. This is the reason why engineers use a safety coefficient to avoid any dramatic effects. [57]

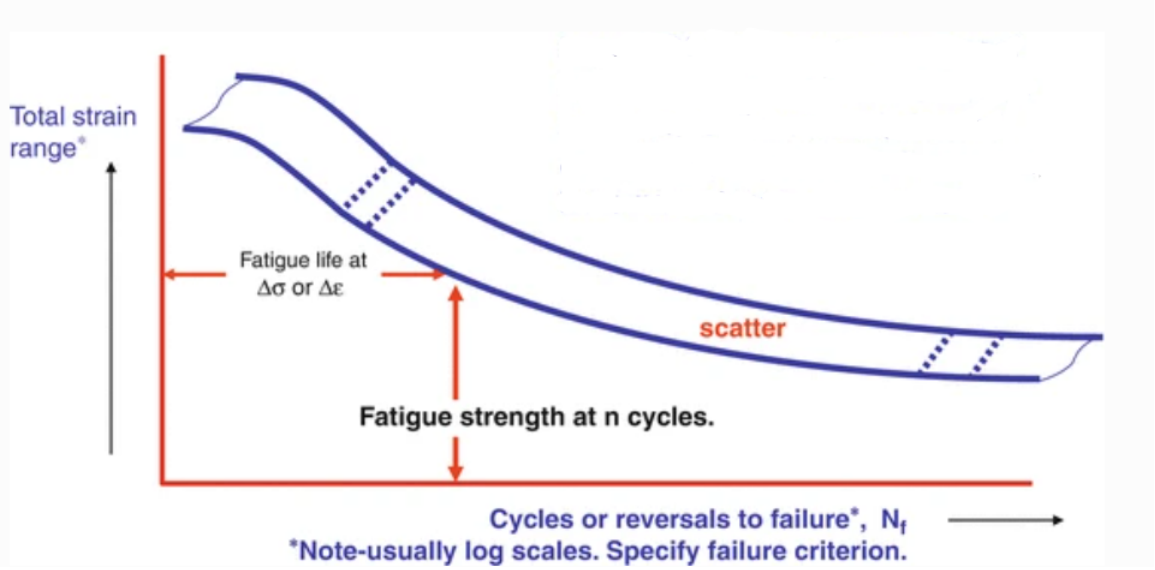


Figure 2.7: Typical Wöhler curve showing the fatigue life of a given material

List of Figures

2.2 Traction tests in the textile sector : a comparison base with tendons in an universal way

Textile materials are synthetic components composed of assembled fibers that have comparable structure with tendons. Mechanical tests has been performed for specific applications, and similar properties have been extracted. Therefore, the process can provide mechanical components to the design of the bits for this thesis.



Figure 2.8: Example of devices used for tensile tests on textile sector

Experiments have been carried out in order to determine some features of a specific fabric such as the required force to tear, stretch or break it. The purpose is indeed to reduce waste and costs, but also to improve the quality of the product and hence, to enhance the client satisfaction. Regarding tensile tests, a device as shown in figure 2.8 is used for some studies. The sample is wrapped around a cylinder at the extremities and can be tested for tear, shear and tensile among others. Some important features such as the tensile strength can be retrieved during tests that are governed by some standards including ISO ones. [58]

The interest of investigating in the textile sector resides in the fact that the fabrication process is controlled decreases significantly the variability within a set of samples which ensures reproducibility

of the results. Additionally, the fiber orientation and structure can be similar to tendons, and some fabrics can have similar properties as they can be elastic and anisotropic for instance [59]. Among the different types of textile products, nonwoven ones are one of the materials closest to tendons in terms of structure as they have randomly fibers orientation. They are used in many fields including the biomedical sector as they are used for the fabrication of operating accessories, bandages or sterilization wrap [60]. They can be also mechanically tested in a device such as in figure 2.8, whose design can be a source of inspiration for the bits that we aim to produce.

2.3 Biaxial testing of biological soft tissues

Mechanical tests on biological samples have become more and more prevalent. From compressive testing of bones to tensile tests on tendons or arteries, the range of the possible tests is wide. Among tensile tests, biaxial tests are conducted by gripping the samples either with clamps, sutures or rakes and stretched along two orthogonal directions as shown in figure 2.9. All those tests enable to extract features of interest of a specific tissue, such as the ones explained in section 3.1.1, for the design of implants and medical devices. Up to today, standardized protocols have not yet been designed for the reasons that will be mentioned further in this chapter. Because of that, the study of Fehervary et al. [61] suggested the use of fitting models using finite element methods and parameters fitting to propose a protocol design for such tests. This would allow to make a relevant comparison between two different studies on the same biological tissue.

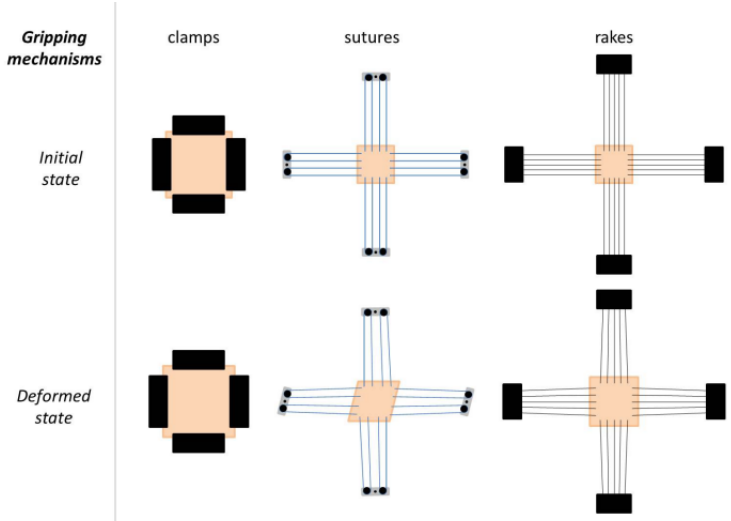


Figure 2.9: Schematic representation of the different methods for gripping samples in biaxial testing.

The devices used for such tests are similar to the one shown in figure 2.10. A rigid metallic platform maintains the tissue stable and allows to adjust its localization with respect to the four linear actuators that transfers forces to the sample. This one is kept in a sterilized environment encompassed by a biocompatible material such as some polymers. Those allow the sample to be fully in contact with air or completely immersed in water. The strain is calculated in a certain region of interest using digital imaging correlation method. Similar curves as for metallic samples can be retrieved by this technique. It allows accurate measurements through the use of cameras and vision lens directly positioned above the sample. The results are useful for several design applications but also to understand the limits of the biomechanics of such tissues especially in the context of some degenerative diseases. [62]

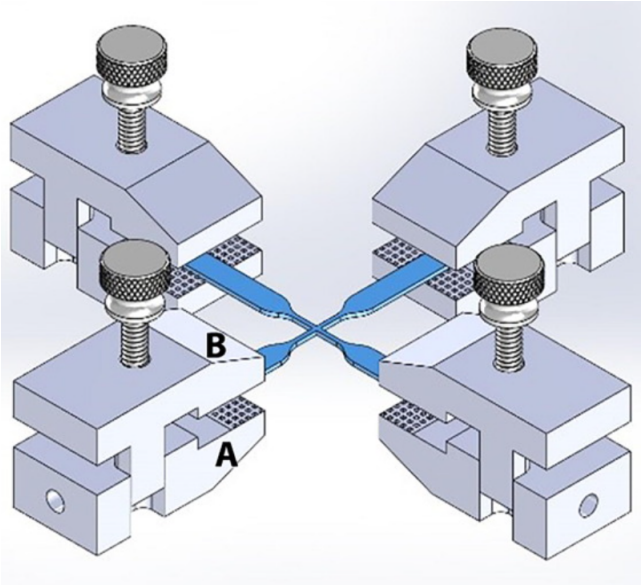


Figure 2.10: Illustration of classical biaxial machine

2.4 Mechanical tests on human tendons to extract their mechanical properties

Many studies have been carried out to extract mechanical properties of the human tendons. The stress-strain relationship has been discovered similarly to metallic samples, and highlighted interesting features that enable to understand the physiology of the tendon. From *in vitro* to *in vivo* studies, with a focus on the impact of sterilization treatments, this section aims to propose an overview of the studies of the mechanical properties of tendons.

2.4.1 Characterization of Achilles human tendon

Achilles tendon is one tendon that is often injured as explained in the previous chapter (section 2.2.2), although this is the strongest tendon in the body. Mechanical testing of human Achilles tendons proved indeed this statement. Tishya et al. [63] performed destructive tensile tests on 11 pairs of consistent human samples (i.e. non damaged) harvested from donors from 35 and 80 years old. The samples included the posterior half of the calcaneus and muscle attachments. The samples were hydrated for the whole time before testing, and did not keep the paratenon tissue (see section 2.1.1). The test has been carried at a elongation speed of $1mms^{-1}$ for one specimen of each pair and $10mms^{-1}$ for the other of the same pair, at room temperature (about 24°C), using a servo hydraulic machine. The way of gripping the samples is detailed further in this chapter.

Cross-head displacement and forces were recorded during the test and the Young modulus were extracted from the linear region of the stress-strain curve. More specifically, the displacement of the tendon body has been measured by a camera, while the grip-to-grip measurement has also been done to retrieve the bone-tendon complex displacement. Four samples from three pairs failed at the bone insertion region while the others failed at mid-substance. For the latter, it seems that the failure occurred at the distal half of the tendon next to the bone insertion. This corresponds to the region with the smallest width which is the location of most Achilles injuries. The paired t-tests revealed no significant differences for failure load and failure stress at the two elongation speed, but the failure stress seemed to be significantly higher for the faster rate. Table 2.1 indicates the properties of the

samples, excluding the specimen that failed at the bone insertion.

Mechanical properties	rate of $1mms^{-1}$ (n=9)	rate of $10mms^{-1}$ (n=9)
Young modulus (MPa)	816	822
Failure load (N)	4617	5579
Failure stress(MPa)	71	86

Table 2.1: Reported mean mechanical properties of human Achilles tendon-bone complex during *in vitro* tensile tests for $1mms^{-1}$ and $10mms^{-1}$

Although the protocol enabled to retrieve reliably the mechanical properties of the bone-tendon complex, significant differences with other works are observed. The testing protocol of Louis-Ugbo et al. [64] provided a value of failure force of 1189N on average, which is roughly four times less than the values of Tishya et al.. The load-strain relationship that they obtained is displayed in figure 2.11. The shape of the graph is consistent with the mechanical properties of the tendon mentioned in section 2.1.4 as we observed three separated regions : a toe region, a linear region and a plastic region. Although the values obtained are completely different from the ones in table 2.1, the behavior of the material remains the same.

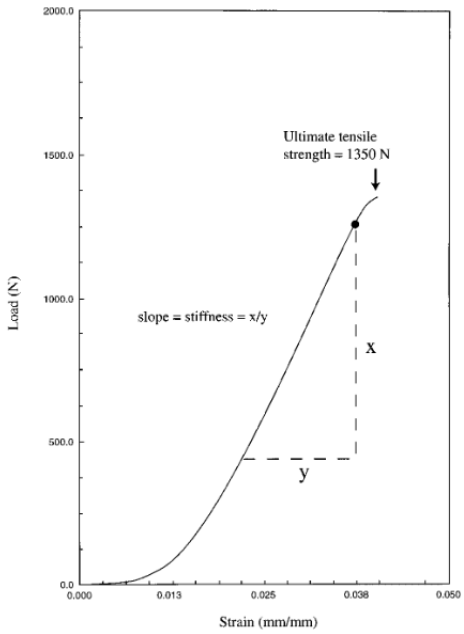


Figure 2.11: Force-strain relationship for the load-to-failure tests

The main difference can be due to the age of the donors, as the mean age of the ones who provided the data in table 2.1 was 52 years old while the donors from the study of Louis-Ugbo et al. were 80 years old on average. However, this high difference should not be attributed to the age only, but it can be also due to the harvesting conditions. Unlike the samples of Tishya et al. study, information of those from Louis-Ugbo et al. regarding storage conditions are not mentioned, except for the fact that they were taken out of the cadavers within 24 hours. This may be suspected that the tendons were not hydrated before testing compared to the other study, so the content of water would have changed which can influence the results.

These hypothesis are supported by the results obtained by Nagelli et al. [65]. The testing protocol and the storage conditions were similar, as well as the mean age of the donors. Hence, they obtained a failure load of 5,649.1 for a rate of $5mm.s^{-1}$ on average which is consistent with the data reported in table 2.1. The fact that this value is higher may be due to the fact that donors were younger on average (46 years old). Additionally, since the properties are history-dependent, the results can have been influenced by all the solicitations over the entire life of the donors, which can differ from one individual to another. For those reasons, it becomes clear that the method has to be thoroughly designed not to induce disparities. This demonstrates that defining standards regarding mechanical properties of human Achilles tendon for cares by allograft purposes is challenging.

2.4.2 Fatigue loading investigations

Fatigue is one very common mechanical phenomenon occurring with tendons. It is defined in Ashcroft's book as involving " *the failure of materials under cyclic loading, where the maximum load can be significantly lower than that required to cause static failure*" [66]. In the case of tendons, it is well known that cycling load induces cellular response leading to structural changes in ECM among others, although the phenomenon is not well understood.

There are two ways for fatigue testing : The samples are cycled to a constant peak load and elongation is monitored for all cycles, or a constant peak elongation is applied during solicitation and the load relaxation is monitored. The first mode is more often attributed to ligaments while the second fits more the tendons. Jennifer et al. [67] reported several studies using *in vivo, ex vivo* or *in vitro* models for characterizing the impact of fatigue on the properties of the tendons and explain the different features that have been extracted.

The *in vitro* models provided significant results regarding the impact of fatigue on structure of the tendons. At the microscopic scale, it seems that cycling loads, even at low intensity, induce changes in collagen arrangement in isolated regions that seem to be associated to damages. Tendocyte arrangement disorders and kinked collagen fibers were also observed as in figure 2.12. However, it has been evidenced that cycling solicitations provoke tendon specialization for specific functions related to the *in situ* load environment, leading to stronger tendons. But the transition point between positive changes and negative changes leading to injury is not known yet. Nevertheless, the studies reported in this review showed across different types of human tendons the link between the applied peak tensile stress and the fatigue life as well as the amount of cycles before failure. Moreover, it also seems that the strain is the main driver of damage accumulation and injury. These results enabled to increase our knowledge about structural changes and cellular response to cycling loads.

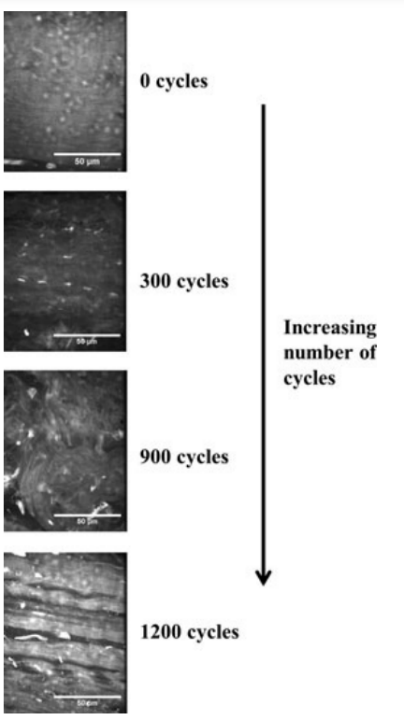


Figure 2.12: Evolution of cracks in bovine extensor tendons over the cycles

The studies using *ex vivo* models, i.e. testing a tissue outside its natural environment but while keeping its viability, brought new conclusions but confirmed also some of *in vitro* models. In fact, the propagation of damages inside the tendon at the microscopic scale, as shown in figure 2.12, has also been confirmed in viable tissues. Moreover, it has been understood that the presence of viable cells influences the load stress in the tissue, which modify its biomechanics and its integrity. Besides, the positive influence of controlled loading has also been proved by the stimulation of DNA and collagen synthesis. Similarly, high loads negative effects have been observed by the increase of the concentration of prostaglandin E2 that we find in case of tendinopathy (see section 2.1.2) as well as the degradation of the mechanical strength. However, those models do not enable to agree on the cells viability during aggressive loading. Nevertheless, the *ex vivo* models completes the *in vitro* ones by bringing insight in the biological effects of cycling loading.

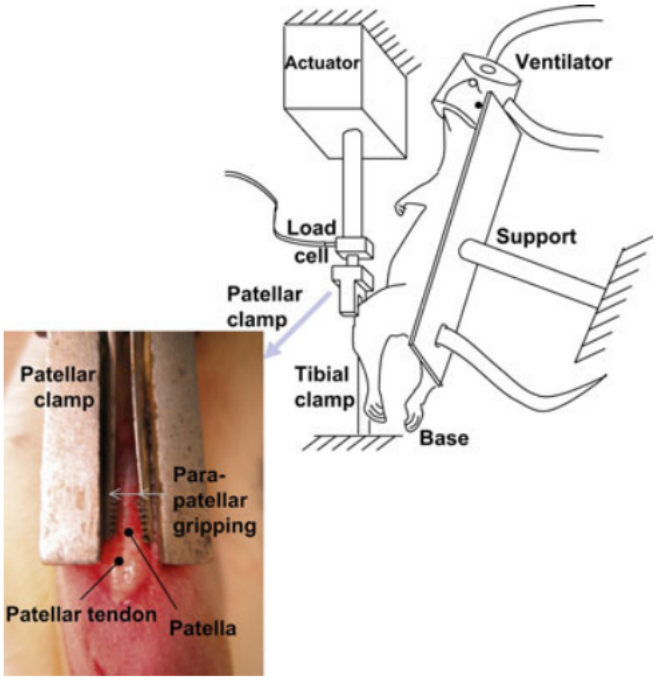


Figure 2.13: Experimental set-up of controlled *in vivo* testing to induce fatigue phenomenon

Unlike the previous models, *in vivo* testing methods enable to represent the native environment of the tendons and its influence on the fatigue effects. The experiments are also most of the time carried out by using animal models for ethical reasons. The interplay between inflammatory cells and mechanical loading can be studied with chemical models, but the most popular methods remain the mechanical ones that induce injuries during cycling loading. Analogously, those models showed the influence of cycling loading on gene expression and protein synthesis regulation, and the presence of inflammatory cells. Moreover, mechanical and biological effects have also been observed during fatigue. In fact, larger tendon size and a reduction of Young modulus and ultimate tensile strength has been observed when repetitive loads have been applied. Similarly, hypervascularity, collagen fragmentation and an accumulation of glycosaminoglycan (a component of the ECM in the tendons) have been correlated with fatigue loading.

Although the influence of the native environment has been taken into account for those models, the results obtained are difficult to reproduce since two native environments from one living being to another are never exactly the same. For this reason, some studies aimed to control the environment of testing by applying specific conditions as in figure 2.13. The animal is anesthetized and placed to a fixed support. The tissue is directly tested *in situ* by a device that controls the movements, in order to assess systematically the tendon mechanisms during fatigue. However, the parallel with human body is not straightforward as the mice locomotion mechanisms are different from human. Nevertheless, all those models helped to understand the impact of fatigue loading on the properties of tendons, and paves the way to further studies.

2.4.3 In vivo-testing with ultrasound imaging

In vivo environment gives different conditions with respect to *in vitro* in terms of humidity and temperature. To show the link between the physiological aspect of the conditions and the mechanical behavior of tendons, Seynnes et al. [68] carried out a qualitative review of the different methodologies for measuring *in vivo* the force-elongation relationship of tendon using ultrasound technique. This approach is very convenient to carry out non-invasive study of the tendon plasticity resulting from

different loading intensities.

To characterize the deformation of the tendons, imaging techniques can be used such as MRI, radio frequency data or ultrasonography. Figure 2.14 shows an experiment using ultrasound imaging that aims to extract the force-elongation relationship of the patellar tendon. The quadriceps and the hamstring muscles are electrically stimulated to provoke an isomeric contraction. The force or the moment are measured at the level of the tibia, and the joint angle measurement in real time is extracted to account for the motion of the knee. A transducer in placed on the knee, aligned with the patellar tendon, for data acquisition. The 2D-ultrasound scan enables to measure the elongation of the tendon and, coupled to the force/moment measurement, gives the desired relationship.

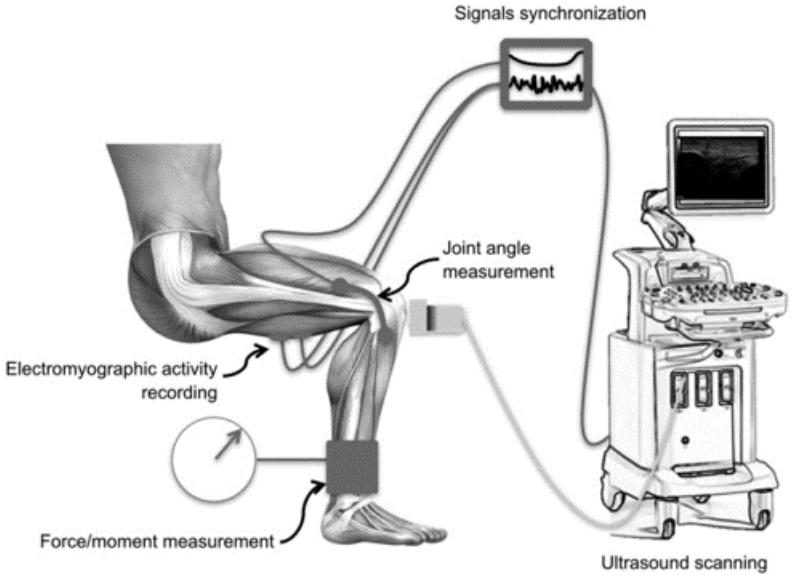


Figure 2.14: *in vivo* force-elongation relationship measurement of the patellar tendon during knee motion. The quadriceps is stimulated to provoke isomeric contraction. An ultrasound scan is performed to measure the elongation coupled to the electromyographic activity

The force transmitted to the tendon is then determined by the transmitted force to the tibia since all elements are assumed to be in series. However, the anatomy and the structure of the knee is very complex, as seen in the previous chapter. This poses several problems to get accuracy in the data, which are difficult to overcome with this method. Additionally, the technique itself presents some drawbacks despite the fact that this is totally representative of the physiological conditions.

Measuring challenges in vivo

As described above, the knee articulation does not constitute a simple mechanical joint. Many tendons and ligaments intertwine, and the structure of the bones as well as the meniscus is complex. As a result, the line of action of the tendon during loading can shift from its rest state, as shown in figure 2.15. Therefore, when the transducer is positioned on the knee before contraction, the measurements can be altered, since 2D-data are generated in the sagittal plane. The displacement is also difficult to quantify during contraction and taking it into account for data processing is challenging. A solution to overcome this consists in acquiring several 2D images from different planes, and use 3D reconstruction to accurately localize the tendon and quantify the elongation, but this poses some constraints during contraction, because the motion is disturbed during data acquisition from different planes.

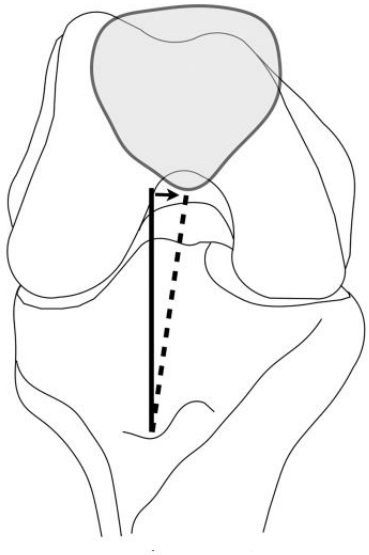


Figure 2.15: Illustration of the shift between the tibia body (solid line) and the axis of the patella apex (dashed line) during quadriceps contraction

Moreover, the size of the transducer can also be a source of errors. In fact, it may be placed in such a way that the displacement at the distal insertion, i.e. at the enthesis, is ignored, considering only the displacement at the proximal insertion, i.e. at the myotendinous region. However, this strong assumption has turned out to be false because the elongation is also influenced by the deformation of the soft tissues and the joint angular rotation. A long transducer utilization will enable the scientists to account for this limitation.

Furthermore, the complexity of the knee joints involves difficulty to catch the morphological features that influence the deformation of the tissues during contraction. As a result, an overestimation of the tendon elongation is possible. In fact, the 3D reconstruction of the image requires a good prior knowledge of the anatomical features. Additionally, morphological changes from one individual to another interfere with this prior knowledge, because the relative motion of the tissues is different. Even if the elongation is based on relative distance between anatomical reference points, this variability makes the elongation difficult to obtain accurately.

Challenges for signal processing and calculation to measure the force on the tendon

Unlike classical tensile tests, the force for *in vivo* testing can only be estimated, which presents the disadvantage of inaccuracy of the computation because of the assumptions made. In fact, the dynamic of the system is reduced to one resultant agonist and antagonist forces aligned along the same direction of the tendon, opposed to each other. In the case of the knee, several muscles act as antagonist muscles, and this simplification is not ensured to be true in this case. Additionally, the muscles of one muscle group work in synergy, which means that one main muscles involves an action and is assisted by the others. This complex relationship is difficult to model, because it is not yet proved that the electromyography of one single muscle represents this synergy. In fact, the amount of force shared by a group of tissues is difficult to predict. As a consequence, the simplification is then too rough and can likely generate errors in the force computation.

Another source of error may come from the image acquisition process itself. In fact, if data are collected from different sources, the constraint of processing time may result in a loss of accuracy

during signals synchronization. Another source of error comes from the fact that ultrasonography constrains the frequency at which images are generated to be much lower than the force sampling frequency. Increasing the number of trials and averaging the data is a way to compensate it.

Finally, the nature of the tendon is such that its properties are history dependent and today, there are no studies that have been able to describe this influence. The resulting high variability among trials, coupled to anatomical differences between individuals, is another important implication to the studies.

Limitation of this technique

The complexity of the human body, both from anatomical and the physiological aspect, poses serious challenges to characterize in a standard way the properties of the tendon. For now, even its resting length is not yet determined in a standardized way. Variability within the same samples due to the history-dependence of the mechanical properties make it very challenging to get comparable results.

The advantage of *in vivo* testing to keep physiological conditions prevents from reaching rupture even for animals for ethical reasons. As a consequence, some parameters such as the ultimate tensile strength have to be estimated, for instance by using curve fitting methods, especially for the plastic region of the force-elongation curve. Coupled to all other error sources described above, this would not give accurate results. Therefore, the use of *in vitro* testing is required to remove out the complexity of the measurements.

2.5 Impact of treatments

2.5.1 Overview of mechanical properties variation due to sterilization processes

There is evidence showing that mechanical properties of the tendons are affected by the type of the process used. Farago et al. [69] reported some studies of different method for sterilization. They compared the Young Modulus of specific tendons for different sterilization processes such as Ethylene oxide exposure, gamma irradiation, supercritical CO_2, Electron Beam or other exposure on chemical substances such as Hydrogen peroxide or chlorhexidine. They ensure that the results were unbiased and that they were based on measurable parameters. Many types of human tendons have been tested separately, such as Achilles tendons, Patellar tendon.

They highlighted some difference in load failure and Young Modulus for a same study that used different parameters for its sterilization process. For instance, a higher gamma irradiation doses reduce significantly the Young Modulus of the tendons tested (Achilles, Quadriceps tendon or Peroneus longus). In fact, the Achilles tendon has been reported to have a Young Modulus of $181.7MPa$ for an gamma irradiation exposure of 18 to $24kGy$ and it drops at $134.75MPa$ for a dose between 38 and $46kGy$. This specific treatment will be detailed further in the next section. Another study showed a drop of 25% of the Modulus of the Tibialis Tendon when it is exposed to an Electron Beam dose between 9.2 and $12.2kGy$ with respect to a dose between 17.1 and $21.0kGy$. Similar observation can be made for load failure in those studies.

The articles described by Farago et al. showed experimental results of same parameters and same tendons. The type of the tendon as well as the sterilization process have a huge impact of the

mechanical properties. However, the data cannot be compared to each other because the conditions of the harvested samples and the environment tests are not perfectly the same. The difference can not be attributed only to the process but we can conclude that all sterilization processes impact the mechanical properties of the tendons.

2.5.2 Impact on tendon after Gamma irradiation exposure

Altered mechanical properties after high dose exposure in dry conditions

As seen before, it has been evidenced that the mechanical properties of the tendon are impacted after Gamma rays exposure. Ren et al. [70] showed a significant decrease in ultimate load and stiffness of irradiated human flexor digitorum superficialis tendons with respect to non-irradiated ones (control group). They used 20 samples (out of 40) from five fresh donors from 26 and 44 years old. While the samples from the control group have been tested immediately after harvest, the ones from irradiated group have been rinsed in phosphate buffered saline solution and stored in packages under vacuum at -80°C until irradiation exposure. This process has been performed on tendons lying in Styrofoam box with dry ice maintaining a temperature between -50°C and -40°C. The dose was equal to 25 kGy for 2.5 hours. The samples have been restored again at -80°C before mechanical tests. This consists in tensile tests with clamps that compress the sample during vertical loading.

By performing a one-way analysis of variance and the Bonferroni post hoc test, the authors found no statistical differences in ultimate elongation between the control group and the irradiated group. However, a significant drop in stiffness and ultimate load has been observed for the irradiated group, which means that the process has weakened the samples. Balsly et al. [71] obtained consistent results with anterior tibialis tendons and semitendinosus tendons as they observed a drop in the tensile strength of the irradiated group with the same dose. Similarly, Conrad et al. [72] showed a drop of stiffness, Young modulus and ultimate stress of irradiated Achilles tendons with respect to non-irradiated tendons (control group).

Despite the impact on the mechanical strength of the grafts, this method is widely used in tissues banks for its effectiveness to eliminate pathogen micro-organisms. A dose of 25 kGy ensures the sterilization but also affects the mechanical properties. This process relies on ionizing radiation that targets the DNA or the RNA of those active pathogen agents that causes damage in DNA basis and sugars, altering proteins synthesis leading to cells death. In the presence of water, the damages to DNA strands are also due to the radiolysis of the water molecules that produces hydroxyl radicals reacting with those strands. The use of irradiation enables to kill those micro-organisms which ensure safety for the patient after transplantation. The loss of mechanical strength has to be compensated with the use of strong tendons such as Achilles tendons or tendons from young donors. [73]

Low dose exposure as pre-treatment

Gamma irradiation in some conditions impacts the mechanical strength of the tendons, but it seems that tendon grafts exposed to a dose less than $15kGy$ prior to any processing steps has no measurable influence of the mechanical strength of the tendon. The study of Cartmell [74] showed that fresh tendons allograft keeps its mechanical properties intact after exposure to gamma irradiation dose of $15kGy$. He used a total of 20 samples, with 10 samples of bone-patellar tendon-bone and 10 samples of gracilis tendon, split into two groups: a group exposed to irradiation and a control group (without any exposure). The tissues were kept its whole form, i.e. they still had adipose and muscles attached, and were not dissected, cleaned nor sterilized, and the tested group have been exposed to gamma rays on dry ice. Then, those tendons were disinfected and stored frozen at - 70°C. All tendons un-

derwent *in vitro* mechanical tests after thaw during night at 4°C and their cross section were analyzed.

For both types of tendons, the author found no significant differences between the two groups in terms of structural or mechanical properties. The absence of complications among patients who underwent an ACL repair using prior-processed tendons support the efficiency of this technique. This could be an alternative of ElectroBeam or more aggressive gamma irradiation process but the presence of important bioburdens could require higher dose or another sterilization process.

2.5.3 Limited impact of Electron Beam exposure

While the use of gamma rays for irradiation process has an impact on the mechanical strength of the tendons in a dose-dependent manner, the Electron Beam method has been proved to have limited impact with specific protocols. Wei et al. [48] observed no significant difference in the mechanical properties between non-treated flexor digitorum superficialis tendons with respect to the ones exposed to fractionated Electron Beam.

The tendons used for this study were harvested from donors from 29 and 47 years old, who do not present any injuries in the forearm nor traces of illnesses markers. Similarly to Ren et al. [70], the samples were lying in a Styrofoam box filled with dry ice. One group were exposed to Electron Beam at a dose of 50 kGy using a 10 MeV electron accelerator. The other group has been exposed, with the same machine, to a dose i-of 2.5 kGy for 32 seconds 20 times (24 minutes for the whole process). The samples have been stored at -70°C for one hour before mechanical testing. The statistical analysis showed a significant impact on the ultimate load and elongation, and stiffness of the tendons exposed to a continuous flow of electrons. While the samples exposed to 20 repetition of continuous electron flow had non significant difference in stiffness and ultimate elongation with respect to the control group. Moreover, it seems that a fractionated exposure has a significant impact on the ultimate load with respect to a continuous exposure, but no significant impact on the Young Modulus has been observed among every groups. The authors came to the conclusion that fractionated exposure to Electron Beam ensures sterilization and keeps the mechanical properties of the tendons which could give better outcomes for tendons repair, which is also confirmed by patients follow-up after transplantation [73].

2.5.4 Long-term impact of peracetic acid treatment

Peracetic acid is a chemical agent used for graft sterilization before transplantation for tissue repair. It has been validated for bone allografts [75] as the strength of this type of tissue is not affected. But tendons are soft tissues that can response differently to this treatment. This is verified by the study of Eras et al. [76] who showed that peracetic acid alters viscoelastic properties of human meniscus transplants.

For this reason, a German study [77] conducted a complete *in vitro* mechanical study using human paired bone-patellar tendons to compare the mechanical behavior of sterilized samples with non-sterilized samples. Cycling loading and load to failure test were performed to analyse the biomechanics and the viscoelastic properties and they found no significant differences, which leads to the conclusion that this treatment does not impact the properties in the short-term.

However, the aforementioned study does not cover the influence of graft incorporation and vascularization on the mechanical properties. This has been investigated with sheep models by Scheffler et al. [78]. They used 16 female merino-breed sheep to assess the influence of this sterilization process on healing and compared the data with the results obtained for 24 sheep receiving a non sterilized

allograft in the scope of their previous study [79]. The long flexor tendon were directly harvested from those animals and immediately stored in sterile bags with ice, then sterilized with 6 hours with a solution containing 2 % of peracetic acid, 96% of ethanol and 2% of aqua ad iniectabila (sterile water). After, the grafts were stored at -18°C in sterile bags before ACL reconstruction. The animals were scarified after 6 or 12 weeks (8 specimens per group) and the whole lower limb was then cut off for testing.

Mechanical testing consisting in drawer test and tensile load to failure tests using a universal machine have been performed to the whole femur-ACL graft-tibia complex. The samples also underwent histological studies to study vascularity and cellularity of the graft. Non inflammatory reactions were found, but a decrease of stiffness and failure load have been observed 6 weeks after implantation. After 12 weeks, a significant diminution of those properties but also stress values have been ascertained. The failures occurred either directly at the graft or by removing from the tibia or the femur insertion. This study provides insight regarding the impact on the healing process after such a treatment, since this is delayed or partially inhibited, but it has to be confirmed with *in vivo* human samples tests. Nevertheless, the impact in short term of peracetic acid on the mechanical properties seemed to be limited, but the healing process can likely be altered by such a treatment. For the patients, the use of this technique ensures sterilization of the tissue but it should require a longer period of rehabilitation.

2.5.5 Ropivacaine administration as a impacting factor

Ropivacaine is a local anesthetic administered to reduce pain after joint surgery but as for peracetic acid treatment, this product may have negative effects on cells lying in the tendons and also on their mechanical properties. To evidence it, Ollivier et al. [80] assessed the toxicity of ropivacaine by testing mechanically fresh human hamstring tendons *in vitro* after having been soaked in a solution containing this product. To do so, they collected 120 segments of this type of tendon from 120 donors and they used two set of tests to demonstrate the effect of ropivacaine on the mechanical properties as well as the influence of the concentration. For the first set, they immersed 30 samples in a 2% ropivacaine solution and 30 samples in a saline solution as specimen control. For the second set, 60 samples were soaked in a solution of this substance : 30 with 2% ropivacaine and 30 with 7.5%. After an immersion of 1 hour, the samples were dried and frozen at -20°C until the time of mechanical testing.

In order to avoid any bias on the results induced by the age, the sex and the level of sport carried before, the authors clustered the samples having similar features together and performed statistical tests on their mechanical properties in order to draw firm conclusions. Hence, they observed a significant drop of the ultimate tensile strength, Young modulus and strain energy (the energy stored because of the strain induced by the test) with the samples soaked in 2% ropivacaine solution compared to the control group. However, no significant difference were detected for the strain at failure. In contrast, they observed an increase of this parameter but also a decrease of the Young Modulus correlated with an increase of ropivacaine concentration, while no significant difference were found in terms of ultimate tensile strength.

They came up with the conclusion that the administration of ropivacaine impacts the mechanical properties as they assume that this substance is toxic for the lying cells that directly mediate the behavior of the tissue under load. Those findings provide some insight on the influence of ropivacaine administration on the tendon strength, but they have to be accompanied by *in vivo* studies to observe the influence of the vascularization of the tissue and its native environment on this effect. Additionally, the remodeling process and the adaptation of ECM and collagen to the exposure to ropivacaine has to be taken into account to further understand the alteration of the mechanical properties. Some

histological and clinical studies may bring new elements regarding this topic.

2.5.6 Mechanical properties of periosteum : a driver for graft stability

Some allografts such as the ones used for Achilles or patellar tendon repair contain a bone block. Therefore, this element participates also in the mechanical behavior of the graft under tensile stress. However, unlike tendons, bones are more prompt to compressive loading so analyzing their mechanical properties under traction is irrelevant. But bones are enveloped by a fibrous soft tissue called periosteum, which shares some similarities with tendons in terms of composition and microscopic structure. Its mechanical properties in traction may play a crucial role in tissue healing process after transplantation like for tendons as discussed previously. For this purpose, Zwirner et al. [81] performed uniaxial tensile tests on this tissue harvested at different location from six human Achilles tendons-calcaneus bone complexes.

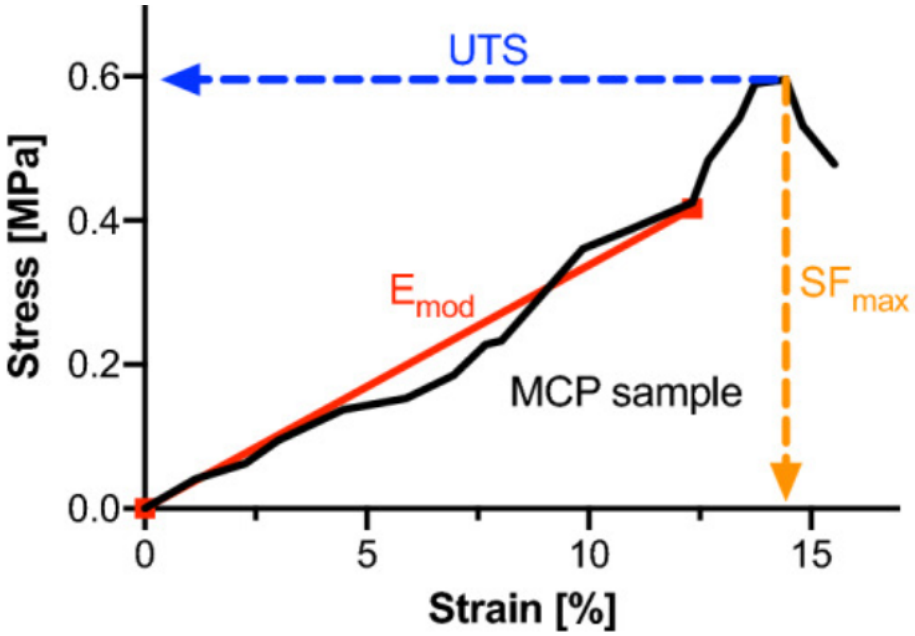


Figure 2.16: Stress-strain relationship of the harvested calcaneal periosteum during load to failure tests

After decalcification and other dissection processes, they retrieved calcaneal periosteum tissues from the bones. The samples were compressed by clamps at the extremities, which were surrounded by a polysiloxane cast to avoid slipping. Elongation were computed by digital image correlation through the speckles patterns drawn with a black pen before testing. The displacement rate was set to 20 mm/min and strain at maximum load, Young modulus and ultimate tensile strength were extracted from the curve plotted in figure 2.16. They retrieved a value of $2MPa$ for the ultimate tensile stress, $16MPa$ for the Young modulus and a maximum strain of 15.5% on average. If we compare those properties with the ones retrieved by Tishya et al. [63] regarding Achilles tendon properties, significant differences can be observed. Although the two tissues are made up of similar components, the Achilles tendon has a Young modulus that reaches $819MPa$ and a maximum strain of 8.8%. This suggests that the constraints are not evenly shared by the two tissues in load, which seems to be consistent since their macroscopic structures are different.

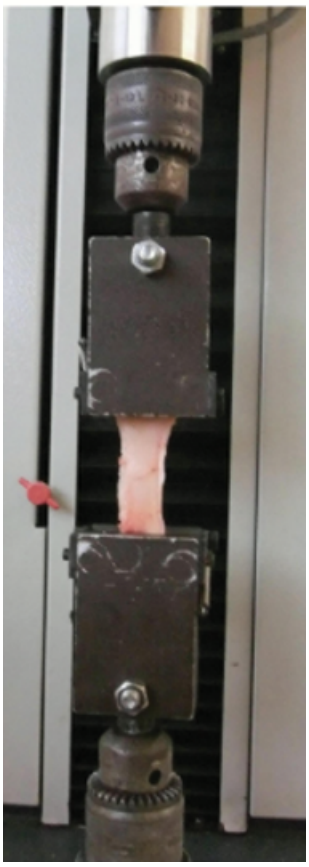
The comparison made before has to be taken with caution as the differences between the two methods may introduce bias in the interpretation. Moreover, disparities in terms of mechanical behavior and structure are also observed within periosteae found on the different bones of the body.

In fact, Kadlub et al. [82] also carried out tensile tests on mandibular and calvarial periosteum and they came up with values of Young modulus between 18 and $70MPa$ on average, which is far from the values in the present study. Nonetheless, a qualitative assess can be made to look deeper into the constraints distribution between two tissues that are similar at the microscopic scale.

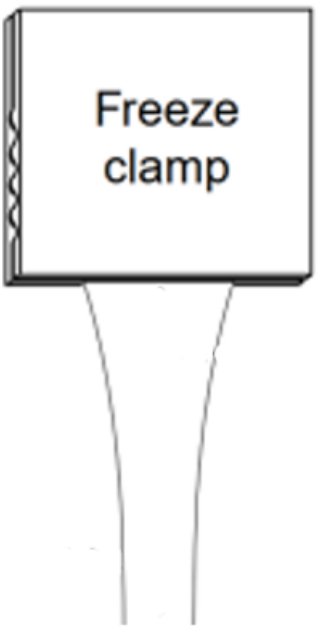
2.6 Overview of the different bits used for *in vitro* studies

As the main objective of this work is to come up with a new model of bits that suits most of the tendons, it is important to look at the types of bits that have been used for tensile stress on tendons in the literature. This section aims to propose an overview of the different models highlighting their advantages and their drawbacks.

As mentioned in section 3.1, the conventional method for securing a sample under tensile stress is to put the extremities between two metallic plates that apply compression as illustrated in figure 2.17. This has been done by Ollivier et al. [80] to study *in vitro* the impact of ropivacaine on the mechanical properties of hamstring tendons. They used a system as shown in figure 2.17a to clamp the free-ends of the tendon and measure the elongation at the edge of the plates.



(a) Classical clamp with two plates bolted together



(b) Freeze clamp variant

Figure 2.17: Clamp systems to lock the free-end tendon

This system prevents the sample from slipping if the plates are sufficiently tightened together, but this induces compressive constraints on the tendon. For metallic samples, this is not an issue because it is a rigid hard material, but tendons are soft and viscous material as explained previously. Therefore, those constraints may weaken the sample and provoke a rupture inside the clamp, which

invalidates the tests. Additionally, the compressive constraints induce deformation on the sample which can alter the measurement of elongation during the tensile test. To overcome this, Tishya et al. used nitrogen-cooled freeze clamp to frozen the extremities of the tendon as illustrated in figure 2.17b. This presents two advantages. Firstly, the frozen area become more rigid which eliminates the tendencies of deformation during compression at this particular area. Secondly, the ice inside the clamp enables a better distribution of the compressive constraints which avoids weakening the sample at the bits. This technique provided convincing outcomes according to some studies [83], but this poses two problems. First, Those clamps are not suitable with samples containing a bone block such as the Achilles samples used for tendon reconstruction (see section 2.3.2). Second, this is not an ergonomic technique in a sense that this requires trained-staff to use it. In hospitals, this would require heavy logistic to use those type of bits.

To overcome the limitation related to the bone block attached to the main body of the tendon, Tishya et al. used a polymer of Polymethylmethacrylate (PMMA) coated with an aluminum layer to embed the bone end of the complex muscle-tendon-bone as illustrated in figure 2.18. The elongation as well as the reference length used for strain computation are measured from the top of the PMMA block.

This solution enables the even distribution of the compressive constraints due to gripping while ensuring stability of the sample during the tensile test. The PMMA has good mechanical properties for such an application. Depending on the polymerization process, the Young modulus of this material can reach 3 GPa [84] which means that it is almost non-deformable during tensile tests of Achilles tendon. The biocompatibility of the material can also be underlined since it can be important for some applications involving non-destructive tests on reusable tendons.

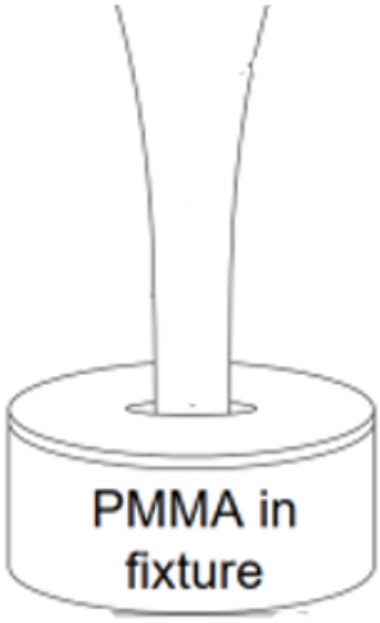


Figure 2.18: PMMA system that embeds the bone block attached to the tendon sample

As for the protocol of Tishya et al., a mix of this system and the one illustrated in figure 2.17b can enable to handle tendon samples with or without bone blocks. However, the fact that the block

is completely embedded may strengthen some regions of the sample, which could induce the rupture to occur in a different region from the natural weak one. This system can actually protect one of the weakest regions in the tendon, the enthesis. While the rupture can be localised there, it could occur elsewhere instead, which will alter the interpretation of the results.

Those systems present some advantages and drawbacks that are not negligible. To go a step beyond those solutions, the objective is to find a bit model that ensures the fixation of the tendon to the testing device without altering its mechanical behavior. For this aim, the present work aims to provide a reliable model that will help surgeons and tissue bank staff to carry out mechanical studies on tendons in order to improve the transplantation delivery system.

2.7 Conclusion

When we look at the mechanical properties of tendons such as Achilles, significant differences are observed in the literature. Those disparities are not only due to the protocol nor the measurement methods. Indeed, they are also due to the fact that the mechanical behavior of the tendons has many random variations from one set of samples to another. Tendons properties are history-depend, which means that the solicitations of the tissue during life has structural and physiological impacts on the tendons because of the cells response to loading. All those elements together make the standard protocol establishment very challenging. This is the reason why the use of textile product for validation of a new tensile test device designed for tendons would be necessary. Nevertheless, it seems that the tendons from the same pair of the same donor has comparable properties.

As explained in the section 2.8, the reduction of discarded tendons can be enabled by the development of new sterilization processes or the improvement of the existing ones. However, this chapter reported some studies that showed the impact of the mechanical properties of some treatments, which could be a serious issue for tissue banks. Therefore, the development of a new system of bits would help scientists to perform mechanical tests on tendons after treatment in order to systematically assess a new protocol of sterilization.

Overall, the main challenge in characterization of the mechanical behaviors in biological tissues, especially tendons, is to extract standard features. As said before, many factors can influence the properties, but even when the conditions are controlled as much as possible, variability can be observed. Indeed, Seynnes et al. [68] reported a difference of 30 % of measurements of the stiffness of the patellar tendon of comparable population with similar testing protocols. Moreover, disparity up to 37% in Achilles hysteresis are also observed in the literature review. Despite, mechanical testing enabled a better understanding of the properties of the tendons and to highlight the influence of decontaminating processes on the mechanical strength of the tendons.

Chapter 3

Mechanical design of the bits

The objective of this project is to be able to carry tensile stress on tendons through a system of bits that will enable to extract relevant features specific to the tendon. To test and valid the design, *in vitro* traction tests will be performed with a classical hydraulic machine. The tests will be destructive-type and the mechanical behavior of the samples through the whole experiment will be analyzed. This will require appropriate bits that fix the tendon for the tests. In this chapter, the mechanical design of the model will be processed.

As seen in the section 3.1, the main way to hold the samples is to clamp it at the extremities. This technique applied to tendons is developed in this chapter, and other alternatives are also proposed. The most convenient system will be determined based on the specifications that are listed in the first section of this chapter, and some mechanical analysis will be carried out to dimension it. The Software used for the design and the simulations is SolidWorks 2022. Finally, a model of bit will emerge and could bring part of the solution of the expansion of the availability of tendon grafts as explained in the introduction.

3.1 Specifications of the system

As seen in the state of the art, the bits that have been covered were suitable for a few types of tendon, either Achilles or patellar tendon among others. To go a step further, the first specification to be determined is the ability of fitting the tendons of interest, with both free or bone extremity. Thereby, the tests could be performed with a large amount of sample-types for some studies.

Secondly, the bits have to be compatible with the traction machine that will be used for the tests. The system has to be in continuity of the machine to perform valid test and should not be bulky. Users should not require any training or specific qualification to be able to use the system.

The bits have also to ensure the sterilized environment for the tendons. The materials in contact with the tendons must remain inert when the samples are placed in order to prevent interference with the biological properties of the tendons. Thus, this requires a specific choice of the material, which will be developed in further sections. Despite the fact that the tests are destructive, the sterility is not a priority for this study, but the validation of the model with a compatible material opens the door to further development.

Finally, the most challenging specification is to design a bit that will not induce rupture nor instability of the sample at the area of gripping. It cannot slip or fall off the bits, and the rupture location of the sample should not be correlated with the design of the model. That will have an

influence on the choice of the system.

3.2 Attachment by drilling

One solution to gripping the samples consists in drilling holes on a limited area on the extremities and gripping the samples with rods that pass through them. Figure 3.1 shows the first prototype that has been imagined and designed. It consists of a parallelepiped rectangle-like support fixed to the traction machine, and three titled rods at 45° to the direction opposite to the traction. The rods are inserted to the extremities of the tendon. Depending on the size, the shape, the type and the consistency of the sample, all or some rods can be used to hold the tendon.



(a) Drilling solution (top view)

(b) Drilling solution (3D view)

Figure 3.1: Drilling solution

3.2.1 Invalidation through Finite Element methods

This solution could enable to deal with several types of tendon and to elaborate a protocol depending on the size of the sample. In fact, it can be assumed that the longer is the tendon, the more holes can be drilled to fix it depending on its thickness and strength. Additionally, this model could fit a tendon-bone complex as the one shown in figure 3.2. This allograft corresponds to a leg tendon scanned in its sterile jar in the tissue bank of Saint Luc hospital. For the tensile tests, the block bone can be placed between the titled rods, which can also be inserted through the tendon tissue. Moreover, the solution could require short length needed to grip the samples which could potentially provide a longer portion of the tendon where the deformation can be measured.

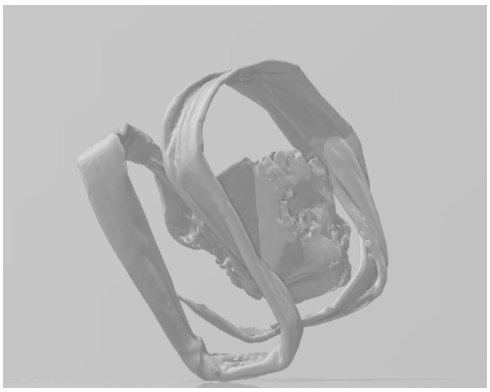
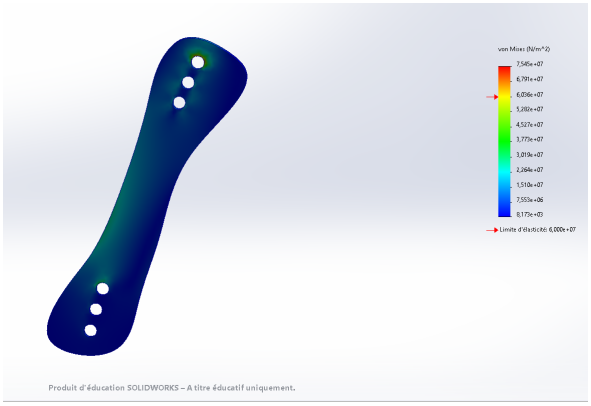
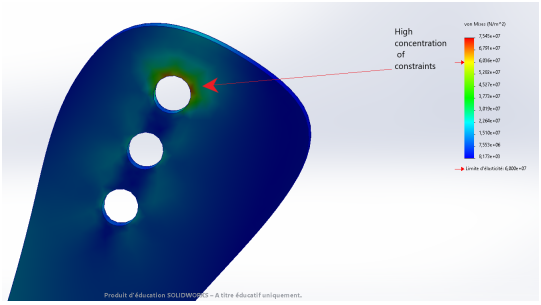


Figure 3.2: 3D scan of a leg tendon from the tissue bank of Saint Luc Hospital

However, several problems are encountered with this solution. In fact, samples with a short width can potentially be impossible to fix correctly and induce tears-off at this particular area of the tendon. Even for the strongest tendons of the body, such as the Achilles tendon, embrittlement at the gripping device could be observed, as evidenced in the simulation pictured in figure 3.3. This simulation has been performed on a sample that has the shape of this particular tendon (3.3a) and that has the same properties as the ones retrieved by Tishya et al. [63]. As the tendon material is not referenced in the data based of Solidworks, the material that has been set in Nylon 101 because its mechanical properties are close to the one of the tendon. The sample has a length of 15 cm and a width of 10 mm, and three holes of a diameter of 3 mm have been drilled at each extremities, separated by 10 mm from each other.



(a) View on the entire material



(b) Zoom on the zone of high concentration of constraints

Figure 3.3: Simulation of tensile test applied on the Achilles tendon drilled by the device

Based on those assumptions, a mesh composed of 16,641 nodes inside 10,185 elements has been automatically generated by Solidworks. Each element has 16 points and has a size ranged from 1 to 3.5 mm. The mesh has been connected following the curves of the sample. An arbitrary force of 4000N has been applied axially, which is a value below the failure force reported by Tishya et al., on the top three holes. The bottom half of the three holes at the other extremity are set to be fixed. By running the simulation, we observe that the constraints are mainly concentrated on the edges, but also at the top three holes. For the highest one, the constraints exceed the yield stress (represented on the scale by the red arrow) which means that permanent deformation occurs at this particular area. Since the force does not reach the failure force of the Achilles tendon, it is likely that tears will appear in those areas in yellow and red with higher value of force, followed by an early rupture. This simulation evidenced the fact that holes on the sample will clearly weaken it which increases the risk of failure at the bits. Although the material is not completely faithful with the tendon, the

results are still relevant and provide an objective reason to discard this model.

3.3 Attachment by compressing

A system that compresses the extremities of tendons can prevent the weakened regions that may occur in drilled samples. But it may also induce pre-constraints on the extremities, which can weaken the sample. Therefore, it is necessary to find ways to compensate for any negative effects caused by such pre-constraints. For this purpose, several solutions are listed bellow.

3.3.1 Cylindrical arrangement with frozen-water

To avoid to have weakened points on the sample and a risk of rupture at the gripped areas, constraints perpendicular to the axis of the sample have to be applied to a large enough area to evenly distribute the constraints. One way to ensure this is the use of frozen water in a cylindrical configuration, as shown in figure 3.4. The principle consists of a cylinder semi-closed in which the extremity of the tendon is inserted. The sample can be either bone-ended or free-ended. If the latter case, the sample can be coiled around a dowel pin and clamped as shown on the left of the figure. The bone-ended sample can stop on the semi bottom cover and is then blocked in the direction of the traction. The cylinder is filled with water that is then frozen by immersing it in liquid nitrogen at -200°C.

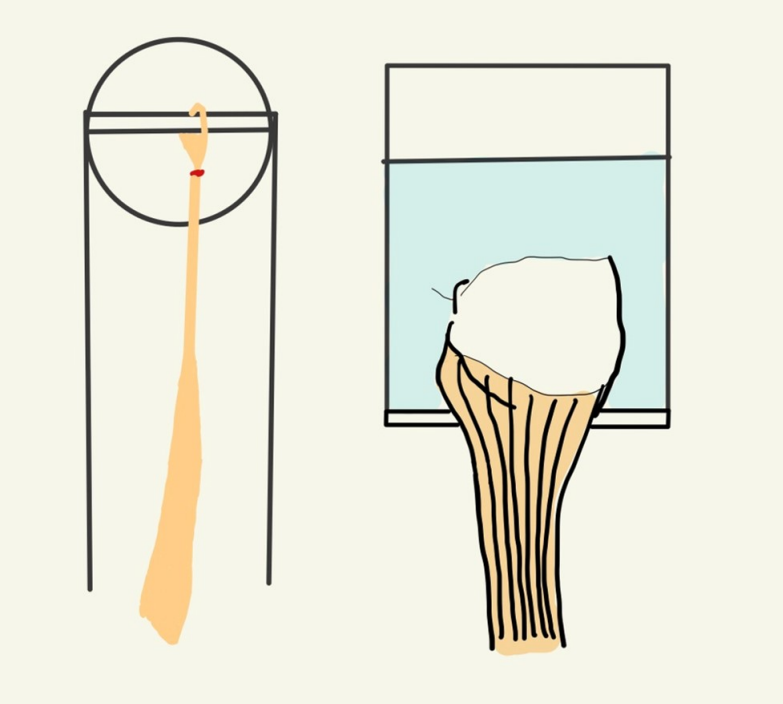


Figure 3.4: Cylindrical configuration with frozen nitrogen

The advantage is that this technique is very resilient in the sense that all sizes and extremity types fit in since the water follows the shape of the area of the sample that is inside the cylinder before freezing. Moreover, the frozen-water ensures to disperse the stress due to gripping and the semi-cover at the bottom or the clamp prevents the sample from slipping on the axial direction, which could invalidate the tests.

However, Nitrogen is a dangerous substance and requires some cautions. In fact, nitrogen presents risks for users of frostbite which can lead to ice crystal formation around their tissues and results then in blisters, frozen muscles or bones or even nerve damage that can require an amputation [85]. Those risks are very high with nitrogen at -200°C.

In addition, This substance is odorless and colorless, and is in equilibrium with air when it is in contact. Thus, air can be nitrogen-saturated which can provoke hypoxia to any individuals around if the airflow is not renewed. It requires thus strict rules for ventilation and nitrogen quantity in the room [86]. It has also a risk of explosion due to the increase of the pressure with the heat provided by the air when the system is immersed in the liquid, which can lead to fire in the laboratory [87].

Although this technique suits some specifications, liquid nitrogen presents high risks of operation and requires strict cautions and qualified staff for the tests. This causes a problem of simplicity and safety for an advanced developed traction system. Additionally, even if we find another substance than nitrogen to freeze water, mechanical properties of the tendon can be altered due to temperature change. In fact, the tests should be performed in a controlled environment (temperature) which is difficult to ensure with such a cold system. Therefore, this technique has to be abandoned.

3.3.2 Cylinder arrangement by compression with two plates

The compression of the free-ends of the tendon reduces the constraints on the sample compared to the drilling solution. However, those compressive constraints are not sufficiently annihilated. In fact, they induce a high force intensity perpendicular to the axis of the tendon in order to create friction that holds it and prevents from moving. One way to compensate it is to get inspiration from the design of some machines used for the traction of the textile tissues as described in section 3.2. In some setups, the fabric is wrapped around a cylinder and sutured at both ends in order to ensure fixation. As the tendon is a viscoelastic material, it can be folded and wrapped around a similar cylinder as the one shown in figure 3.5. Instead of sutures, tendons can be hold by compression at both ends. The clamping can be induced by two semi-cylinders sliced at the center of the main mechanical body. Both pieces can be then screwed to compress a portion of the tendon, and the outer surface can enable the coiling. The combination of those principles can ensure a stable fixation of the sample while reducing the compressive constraints. The idea seems to be promising and can be a base for further analysis.

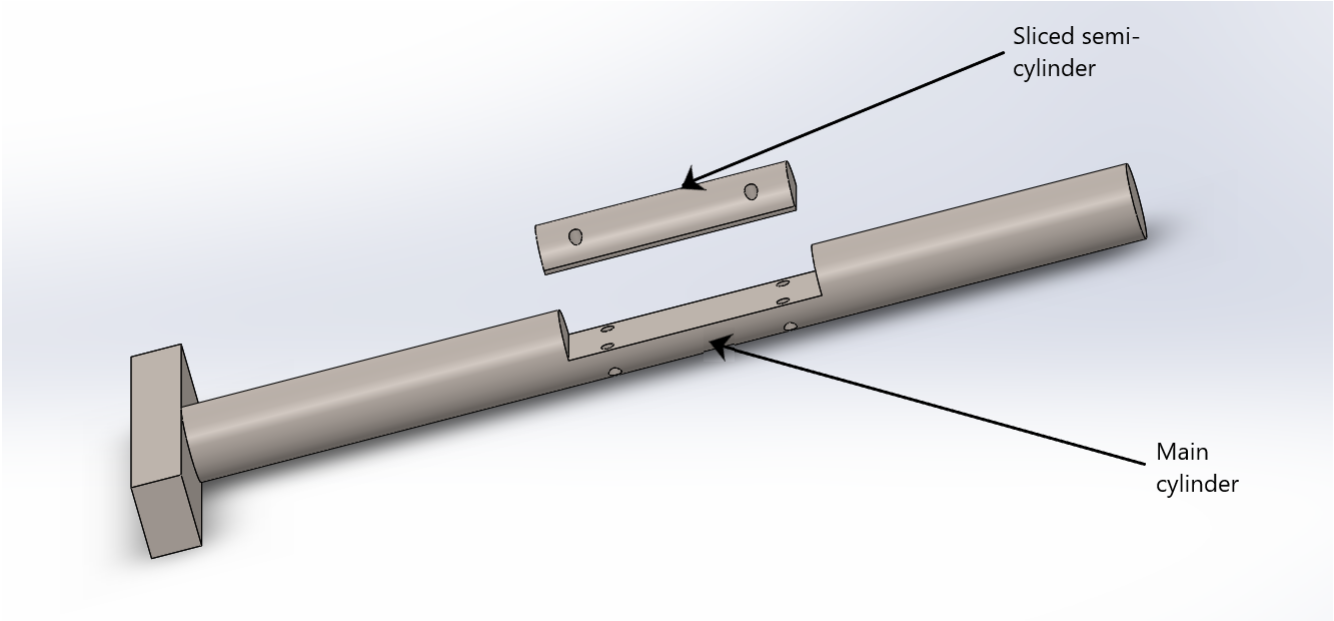


Figure 3.5: 3D-view of the proposed design with cylinder sliced at the center for clamping the sample

3.3.3 System to lock the cylinder

The idea described above presents the advantage of distributing evenly the gripping constraints. After placing the sample, the cylinder needs to be locked in order to prevent any movements of the device which could potentially interfere with the results of the tensile tests. Two degrees of freedom have to be blocked : the translation in the direction of the cylinder axis and the rotation around this axis. Some solutions that could suit the requirements are described bellow.

Connecting rod-crank system

A simplistic assumption can be made on the linear movement as it can be considered that the cylinder is held by two pillars that impede the cylinder from translation at all times. To prevent the main cylinder from rotating, a proposed model consists in converting the rotation into a linear movement and using the principle of clamping to immobilize the system. This can be executed by a crank-rod mechanism similar to the one used in car engines. Figure 3.6 shows the system designed for this purpose. Several pieces are assembled together to provoke a translation of the slider thanks to the connecting crank that converts the motion. The slider can be blocked by clamping on the guiding rails through screws and bolts. When the final position of the cylinder is reached, the screws and bolts can be tightened on the rails which provokes an immobilization of the whole mechanism. To match the angular position of the cylinder with the linear one of the slider, needles have been added but are not part of the bits design. The relative needle is integral with the main cylinder and indicates the angular position as it rotates. This is compared with the reference needle attached to a fixed cylinder coincident with the moving one.

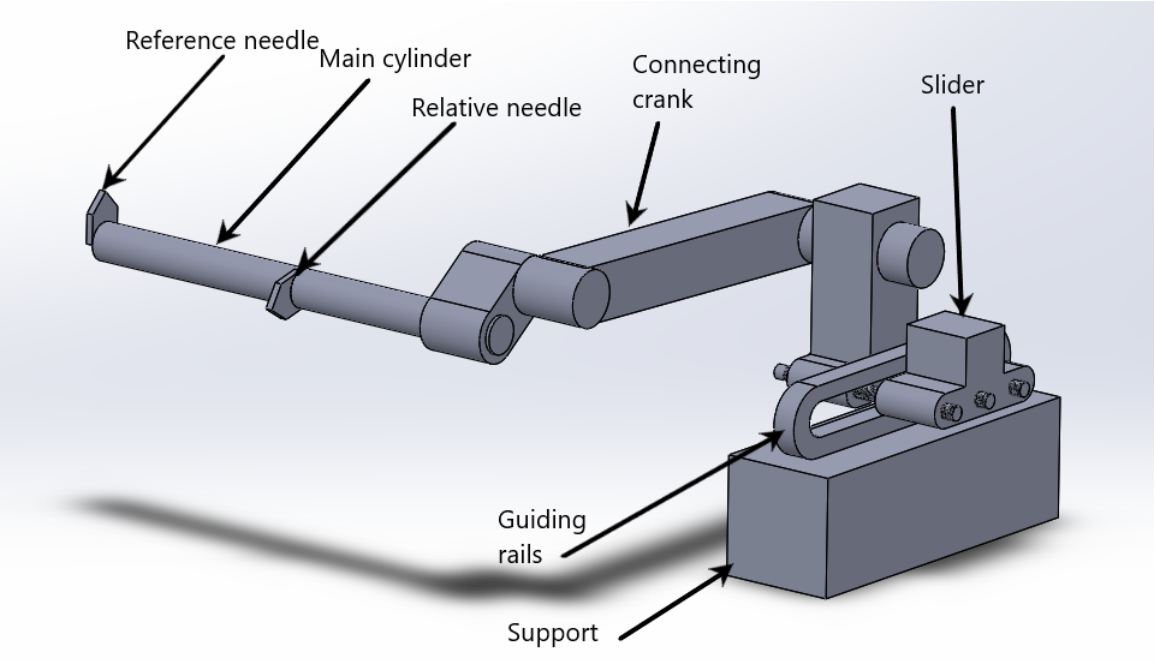


Figure 3.6: Design of the complex rod-crank system that locks the rotation

The proposed system can be highly versatile as the final position of the cylinder is continuously adjustable. In fact, there is no preset positions as the locking principle lies in the friction on the rails. This flexibility in the final set position can contribute to meeting the requirement of the suitability to all possible types of tendons. However, several problems regarding the design are encountered. First, two copies are needed for each ends of the sample, which would take a lot of space in the device. The system would become too bulky compared to the added value of such an external element. Secondly, the system is very complex and is likely to induce several torques on its sub-elements which has to be compensated. This would even complicate the system and make it impossible to produce. The bits would be not ergonomic and a disproportionate amount of materials would be needed only to hold a small sample of tendon. Therefore, the development of this locking system is abandoned.

Friction screws

To reduce the size of the model while preserving its versatility, a proposed solution could be the use of friction screws. This type of screw are engineered to generate a frictional force when they are tightened against a moving surface in order to keep it in position. This much more compact solution does not require to convert the rotation into a translation and can also contribute to locking the linear movement of the cylinder along its axis. Figure 3.7 shows the locking mode that is proposed for this solution. The screw turns above the cylinder and enter into contact with it which creates friction to lock it. Several screws can be placed along the axis of rotation to enhance the locking system.

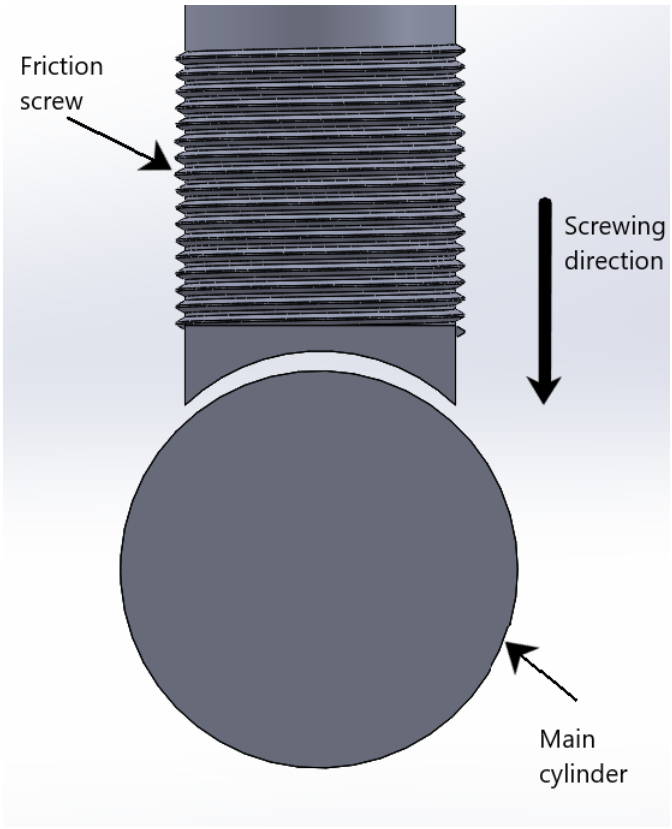


Figure 3.7: Example of friction screw used to lock the rotational movement of the cylinder, all designed with SolidWorks

Although the simplicity and the versatility of this solution is very well optimized, two problems are encountered : First, the small surface of contact between the screws and the cylinder results in insufficient friction being generated which could finally induce movements. In fact, if the Achilles tendon is tested, force magnitudes up to 5500N can be generated perpendicular to the cylinder axis. As the tendon is expected to be coincident with the cylinder, it could generate torsion, as covered further in this chapter. Therefore, it would require a high amount of friction force to prevent any motion during the tensile tests which is possibly not ensured by the use of friction screw. Secondly, the efficiently of the mechanism depends also on the quality of the surfaces in contact. In fact, users have to ensure the absence of any contaminants that can diminish friction such as oil or dust, or even water, which is clearly present in the context of the tendon use. This would require several procedures for the tests performed in a clinical environment which can be not handy in practice. Additionally, roughness of the materials has to be perfectly tuned at the machining process in order to provide a friction coefficient sufficiently high. This can be difficult to reach in real life. Third, the locking ability is likely to degrade over time as the quality of the surface is affected after each use. Consequently, the use of friction screw is not a long term efficient solution to lock the system.

Dowel pin

To ensure sufficient contact with the cylinder to lock its rotation, holes can be drilled across the cylinder and the pillars that hold it, and a dowel pin can be inserted inside. Figure 3.8 shows an example of the dowel pins that can be used for this solution. It only consists of a simple mechanical component that is inserted inside the drilled cylinder. The areas outside can be in contact with a fixed object such as the pillars holding the cylinder in order to immobilize the system. This would enhance stability as no movement are generated (both rotation and translation) when the dowel pin are inserted, and improves also the load distribution across the connected components. The force that the system can bear can be thus higher while keeping the cylinder fixed. Additionally, this solution

is a cost-effective method as the design is simple and widely available. It offers also the simplicity in assembling and disassembling though the whole tests that will be performed on several tendon samples.



Figure 3.8: Example of Dowel pins used in the industry

However, the gain in stability comes with a cost of the flexibility in the desired positions of the cylinder. In fact, one hole across it enables two final positions at 0° and 180° and there are no intermediate ones. This lets us a reduced fine-tuning possibility when the tendon is wrapped around the cylinder. Moreover, the system requires a high level of machining precision as all elements have to fit with each other with a very tight tolerance. As before, the continuous use of the system may results in wear that could lead to deformations of the different components. As a consequence, loosening can be more important between the pillars and the cylinder which can provoke some movements in between. Despite all those disadvantages, the design can be kept for further consideration in the design process.

Shaft support with hose clamp

In order to keep the freedom in the set positions of the cylinder while ensuring the stability of the system during the tensile test, an alternative solution would be the use of a shaft support with hose clamp as shown in figure 3.9. The component is fixed to the support and the cylinder lies at its extremity inside the main hole. When the desired position is reached, the lever is pulled and locks the cylinder by tightening the hole. Friction holds the cylinder with a high surface contact. Unlike the friction screw, this mechanism offers the stability during the tensile tests and is also easy to implement, assemble and adjust.



Figure 3.9: Example of shaft support with hose clamp equipped with a clamping lever proposed by Misumi

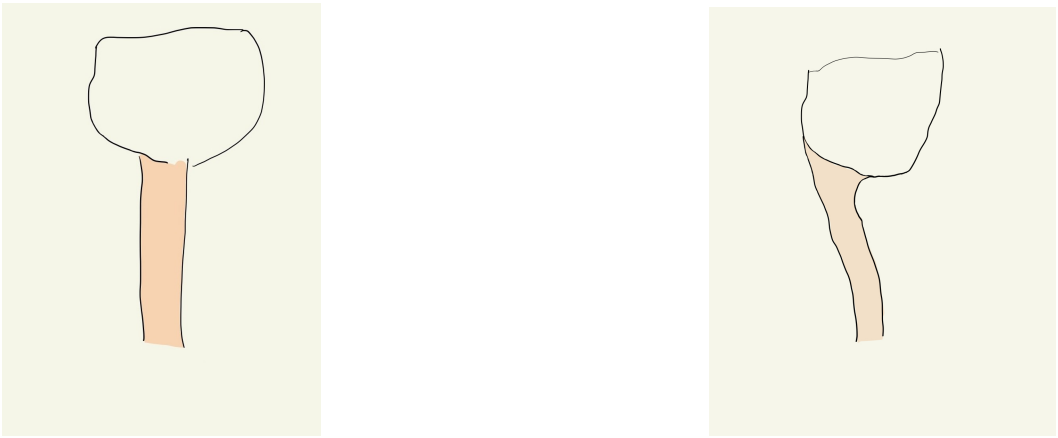
As for the other mechanisms, wear due to continuous use of the device may affects the surface finish influencing the friction generation and the locking effectiveness. Moreover, the surface needs to be dry and cannot be exposed to oil or water as the friction coefficient may be reduced. Furthermore, the surface contact between the shaft and the cylinder can be too large to enable the rotation of the cylinder even without tightening. In fact, the metal-to-metal contact may naturally induce high friction which could affect the ability of rotating the cylinder. To prevent this problem, a high level of precision is required to ensure a fine tuning of the dimensions in order to fulfill the desired function. Nevertheless, this solution seems to suit the requirements and could provide effective results, but a study in torsion has to be carried out to dimension the system.

3.4 Added grippers to bone extremity

The clamping cylinder system described previously is a good solution for free-ended tendons but an extension of the model is required to include the samples with a bone-block attached at one end. To be faithful with the physiological direction of the tendon traction, a good solution consists in gripping the bone around the tendon and let the soft tissue follow the direction of the solicitations. This can be done by simple grippers attached to the same support as we will develop further in this section.

3.4.1 Type of bone insertion to consider

Before starting the design of the grippers, it is important to look into the bone insertion types. In the context of tendon repair surgeries, the provided grafts with a bone block are widely used as explained in chapter 1, and the geometry of the bone-tendon complex differs from one graft to another. In fact, we can find two types of insertion as drawn in figure 3.10. The tendon can be inserted at the center of the bone block (3.10a) or tangentially to it (3.10b) such as the Achilles tendon graft. This has an influence on the design of the grippers as they have to suit both type of insertion. In fact, the contact surface has to be adapted to the geometry of the sample in order to ensure stability of the system.



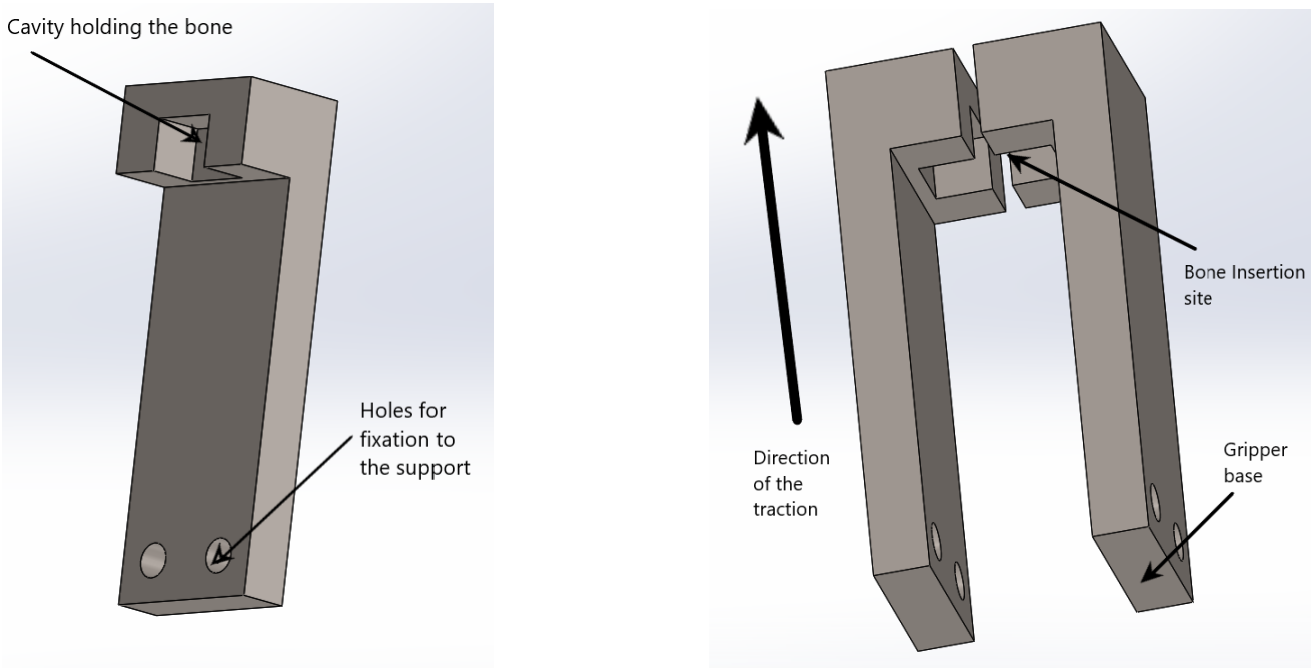
(a) centered tendon-to-bone insertion configuration

(b) tangent tendon-to-bone insertion configuration

Figure 3.10: tendon-to-bone insertion configurations

3.4.2 Adapting gripper configuration

The consequence of those two type of gripping is the requirement an adapting system. The first element to consider as a base is a gripper system for central-bone insertion. In order to be as close as possible to the configuration of the physiological solicitation, the system that is proposed in figure 3.11 enables to hold the bone only and let the tendon lie between the grippers in the configuration in 3.11b. This component designed in 3.11a is composed of a square cavity inside which the bone gets in contact with the inner surface. The gripper is fixed to the support perpendicular to its axis with screws or dowel pins.



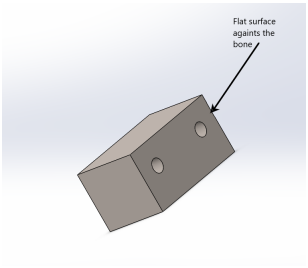
(a) 3D-view of the grippers used to hold the bone block

(b) 3D view of the system configuration

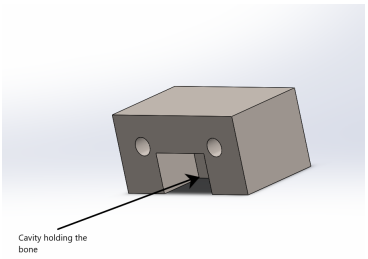
Figure 3.11: Design of the grippers configurations

To fit both insertion types, the design of the grippers has to be more versatile. In the case of centered insertion type, the bone-block can be inserted inside both cavities of the grippers. But for the tangent insertion type, only one cavity is needed to hold the block, and a flat face can come

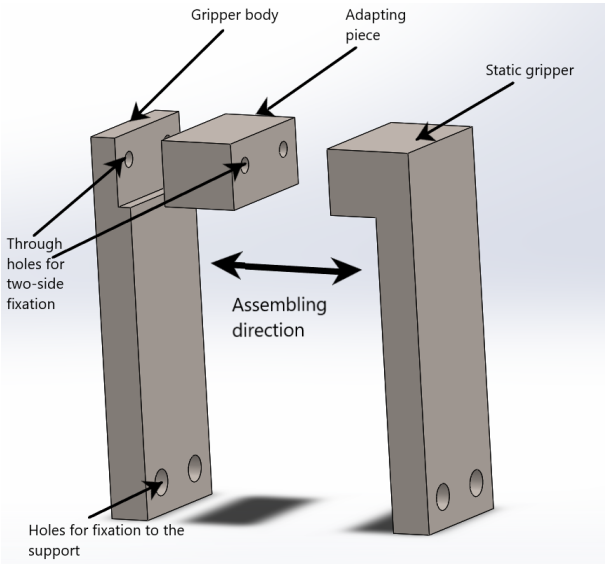
into contact with the tangential insertion area on the other side of the block. To enable both cases in the same design, a proposed idea viewed in figure 3.12 consists in splitting one gripper into the main body and an intermediate component. This one has a flat side (3.12a) and a cavity (3.12b) on the other side that can be both in contact with the sample. Through holes are drilled and aligned with the main body of the gripper to which it can be attached from each sides. The assemblage is aligned with a static gripper (3.12c) and gives two possible configuration with the same components.



(a) Flat face view of the intermediate component



(b) Cavity view of the intermediate component



(c) Assemblage view

Figure 3.12: 3D view of the designed grippers. The intermediate piece is aligned with both grippers and enables both configurations

This model of grippers presents the advantage of versatility and keeping the physiological direction of the traction of bone-ended tendons. This would show the behavior of such a sample and highlight its strongest and weakest zones. Those grippers can be attached to the same support as for the cylinder, and the user can assemble one model or another depending on the sample type. However, one limitation of this design is the fact that the contact surface between both materials can be irregular giving the fact that the bone block does not have flat surfaces. This can provoke a high concentration of the constraints on the bone during traction and lead to local deformation. This problem is not encountered with the use of PMMA (see section 3.6) but it still offers the advantage of simplicity as the PMMA requires additional processes to give the shape of the hold sample. Since the bone-block is a hard material that withstand relatively high constraints in compression, the potential damages caused by the grippers on the bone should not be significant. In fact, we can assume that the weakest region of the tendon-bone complex is not localized in the bone if the sample is correctly treated. For destructive tests, the proposed system should be suitable and can be conserved for further studies.

3.5 Two merged systems outcome

The two subsystems described above can merge and give one model of bit. Figure 3.13 shows the combination of them, giving a prototype that has been chosen for further analyses. The main support holds the pillars that bear the rotating cylinder with the semi-cylinder cover and the clamping site in between. The main cylinder is expected to be immobilized by dowel pins inserted inside the pillars. For the bone-end extremity, the pillars-cylinder complex can be removed out and the grippers are placed inside the grooves at the center. They are attached to the main support also with dowel pins. It has to be noted that the solution of fixing the cylinder with dowel pins is kept for further studies, but the use of a shaft support is not excluded in place of the pillars.

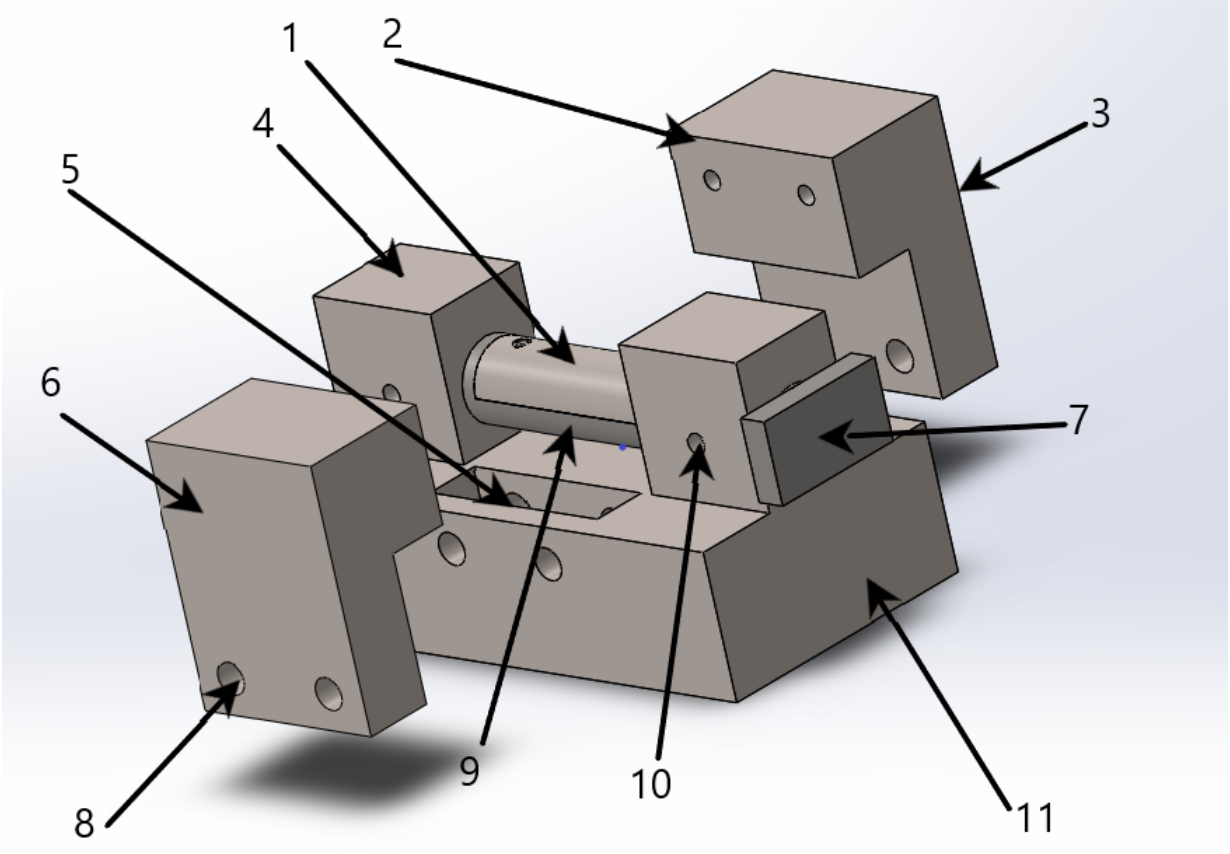


Figure 3.13: 3D-view of the merged model of bit. 1: Semi-cylinder that clamps the free-end of the tendon before coiling. 2 : Detachable hybrid piece with flat face and cavity on the other side. 3 : Hybrid gripper assemblage. 4 : Pillars holding the rotating cylinder. 5 : Groove for the fixation site of the grippers. 6 : Simple model of gripper with cavity. 7 : Handle to facilitate the manual rotation of the cylinder. 8 : Through holes for the dowel pins fixating the grippers to the support. 9 : Main cylinder with a flat surface at the center for the clamping site. 10 : Through holes for the dowel pins immobilizing the cylinder during the test. 11 : Main support attached to the traction machine.

The model shown in figure 3.13 is adaptable for both bone-ended and free-ended samples, and the principle of coiling enables to deal with several size of free-ended tendons. The clamping system offers the ability to hold the tendon and ensure stability like the system shown in section 3.6 (figure 2.17) but instead of frozen clamp to reduce the compressive constraints, the coiling system around a metallic component is preferred. This has the advantage of simple usage and does not require heavy facilities to perform the traction tests. The whole principle is expected to ensure stability of the samples in traction but the whole design has to be assessed by prototypes and simulations.

3.6 Prototyping with a 3D-printed model

After completing the mechanical design on SolidWorks, a prototype needs to be built for the purpose of design validation. It has to be noted that some simplifications are made. First, the Shaft support with hose clamp is not modeled, and is replaced by simple pillars at both ends of the cylinder. Second, the pieces are not attached to each other as the screws are not used with the material of the prototype. Third, the dimensions of the system are approximated and sometimes overestimated based on the efforts applied on the different components. This process aims to assess the different features of the design, and further studies will be carried out for fine-tuning.

The technique used to enable several iterations in a low cost way and in a short time is the 3D printing, especially with the technique of Masked Stereo-lithography Apparatus (MSLA) [88]. This one is preferred to Fused Deposition Modeling (FDM) because we have to handle irregular geometry with holes that require a certain resolution. Figure 3.14 shows the principle. A plate containing the model is bonded to a LCD screen. This is exposed to a LED light that emits UV rays to polymerize the layers of resin to form the object. Then, the platform on which the object is glued is rinsed with 95% ethanol to remove non-polymerized resin. Residual ones are removed by exposing the object to UV rays during 20 seconds. This process can be repeated several times to create prototypes with different scales and parameters to validate the model.

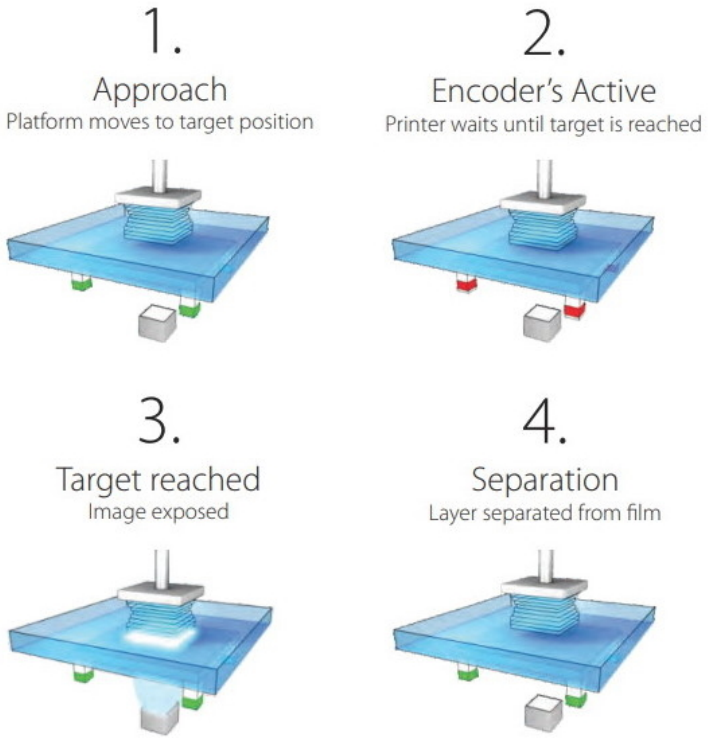
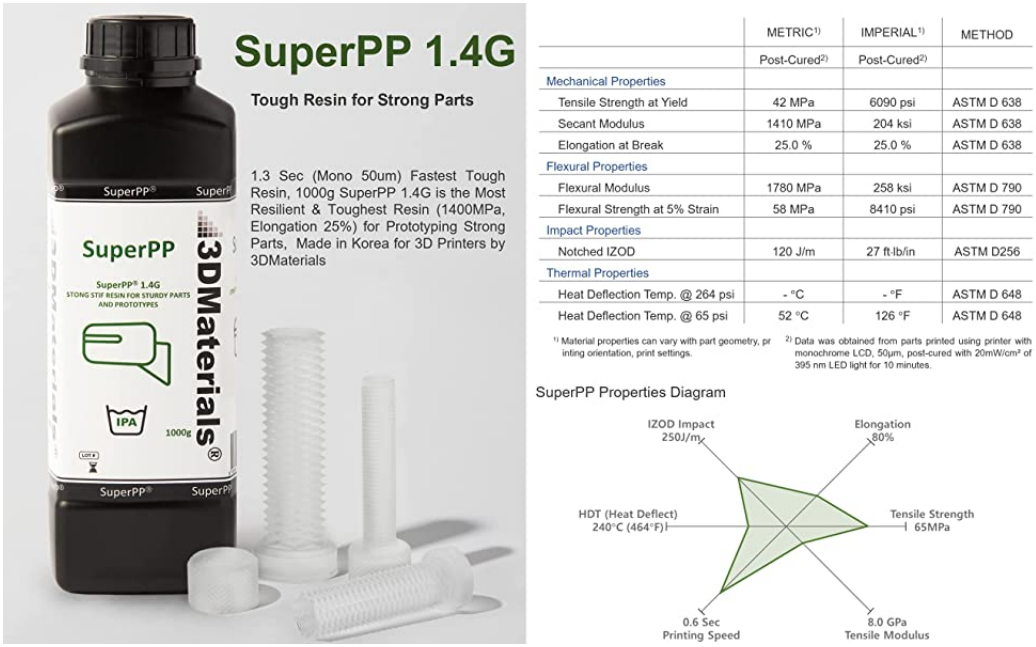


Figure 3.14: Illustration of the principle of the MLSA 3D-printing technique used for prototyping

The 3D-printer used is the Photo MonoX that has a pixel size of $50\mu m$. Photon Workshop V2.1.29.RC12 software enables us to set the parameters of the printer and reorient the different parts of the model in order to ensure a high quality of the prototype. The resin used is Super PP Superfast produced by 3DMaterials (Figure 3.15 [89]) because of its properties. In fact, we need a rigid and solid resin to withstand traction in the cylinder, even though the tests do not reach a high constraint. The tensile stress of this resin is equal to 42 MPa and does not elongate that much (25%) at the rupture. Therefore, the mechanical properties of this resin are closer to our application than many others and can enable to create a relevant prototype.



	METRIC[1]	IMPERIAL[1]	METHOD
	Post-Cured[2]	Post-Cured[2]	
Mechanical Properties			
Tensile Strength at Yield	42 MPa	6090 psi	ASTM D 638
Secant Modulus	1410 MPa	204 ksi	ASTM D 638
Elongation at Break	25.0 %	25.0 %	ASTM D 638
Flexural Properties			
Flexural Modulus	1780 MPa	258 ksi	ASTM D 790
Flexural Strength at 5% Strain	58 MPa	8410 psi	ASTM D 790
Impact Properties			
Notched IZOD	120 J/m	27 ft-lb/in	ASTM D256
Thermal Properties			
Heat Deflection Temp. @ 264 psi	- °C	- °F	ASTM D 648
Heat Deflection Temp. @ 65 psi	52 °C	126 °F	ASTM D 648

[1] Material properties can vary with part geometry, printing orientation, print settings.
[2] Data was obtained from parts printed using printer with monochrome LCD, 50µm, post-cured with 20mW/cm² of 395 nm LED light for 10 minutes.

Figure 3.15: Properties of the SuperPP resin

3.6.1 First trials with low scales

The really first iteration in the process aims to enable us to tune correctly the parameters of the printer. Table 3.1 contains them for the two first trials. Normal exposure time is related to the exposure to UV rays per layers. The off times is the time during which there is no incoming rays on the constructing object after the exposure. Bottom layers require particular attention because it is precisely the location of the fixating area to the plate. Therefore, we need to tune a specific exposure time for a given number of layers to ensure the fixation, the time thus has to be longer.

	1st trial	2nd trial
Layer thickness (mm)	0.05	0.05
Normal exposure time (s)	1.8	2.0
Off Time (s)	0.5	0.5
Bottom Exposure Time (s)	10	30
Bottom Layers	4	4

Table 3.1: Parameters of the printer for the two first prototypes

It has to be noted that the model has been modified in order to reduce the amount of resin that we use and to make the process easier without affecting the mechanical function of the device. In addition to the modification explained before, the threads where the elements are expected to be screwed have been removed. Moreover, materials have been removed from the support because it does not have to be thick at this stage. Therefore, some holes have been drilled in the corners and at the extremities behind the pillars that hold the cylinder (Figure 3.16). For the first versions, the handle has been removed in order to assess the ability of rotating the cylinder.

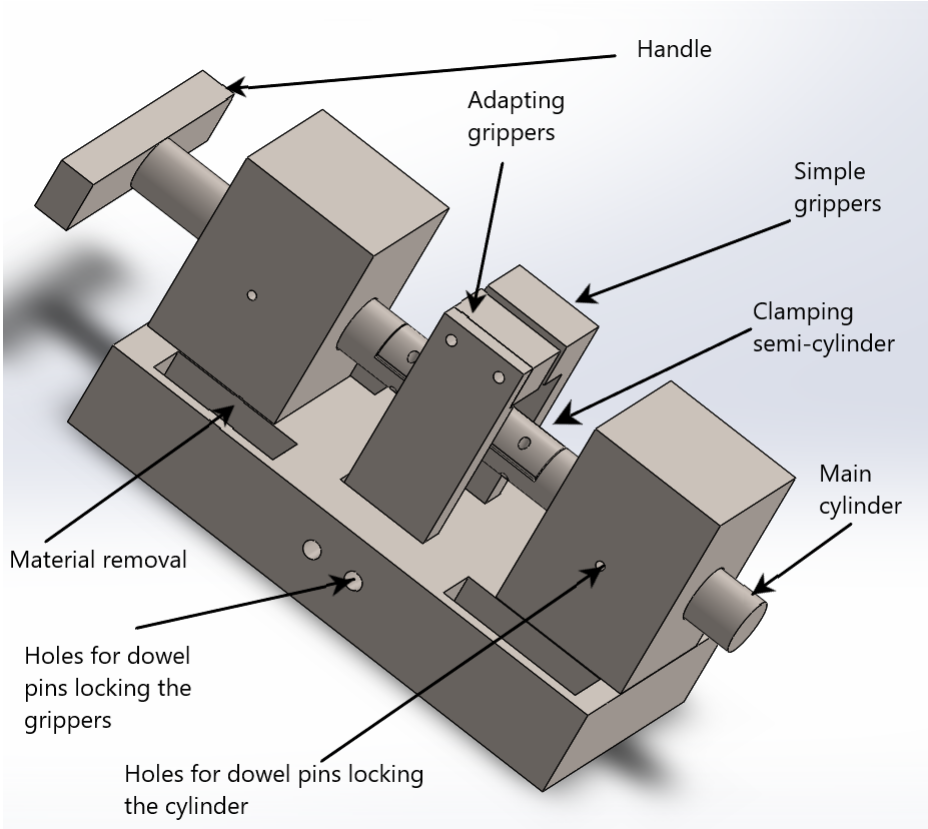
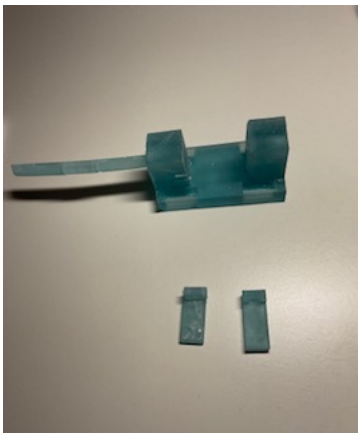


Figure 3.16: 3D view of the designed system with adaptation to the 3D-printing process

Figure 3.17 shows the two first prototypes at 0.2-scale (3.17a) and 0.3-scale (3.17b). The 0.2-scale version contains wheelbase in some pieces and the holes are not correctly drilled. But it shows that we need more looseness between male-pieces and female-pieces (cylinder and support, semi-cylinder cover and cylinder) which is something that was corrected in the second version of the 0.3-scaled model.



(a) First trial 0.2-scale and normal exposure time of 1.8 seconds



(b) First trial 0.3-scale and normal exposure time of 2.0 seconds

Figure 3.17: First 3D-printed prototypes

The third trial illustrated in figure 3.18 shows that we needed in fact more looseness (the diameter of the hole in the two pillars is 1 mm larger than this of the cylinder). This version did not need to put support on the surfaces as we ensured flat surfaces at the base, which allowed us to pose the model on the plate of the 3D-printer so that it gives smooth surfaces. This is also the first version

that allowed us to fix the grippers and drill the holes inside which the two dowel pins are expected to be inserted. The relative distance between the cylinder and the cavity at the top of the grippers in contact with the bones seems to be correct, as well as the relative length of the cylinder with respect to the support. However, this version shows that we need in fact to add a small handle at the end of the cylinder to facilitate the rotation of this piece during the tests. Therefore, it is expected to be added for the next trial. Finally, this version showed us that the settings of the printer ensures a good quality of the prototype, which can be repeated for a scaled-up one.

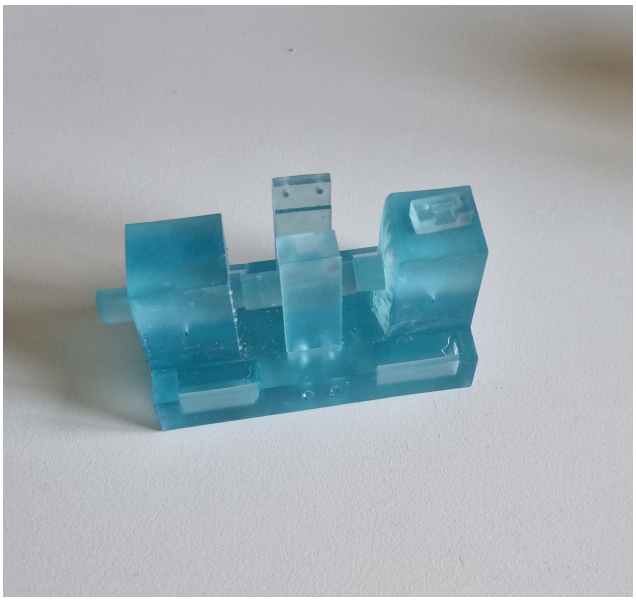
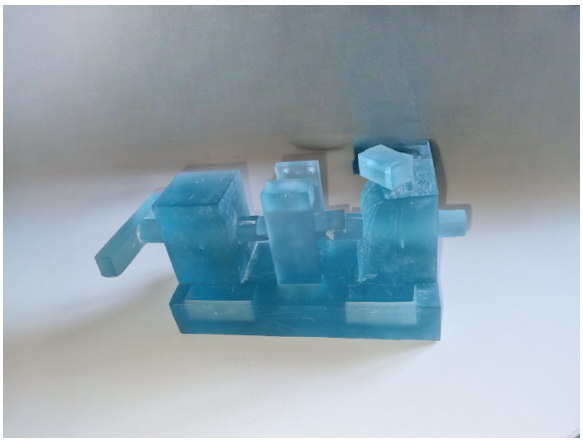


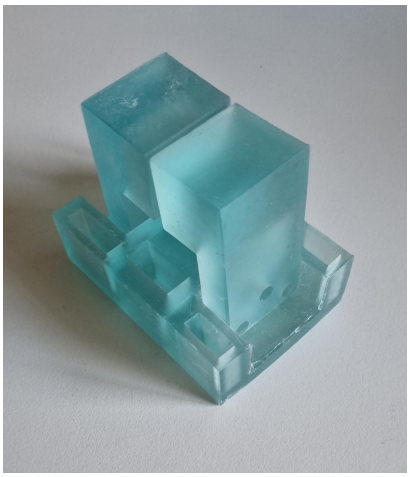
Figure 3.18: Corrected trial of the 0.3 scaled model

3.6.2 Scaled-up trial

Validation of the relative distances were made, the next step was to obtain a bigger model with realistic dimensions. Due to the size of the 3D-printer, the printed model is no more than 0.65 scaled up. However, it remains consistent in a sense that the real dimensions have still to be determined by different tests, simulations and analysis.



(a) 0.65 scaled prototype of the model



(b) 0.65 scaled prototype of new grippers model

Figure 3.19: Scaled-up 3D printed prototype with corrections on the grippers

Figure 3.19 shows the last trials of the 3D printing. Figure 3.19a is the scaled up prototype of the figure 3.18 with an added handle. The holes in the support perpendicular to the main one for the cylinder could not be drilled due to orientation constraints in the printer. Therefore, the dowel pins that block the rotation of the cylinder could not be tested, as well as the one that fix the grippers. Yet, the cylinder seems to be convenient for the tests with free-free extremity tendons, and its dimensions seem to be realistic.

However, the design of the grippers encounter some problems. Indeed, it has been highlighted that a torque is created by the traction of the bone-tendon sample on the grippers, that is not well compensated. The shape seems to be too simplistic which is the reason why a revisited version has been proposed and printed, as shown in figure 3.19b. Here, we have reproduced only the portion of the support that is between the two pillars to model the way of fixing the grippers. This version proposes to widen the insertion area of those pieces on the support, and make them thicker to resist to the flexion induced by the traction in the vertical direction. This version should be more convenient and ensure a mechanical strength that is require to withstand the constraints.

3.6.3 Design features outcome

The combined version of the model highlights the specificity of the design. In fact, some problems may occur if it is reproduced as such in stainless steel. First of all, the holes for the dowel pins could pose problem because the cylinder is free to move in the axial direction, which could prevent the passing of them. We thus have to find a way to prevent the cylinder to rotate and to translate in a more efficient way. That is the reason why a shaft support should be more convenient, as explained in section 4.3.3. Moreover, the system will be super heavy if it is manufactured in metal, as we will see in the next chapter. The support then needs to be smaller and the size of the pillars reduced. In fact, the version in metal is expected to weight 17 kg per bit approximately according to SolidWorks.

This 3D-printing step enables us to validate the way of fixing tendons on the bits but some details need to be adjusted before machining. Moreover, several raw dimensions need to be tuned accurately with some mechanical studies of the different efforts, and some standards of external pieces as well. Nonetheless, this step of first prototyping provides a concrete tool to validate the overall design.

3.7 Material of the bits

The material of the bits is influenced by the type of application and the efforts born by the system. As the efforts could be relatively high, the use of metal is required. In the medical device systems, the most common metals used are titanium and stainless steel [90], and more precisely grade 301, 304L or 306L. The selection of the material must be among those metals. In fact, we aim to develop a model of bit that is validated for *in vitro* studies using destructive tests, but non-destructive tests in a sterile environment is the outlook of this thesis. Therefore, the selection of the material considering this requirement can be a base for the next step. To determine the most suitable material for this application, two criteria are considered : the cost and the mechanical properties. The former discards titanium and stainless steel grade 306L as they are the most expensive ones for no significant added value in this context. In fact, those materials are specifically used for implants because of their high biocompatibility, which is not necessary at this stage. The second criteria is related to the ability of the material to withstand relatively high constraints and to deform really minimally itself during the tests. As we will see later, some elements of the model are subject to flexion and torsion, and their

ability to bear those efforts rely first on the material and its mechanical properties.

Stainless steel grade	Young Modulus (MPa)	Yield stress (GPa)	Ultimate tensile strength (MPa)
301	200,000	400	600
304L	190,000	207	517

Table 3.2: Mechanical properties of interest for the two stainless steel grade considered

In the context of traction testing, the elastic deformation and the elongation in function of the efforts are important to consider. To quantify them, The Young Modulus and the Yield stress of those materials are the appropriate indicators. In fact, the higher the Young Modulus is, the stiffer the material. Similarly, the higher the yield stress is, the better the material can bear the efforts without any non-reversible deformations that can lead to failure after several tests. The latter property is quantified by the Ultimate tensile stress. Table 3.2 displays those mechanical properties for the two type of stainless steels. The data are retrieved from the SolidWorks data base. The stiffness of the two materials is quite similar, but a huge gap in observed between the two in terms of the ultimate tensile strength. Although the break point occurs at high constraints, it seems that the 301 grade has a significantly higher elastic region than the 304L. This is an important feature as we want to reach constraints up to 5500N (see subsection 3.4.1) without any plastic deformation. Therefore, this material made of 8% of nickel [91] will be selected.

3.8 Adjustment of the model for the machining process

The 3D-printing step enabled to assess concretely the model of bits and highlight some features. Several modifications have to be made before the machining process, based on the conclusion drawn in subsection 4.6.3 and the characteristics of the metal. External components will be assembled to the machined ones. The model will be split into the cylinder and the gripper assembly, and the two will merge for the validation of the design.

3.8.1 Cylinder assembly

Some constraints of the machining process have to be taken into account. First of all, it is impossible to obtain right angle corners inside a component as the ones on the clamping region of the cylinder. In fact, mechanical leaves due to the machining tools will always occur. This specification can also be taken positively into account as it prevents high concentration of constraints due to the sharp corners. Furthermore, the model has to be split into several pieces that are screwed together, otherwise the process would cost a lot of material to create one whole component. Simple geometric features are required for such a process. In addition to that, the process has a limited precision in terms of dimension of the system. This particular characteristic has a strong impact when some pieces have to fit others. In fact, the components will be screwed and aligned which requires high level of precision. For this reason, tolerance has to be introduced.

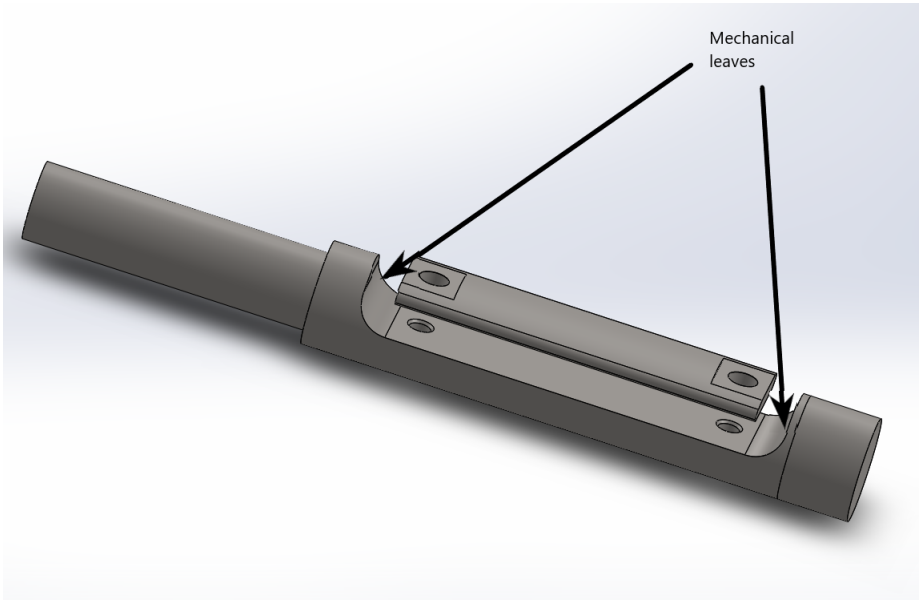


Figure 3.20: Revisited version of the clamping cylinder and its cover

The first modifications involve the clamping cylinder and its cover. First of all, the radius must ensure integrity of the system while offering sufficient coiling potential to the tendons. As the cover does not bear the constraints, its size can be minimized. The minimum radius of the mechanical leaves is two millimeters. Therefore, this is the radius that can be set for the cover. Flat surfaces will be incorporated at the insertion site of the screws, and through holes will be drilled to ensure clearance between the cover and the main cylinder. In fact, the thickness of the tendon varies from one specimen to another and the system has to fit the different dimensions of the tested tendons. Regarding the cylinder, mechanical leaves have to be added at the corners of the flat surface as shown in figure 3.20. Moreover, the translating motion of this component has to be locked easily. For this reason, an enlargement of its radius has been proposed to make a stop with an holding support. This enables to lock the motion to one direction, and the other would be handled by another component described bellow.

3.8.2 Grippers assembly

Similarly, the design of the grippers has to integrate mechanical leaves. Indeed, the support contains inner right angled corners in the initial design which is impossible to produce. This would affect the insertion of the grippers to this piece. Therefore, mechanical leaves have to be incorporated to ensure that the components fit each other as shown in figure 3.21. Mechanically, this feature does not influence the integrity of the system during tensile tests, it can be thus introduced.

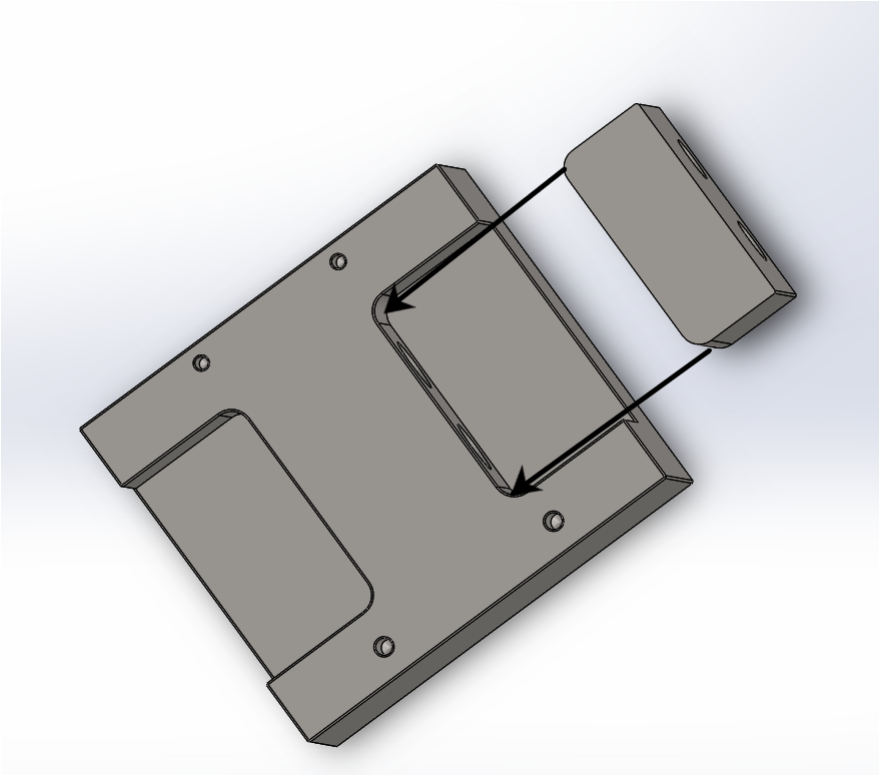


Figure 3.21: top sectional view of the gripper insertion to the support

As opposite to the clamping cylinder, the grippers contain outer sharp cutting edges. To avoid any injuries, non-functional chamfers are introduced in the design for every sharp edges of the model. Finally, the shape of the bone block can differs from one sample to another. In can be indeed more rounded such as the calcaneal bone of the Achilles samples or flat such as the patellar tendon. For this reason, a removable component can be screwed inside the cavity of the of the gripper to ensure contact with the bone. In addition to that, this component reinforces the main body of the gripper during solicitation, especially when the highest values of load are reached with the Achilles tendons. For this reason, the cavity can be opened on the two sides in order to simplify the geometry of the component. Figure 3.22 shows the final version of the grippers. With this adaptation, the design can be machined and functional.

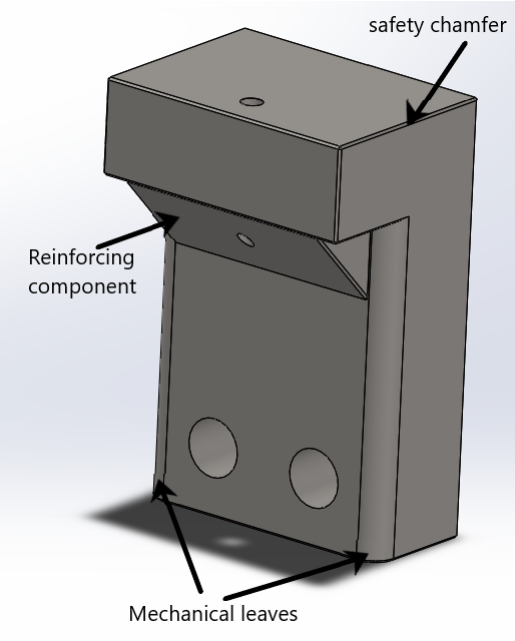


Figure 3.22: Final version of the grippers

3.9 Analytical study of the dynamic

The next step of the design is to determine the dimension of the system by studying first analytically the efforts born during the tensile tests. The most sensitive component is the cylinder as it bears two type of solicitation : torsion and flexion. Both efforts will be quantified further in this section.

3.9.1 Analyze of the flexion of the cylinder

To study the flexion of the cylinder, a 2D-beam problem is proposed and will enable to determine the optimum radius of the cylinder to ensure nor plastic deformation while ensuring a coiling that is sufficient to hold the tendon. First some assumptions are here made :

- The cylinder is considered to be a beam, which means that the dimensions of the sections are much lower than its length (the larger dimension is less than the length divided by 10) [92]
- The section of the beam is uniform and is here a perfect circular
- The middle fiber is planar (straight)
- The beam is uniform (same density over all portions)

In our configuration, the beam has a length of $L = 129mm$, undergoes a force at its center and is held by two structures (either dowel pins or support shaft) at $d_1 = 47.5mm$ from the left side and at $d_3 = 12mm$ for the right, spaced of $d_2 = 69.5mm$ apart (figure 3.23) . It has to be noted that those dimensions are optimized to reduce the weight of the system and the lever arm on the beam. This is also determined by the additional components preset by the manufacturer and the typical sizes of the tendons.

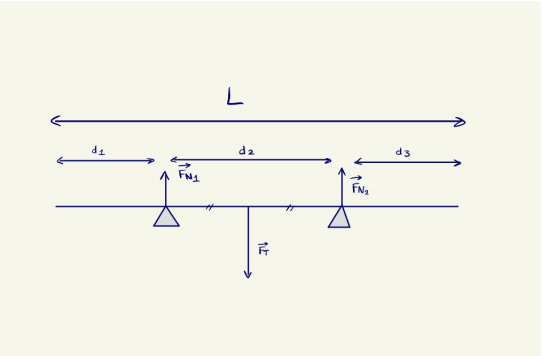


Figure 3.23: 2D problem of the cylinder-beam flexion

The system bears a traction force F oriented toward the bottom and two normal forces F_{N_1} and F_{N_2} toward the top. The traction force F is supposed to reach the maximum level observed in the literature, which means that it can be equal to $5500N$. By considering a reference point at the holding point on the right side, the torque generated by this maximum force is equal to :

$$M = F * d = 5500 * 0.0695/2 = 191.125Nm \tag{3.1}$$

where F is the maximum force and d is the lever arm. In this problem, the material used the bits is supposed to be the stainless steel 301 as seen in the previous section. Therefore, the data used are the one displayed in table 3.2.

The first step consists in applying Newton and Euler's law to get the value of force and torque. In the direction perpendicular to the cylinder axis, we get :

$$\sum \overrightarrow{F} = \overrightarrow{0} \leftrightarrow \overrightarrow{F_T} = \overrightarrow{F_{N_1}} + \overrightarrow{F_{N_2}} \tag{3.2}$$

With Euler equation, we can obtain the value of the different moments applied on the pillars with respect to this applied on the center calculated in equation 3.1, with a reference point at the right extremity of the beam :

$$0.012 \cdot (-\overrightarrow{F_{N_2}}) + 0.04675 \cdot \overrightarrow{F}_T + 0.0815 \cdot (-\overrightarrow{F_{N_1}}) = \overrightarrow{0} \tag{3.3}$$

By resolving the equation 3.3 with equation 3.2, we get for the normals ;

$$\begin{cases} \overrightarrow{F_{N_1}} = \frac{0.04675-0.012}{0.0815-0.012} F_T = 2750N \\ \overrightarrow{F_{N_2}} = F_T - \overrightarrow{F_{N_1}} = 2750N \end{cases}$$

According to Hooke's law, the maximum stress is directly linked by the torque calculated in equation 3.1 by :

$$\sigma_{max} = \frac{My}{I} \tag{3.4}$$

Where M stands for the torque, y represents the distance of the point where the force is applied with respect to the neutral axis (which is here the axis of the cylinder so y is equal to the radius of the cylinder) and I represents the moment of inertia of the cross section, which is equal to $\frac{\pi r^4}{4}$. Therefore, the inertia must be such that this maximum torque induces a value of the stress that does not exceed what we plan, which means that the radius should be equal to :

$$r = \sqrt[3]{\frac{4M}{\sigma_{max}\pi}} \tag{3.5}$$

To ensure no plastic deformation, we need to remain far enough from the yield stress of the material. Figure 3.24 shows the values of the radius that we have to set to obtain the corresponding stress that is born by the system in solicitation. We see that before $100MPa$, the radius should be quite huge and decreases significantly with the increase of the stress. However, it starts to reach a plateau with stresses next to $300MPa$ as the increase of the stress does not reduce very much the radius. As we have to ensure a consistent mechanical strength, which means that the beam should not be permanently deformed, a maximum tolerated stress should be equal to $150MPa$. This would also ensure a resistance to fatigue which would make the device convenient for long-period studies.

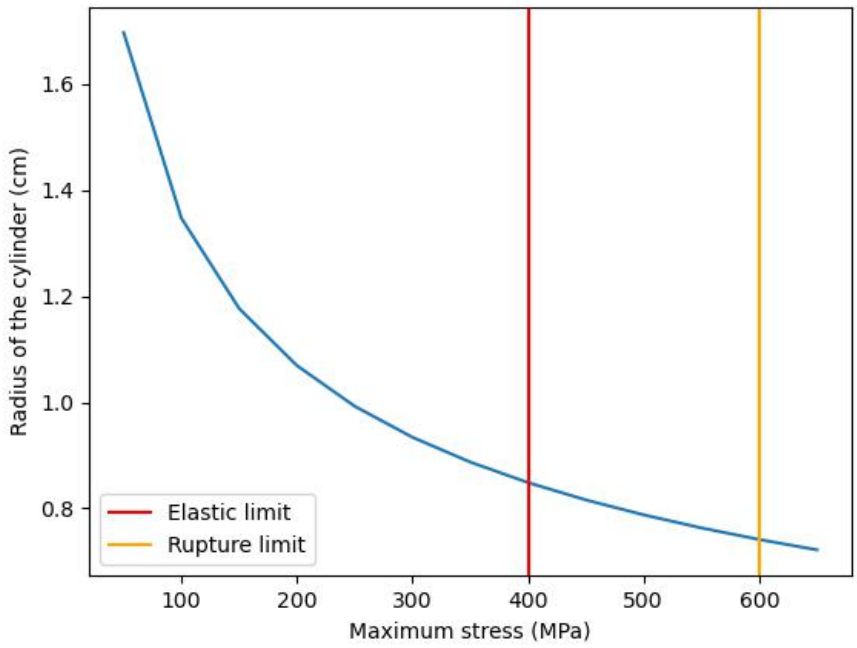


Figure 3.24: Values of the radius with respect to the maximum tolerated stress

By replacing the variables of equation 3.5 by their values, we get **r = 11.75 mm** and we will keep $12mm$. This value overestimates the minimum value of the radius that induces permanent deformation. In fact, a maximum stress of $150MPa$ has been considered to be the safety limit which is lower than the minimum stress that induces the plastic deformation of this kind of steel. However, we had to strongly impose those security because the force is actually exerted on a semi-cylinder at the center, due to the biological constraints and the design. Therefore, strong caution has to be taken with the radius of that cylinder but this mechanical analyze should be confirmed with biological data.

Now let us see how the beam will bend. In fact, we have to minimize the bending because it can interfere with the results of the elongation of the tendons. In fact, we will use the displacement measure of the crossbeam of the machine although we will get the relative displacements of two needles that are attached to two points of the tendon (see figure 3.25).

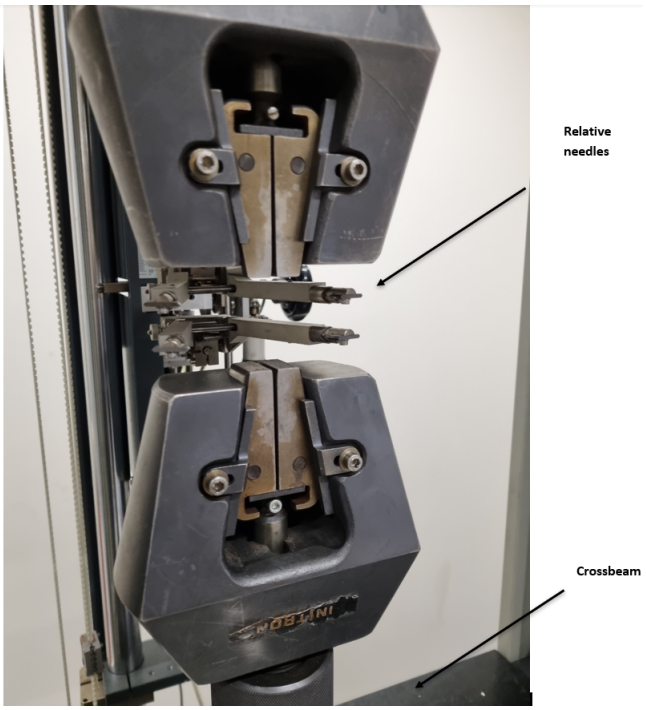


Figure 3.25: Traction machine Zwick and Roll that will be used for the tests

Therefore, we need to prevent the measured to be biased by the bending of the beam. To concretely estimate it, we will use the Hooke's law that gives us the radius of curvature :

$$R_c = \frac{EI}{M} \tag{3.6}$$

Where M stands for the toque calculated in Equation 3.1, E refers to the Young modulus of the material and I represents the inertia as in Equation 3.4. By replacing, we get a radius of curvature of $17.04m$ which means that the center of the beam moves by $0.12mm$. In fact, if we consider this radius of curvature, we can get the distance between the center of the beam before maximum charge and after as shown in figure 3.26.

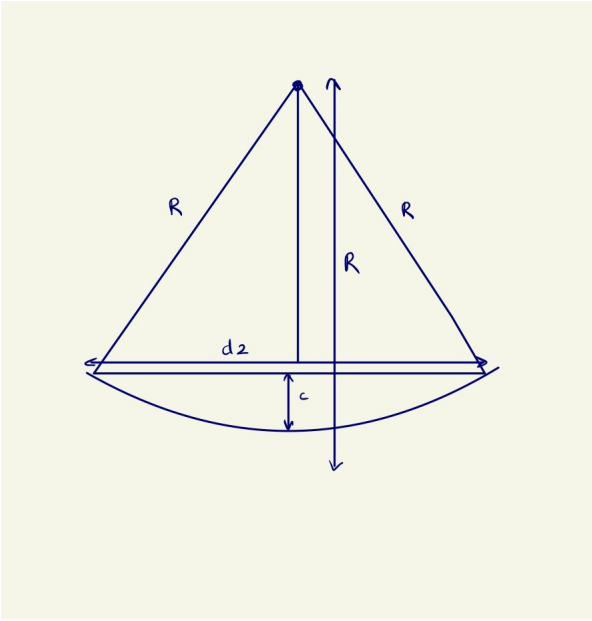


Figure 3.26: Bended cylinder-beam at maximum constraint vs straight beam

The distance at which the center moves at this maximum flexion, c, can be extracted thanks to Pythagore rule :

$$c = R_c - \sqrt{R_c^2 - (\frac{L}{2})^2} \tag{3.7}$$

Where L is the total length of the beam and R_c, the curvature. The calculated radius ensures a minimum bending and no undesired deformation of the system during the tests. However, we have to confront this radius with the typical sizes of the different possible tendons that can be tested. In fact, tendons have to be rolled-up by the cylinder to prevent from slipping and to ensure a sufficient length between the bits for the tests. In fact, the radius should be as low as possible to reduce the risk of protecting weak portions that should break due to the traction.

3.9.2 Analyze of the torsion of the cylinder

The torsional stress is generated because of the locking system that prevents the cylinder from rotating. Figure 3.27 illustrates the problem. A torque is created by the tendon that is coiled around the cylinder, whose lever arm is equal to the radius of the component. If we consider the same level of force as for the flexion, we obtain by the equation 3.1 a value of torque of $66Nm$. By the equation 3.4, we get a maximum stress of $48.63MPa$ if we keep the same radius as the one retrieved in equation 3.5. This is far low from the yield stress, and this short analytical analysis validates the value. But those calculation have to be completed by a simulation because some simplification has been made to compute the value of the radius. Nevertheless, this section provided an overview of the stresses born by the cylinder and allowed for the determination of the radius that will be tested in the subsequent analysis.

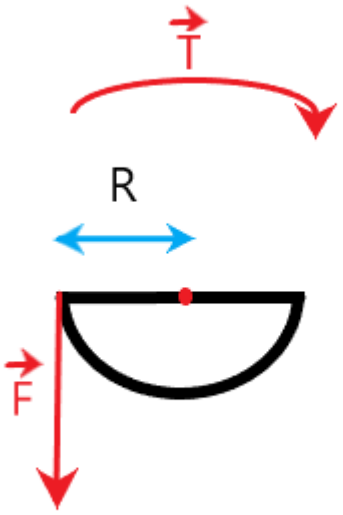


Figure 3.27: Illustration of the torsion problem during tensile tests

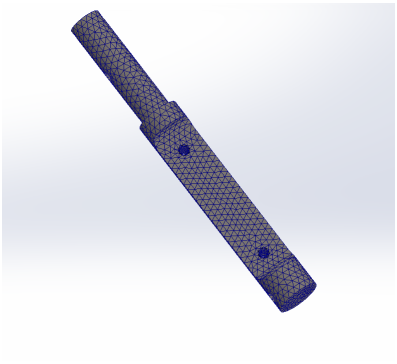
3.10 Finite Element method to simulate the efforts

The second step to determines the dimension of the system is to simulate the efforts. To do so, the extension of Finite Element Methods (FEM) is used for the different components of the system. Two pieces that bear the efforts have to be studied : The cylinder and the grippers.

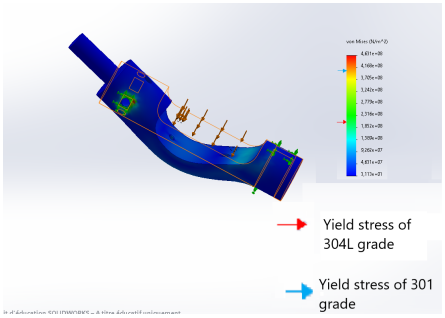
3.10.1 Simulation of the efforts born by the cylinder

Flexion study

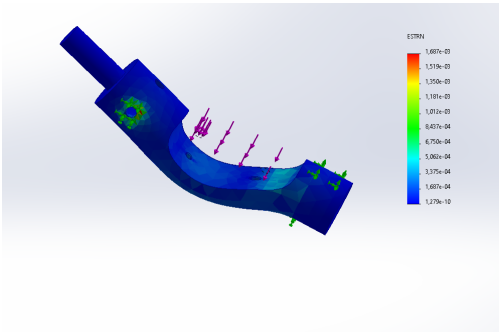
The study of the flexion will enable to choose between the support shaft with hose clamp or the dowel pins inserted inside the pillars holding the cylinder. In fact, holes in this component will be taken into account and the impact of this effort is here studied. Let us look at the configuration where holes are inserted to let the dowel pins pass across the whole object. As for the simulation on the Achilles tendon in section 4.2.1, each element of the mesh generated by following the curves of the object has 16 points and has a size ranged from 0.8 and 2.4 mm. For this configuration, the mesh contains 11690 sharing 18594 nodes. Figure 3.28 shows the results obtains by the simulation. The mesh on which the efforts are simulated is displayed in 3.28a. We applied a force of 5500N which corresponds to the maximum force that can withstand the Achilles tendon. It has been assumed that the elements inside the holes are fixed (green arrows) since this is the location of the holding dowel pins. A traction force is assumed to be evenly distributed across the flat surface at the center of the object (brown arrows) and oriented perpendicular to the axis of rotation.



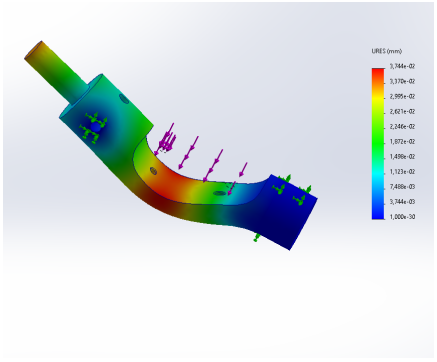
(a) Cylinder mesh automatically generated



(b) Modeled constraints distribution across the whole component



(c) Modeled deformation of the cylinder



(d) Modeled displacement of the cylinder

Figure 3.28: Results of the simulation of the flexion effort born by the cylinder with the drilled version

The constraints represented in 3.28b show that the range contains the Yield stress. If we look into details, it seems that the highest concentration of constraints is localized precisely at the holes. Those constraints overcome the yield stress which means that at the end of the tensile tests, permanent

deformation will remain at this location. This is exactly one of the concerns explained before with wears occurring at the insertion site of the dowel pin. It proves that this solution has to be abandoned as we will focus on the support shaft variant.

Regarding the constraints at the other locations, it seems that most of the regions do not reach high level of stress (blue regions on the object). However, it can be observed that constraints are also quite important at the interface between the cylinder and the semi-cylinder region. This shows that a sufficient curvature shape needs to be ensured instead of sharp corners. This detail is incorporated in the design. Finally, the deformation shown in 3.28c across the whole component does not exceed 0.16% which means that the bit system remain stable and efficient at this particular location. Moreover, short deformation amount ensures long-term durability of the system because of the reduced potential to fatigue. In addition to that, the motion of the cylinder during the flexion will not interfere significantly the results as evidenced in 3.28d. In fact, the maximum value of displacement is reached at the center of the surface (in red) but does not exceed 0.03744 mm.

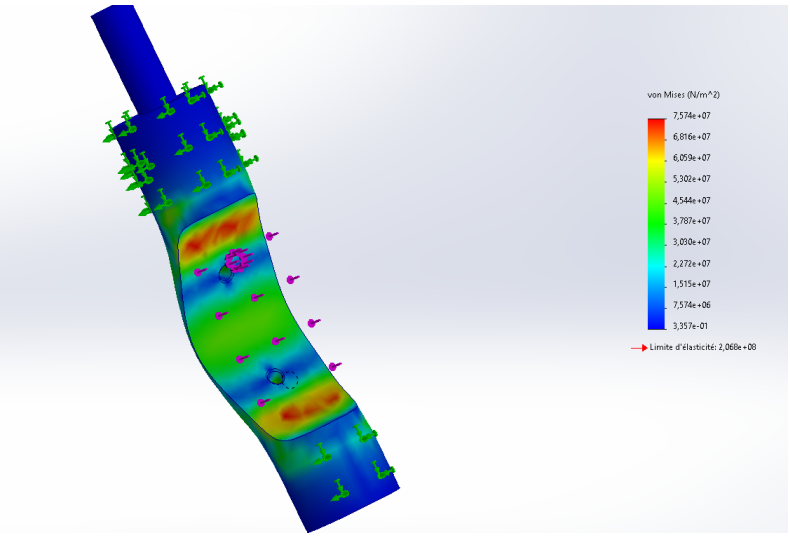


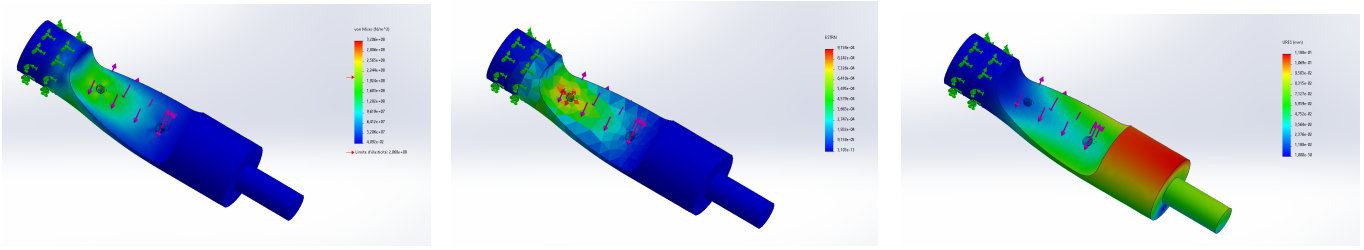
Figure 3.29: Simulation of the constraints across the whole component for the configuration without the dowel pins

In contrast, the simulation provides significant outcomes when the cylinder is not drilled at the insertion of the dowel pins, as evidenced in figure 3.29. The mesh has been slightly modified to contain 15960 nodes distributed in 10016 elements since the surface of the component is reduced due to the absence of the hole. In this simulation showing the constraints distribution, it can be seen that the level of stress, for the same conditions, never reaches the yield modulus. In fact, an order of magnitude separates the highest value from the maximum stress in the elastic region of the material which means that the geometry of the object as well as its material suits the requirement in terms of mechanical strength. As a result, the use of dowel pins to block the cylinder is abandoned and the present study will focus on the option involving a support shaft.

Torsion study

As the locking action of the cylinder to prevent from rotation creates constraints of torsion, it is important to look at the behavior of the object when it is subject to this kind of solicitation. In the simulation shown in figure 3.30, the mesh of the configuration without holes has been kept, and solicitations is torsion have been applied. To do so, a fixed geometry condition has been imposed at the left side of the object (green arrows), and a torque has been applied at the location of the flat surface (pink arrows) with a magnitude equal to the previous force level multiplied by the radius of

the central portion.



(a) Modeled constraints distribution across the whole component

(b) Modeled deformations across the whole component

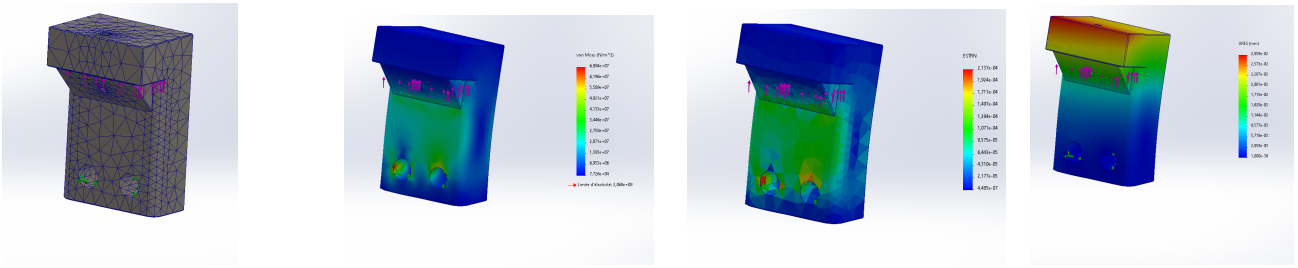
(c) Modeled displacement of the elements of the cylinder

Figure 3.30: Results of the simulation of the torsion effort born by the cylinder with the drilled version

If we look at the constraint distribution displayed in 3.30a, it can be noted that some regions of the cylinder bear constraints that are higher than the yield modulus. It means that the tensile test of an Achilles tendon will induce irreversible deformation at those areas when the sample fails. Those weakest regions are also located around a hole, which corresponds here to the screw insertion site. However, the radius should not be increased to overcome it because the coiling potential of the tendon will be affected. Additionally, the screws are directly in contact with the weakest regions, which means that they will also bear the constraints in torsion. That will then release the stress around the insertion sites, leading to elastic deformations.

3.10.2 Simulation of the efforts born by the grippers

The second set of elements that is directly concerned by the efforts is the pair of the grippers. During tensile tests of a bone-tendon sample, the bone block is in contact with the upper part of the grippers which create a torque on the components. Therefore, it is important to quantify accurately those efforts at the highest failure forces that the system can encounter.



(a) Automatically-generated mesh for the simulation

(b) Modeled constraints across the whole component

(c) Modeled deformation of the elements of the grippers

(d) Modeled displacement of the elements of the grippers

Figure 3.31: Results of the simulation of the traction effort born by the gripper

Figure 3.31 shows the results of the simulation performed on the clamp-plate assembly. The mesh displayed in 3.31a has been automatically generated by Solidworks and contains 11,721 nodes shared by 7,120 triangles. To be faithful with the reality, a fixed geometry has been imposed on the lower half of the two holes through which the dowel pins are inserted. An evenly distributed force on the plate of a magnitude of 5500N as before has been applied vertically.

As evidenced in 3.31b, the constraints are much lower than the yield stress of the material. In fact, the maximum value observed in the simulation is 6.884×10^7, which is 66% times less. This ensures a

high safety margin and validates the model and its dimension. Additionally, the deformations (3.31c) occurring on the top of the grippers do not exceed 0.02%, which would not interfere significantly the measurement of the elongation of the sample. This is also confirmed by the displacement shown in 3.31d as the elements do not move more than 28 μm away from the initial position.

3.11 Validation of the design

The simulations shown previously proved that the system can withstand high values of loads observed in the literature. Safety margin has been also ensured by setting the current dimension of the components. In fact, some assumptions have been made for the simulation, and higher values of load can be observed in the future. But the current dimensions of the system seem to be at the optimum between material saving and sufficient strength to ensure integrity during loading.

Regarding the cylinder assembly, some alternatives considered for the final solutions can be discarded. In fact, the simulations shown that the drilled version with dowel pins induces high concentration of constraints in flexion at the location of the through holes. Non-reversible deformation can occur at highest values of loads which jeopardizes the integrity of the bits. Therefore, the option of a support shaft with hose clamp is preferred. To compensate for high friction during the rotation of the cylinder during setup, a bearing housing is added at the other end of the cylinder. In addition to this, a handwheel is attached to it to increase the lever arm of the user when the user rotates the cylinder. Figure 3.32 shows a front sectional view of the assembly. The bearing housing supports the cylinder and a knurled handwheel is added at the extremity. The enlargement of the cylinder section makes a stop to the bearing housing to lock the translation to one side. Between those two added components, a ring is wrapped around the cylinder to make a stop to the other side of the bearing housing while preventing from interference between rotating components and fixed ones.

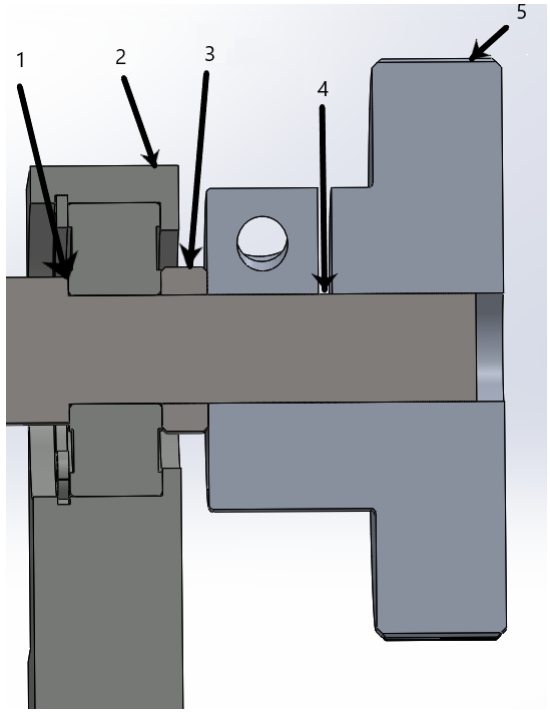


Figure 3.32: Sectional view of the cylinder assembly. 1 : Enlargement of the section of the cylinder to make a stop to the bearing housing. 2 : Bearing housing on one end of the cylinder. 3 : Ring separating the knurled handwheel from the bearing housing 4 : Clamping cylinder inserted across the additional components. 5 : Knurled handwheel

Figure 3.33 shows the final design of the cylinder assembly. A support shaft with hose clamp bears the cylinder at one end to lock the rotational motion when the final position is reached. Total freedom regarding the possible angular positions is ensured as the system does not preset it. On the other side, a bearing housing holds the cylinder and makes stop to it to prevent from translation. To further enhance the rotation during the set up of the experiment, a knurled handwheel is added at the extremity of the system. Between those two supporting components, a flat surface is sliced on the cylinder for the clamping area. The tendon lies on it and is compressed by the cover screwed on the cylinder. Then, the rotation occurs to coil the biological tissue around the cylinder. All those pieces lie on a support that is then fixed to the traction machine. To clamp the samples, two knurled knobs with steps are screwed to manually tight the cover to the main cylinder. This would make the system more easy to handle.

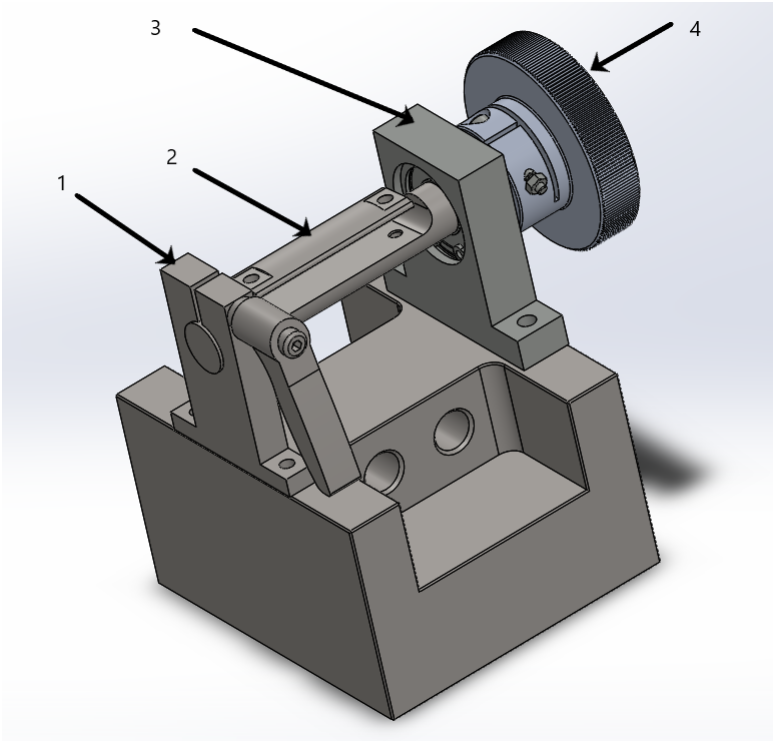


Figure 3.33: Final design of the cylinder assembly adapted to the metallic version. 1 : Support shaft with hose clamp that lock the rotational motion of the clamping cylinder. 2 : Clamping cylinder-cover assembly. 3 : Bearing housing. 4 : Knurled handwheel

Regarding the grippers assembly, two types of grippers have been proposed for the simplification of the system. Instead of having an adapting piece for one gripper as shown above with figure 3.12, it is preferred to have a one-block piece that can be inserted into the fixation area of the main support. The last version of the gripper insertion that has been 3D-printed (figure 3.19b) will be kept. As before, non-functional chamfer are added to avoid any cutting edges. Two dowel pins are inserted through the components to fix the grippers to the support and immobilize them during tensile testing. The insertion area for the grippers are aligned perpendicular to the axis of the cylinder in the previous assembly. This is to save room and to avoid the system being bulky. Figure 3.34 shows the gripper configuration. The same support is used for those components as the elements of the cylinder configuration are removed from it. This allocate rooms for this configuration. Either two hollow grippers are fixed or only one in front of a flat gripper is mounted.

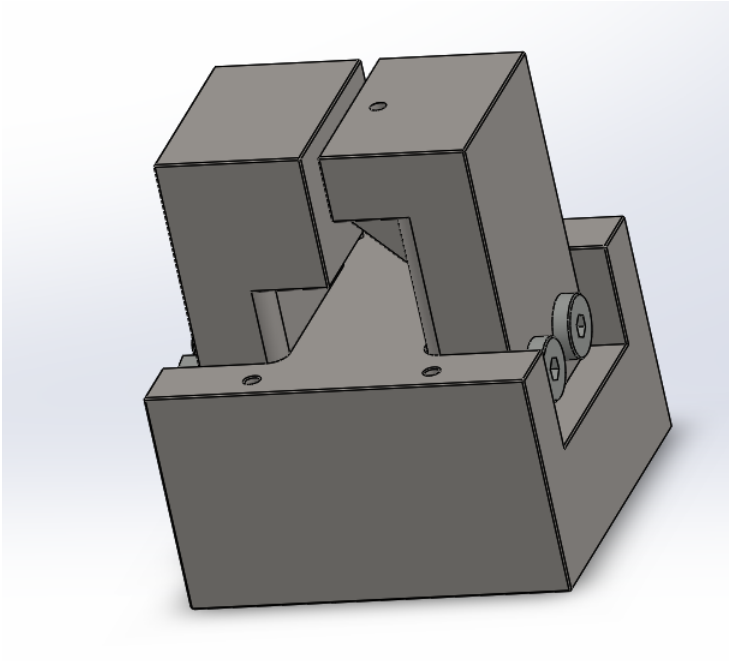


Figure 3.34: Final design of the grippers assembly adapted to the metallic version

To fix the bits to the machine, a support shaft is mounted in series with both elements. Figure 3.35 shows the type of component that links them. A flat support at the bottom is drilled to pass screws fixing the bits to this support shaft. The shape of the holes is the same ones as on the bottom of the bits support. On the upper part, the hollow cylinder fits a shaft of the machine and is fixed to it by a large dowel pin inserted perpendicular to the axis.

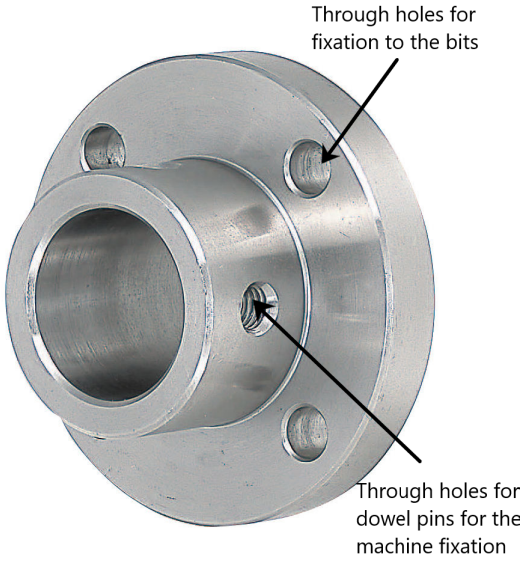


Figure 3.35: Support shaft attaching the bit to the traction machine

This final version of the bit fits the requirements addressed at the beginning of the chapter as it enables to test various type of samples without being bulky. The last step of the design concerns the dimensions of the components. The cylinder radius is set by the mechanical constraints, but the grippers and the flat surface at the center of the cylinder needs to be sized based on the typical sizes of the grafts. In addition to that, tolerances are introduced to ensure that the pieces fit each other.

Based on that, the other dimensions are set accordingly, with the aim of material saving and integrity conservation.

3.12 Final dimensions based on allograft data and the external pieces

Some components need to have the proper dimensions that enable them to fit the samples. For this purpose, data about the typical size of tendons have been transmitted by the tissue bank of Saint-Luc hospital in Brussels. The dimensions of the tendon allografts harvested in the past 2 years have been retrieved from the data base, and a statistical analyse has been carried out.

The tendon used for the analysis are the Achilles tendon with bone-end, free-ended extensor tendon, free-ended tibialis posterior tendon (TPT), tibialis anterior tendon (TAT), hamstring and patellar tendon. Those are the main ones used to provide the allograft for tendon repair. Therefore, their dimensions are the most relevant to set the ones of critical components such as the main clamping cylinder and the grippers.

Type of tendon	n	Mean width (cm)	Minimum width (cm)	Mean length (cm)	Minimum length (cm)
Achilles	68	1.79	1	27.56	19
Extensor	73	0.546	0.3	26.07	18
TPT	72	0.951	0.1	28.92	23
TAT	61	3.11	1.7	24.45	7.5
Patellar	65	2.92	2	4.99	3.5
Hamstring	62	3.14	1.7	24.48	7.5

Table 3.3: Dimension of the free-ended tendon

The initial data set pertains to the free-ended tendons, and their respective dimensions are presented in Table 3.3. The dimensions of particular interest in this context are the width and length of these tendons. This will validate the length of the semi-cylinder as well as its radius. The minimum value and the mean have been retrieved for both dimensions. To ascertain the appropriate radius of the cylinder, the problem of flexion developed in sections 4.9 and 4.10 led to the conclusion that the value should be sufficiently high to prevent permanent deformation or significant displacement of the component. However, it should not be excessively high in order to maintain a desirable coiling potential. In fact, the portion of the sample that is wrapped around the cylinder corresponds at least to a length equal to half of the cylinder perimeter. This minimum length is required at both extremities of the tendon and would release the compressive constraints of the clamping system.

Therefore, a length of about 3.8 cm is needed to hold the sample in the bits, with a radius of 1.2 cm. In the table 3.3, it seems that the tendons are sufficiently long on average and offers an important amount of their length to study the elongation. But some specimens belonging to the TAT type are sometimes relatively short as some samples are only 7.5 cm long. As a consequence, the radius of 1.2 cm seems to be at the optimum and enables the shortest samples to be coiled only once, while the longest ones have a higher coiling potential. It has to be noted that some samples such as some form the Patellar type has to be discarded for the tests as they do not offer a sufficient length. The clamping system is the only principle that can be used to hold the tendon, but it is not sure whether

this is adequate. As it does not represent a significant proportion of the specimens, it does not affect the versatility of the model.

It has to be noted that the tendon does not necessarily have a constant width over its whole length. The width displayed in Table 3.3 corresponds to the smallest ones, but data on the largest portion of the tendon is lacking. Nevertheless, the values reveal certain characteristics that need to be considered. In fact, the samples are generally very tight as their width are ranged from 0.1 to 3.14 cm. This indicates that the compressive force in the clamping surface can be applied to a very small area of the tendon, which induces high values of constraints. In order to avoid weakening the tendons, they have to be coiled more than once. It seems that the tightest specimens offer a long portion of test and that would enable to coil it. That validates also the value of the cylinder radius found previously.

Regarding the portion length of the clamping semi cylinder, the problem is similar. It has indeed to be small to diminish the lever arm in flexion, but it has to be large enough to avoid the tendon to be fold too much if the surface is too small. This problem can be encountered with the Achilles tendon. In fact, at the free-end of the sample, the width is on average equal to 6.8 cm according to some studies [93]. The simulations detailed above have been carried out with a clamping surface width equal to 5.3 cm (between the screws) and provided significant results regarding the constraints. In order to remain far from the critical values of constraints, it has to be imposed such as value of clamping surface length. Some specimens of Achilles tendon could constitute the limit case of the system, but as for the Patellar tendon, this does not represent a high proportion of the available samples. Additionally, folding the sample at the extremities of the clamping surface should normally not weaken it.

Type of tendon	n	Mean length (cm)	Maximum length (cm)	Mean width (cm)	Minimum width (cm)	Mean height (cm)	Minimum height (cm)
Achilles	64	4.47	6.5	3.1	4	1.98	3.2
TAT	71	2.36	3.3	2.07	3	1.44	2.4
patellar tendon (patellar end)	62	4.35	5.2	3.55	5	2.15	3
patellar tendon (tibial end)	62	6.5	9	2.25	1.4	1.3	0.5

Table 3.4: Dimension of the bone-block attached to the tendon

Regarding the bone block dimensions, the data retrieved in table 3.4 will enable to set the size of the cavity inside which the block is held. Figure 3.36 shows the geometrical configuration of the subsystem. The length and the width correspond to the cross section of the bone while the height is the dimension parallel to the tendon length. This runs parallel to the outer edges of the grippers. The mean has been calculated over the samples to retrieve a trend, and the maximum value has been spotted to study the limit cases that can pose a problem of fitting. The gripper cavity has to be designed to accommodate the section defined by the height and length of the bone block. In order to prevent the system to be bulky, lateral walls will not be present in the grippers. This would let the largest bone block lie beyond the contact surface. The width of the samples of interest does not exceed 3.55 cm which means that each gripper would contain half of it. Therefore, a cavity depth of 2 cm is enough to hold the bone block. Similarly, the length never exceeds 9 cm. However, this does not happen very often as the mean values are ranged between 2.36 and 6.5 cm. In the simulation, a length of 6 cm has been chosen to provide ample space for the dowel pins at the bottom. This

dimension constitutes a compromise between a sufficient contact surface and an compact system. Therefore, this length will be maintained for the dimensions.

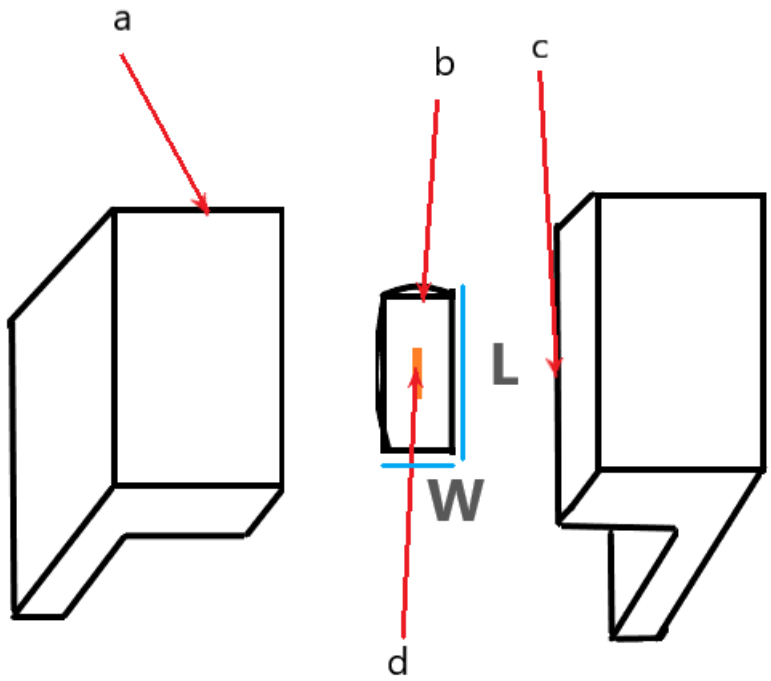


Figure 3.36: Schematic Top view of the block bone insertion into the system. a : One paired gripper with cavity. b : Bone block of a sample. c : Contact edge of the gripper along which the sample lie during the test. d : Tendon insertion to the bone block.

Finally, the manufacturer sets the dimensions of the external pieces such as the support shaft with hose clamp. For this component, the tolerance has been defined as H7 for the main hole, indicating that the actual diameter cannot exceed the theoretical diameter by more than 40 μm. To ensure the fitting of the two components, a h7 tolerance is imposed to the diameter of the corresponding side of the cylinder. Similarly, the manufacturer ensures that the diameter of the hole for the bearing housing will not be 7 μm shorter or 20 μm larger than the expected one. Therefore, a stronger tolerance corresponding to g6 has to be imposed at the other end of the cylinder following this recommendation. Regarding the dowel pins fixing the grippers, a tolerance of +50 μm is indicated which should fit one of the hole diameter of the grippers and the main support component.

The dimensions of the bits enable to obtain a device weighting between 5 and 7 kg depending on the configuration. This is between 60 and 70% lighter than the 3D-printing version. As a results, the system can be used to perform successive tests. The biological data provided by the tissue bank of Saint Luc hospital confirmed the dimensions of some critical components of the system in such a way that the efficiency of the device is ensured.

3.13 Technique used for machining

The two main techniques that have been used to make the machined components are Grinding and Turning. Figure 3.37 shows their principle. Grinding is a process utilizing an abrasive wheel

that removes material from a workpiece in order to shape the component. This highly accurate technique enables to reach tight tolerances and obtain the shapes of those bit elements. To create circular shapes, turning process is preferred. Similarly, a tool is utilized for material removal, but the workpiece here rotates around itself and the tool is in contact to shape it.



(a)



(b)

Figure 3.37: Pictures of the machining processes used : Grinding (a) and Turning (b)

To make the main support on which the support shaft lie, the bearing housing and the grippers, a block of stainless steel underwent the grinding process to shape them. The wheeled tool removes material to create the insertion areas of the grippers, and the holes for the dowel pins have been carried through the boring process. To allow fixation of the external pieces holding the clamping cylinder, threads have been created on the support with a tap according to their preset dimensions.

Similarly, the grippers have been manufactured using Grinding and Boring processes. To build the cylinder, another stainless steel block underwent the turning process. Holes have been drilled and a thread has been created. The clamping surface has been sliced using the Grinding process to remove material from this area. Finally, the covers underwent also the Turning process and through holes have been drilled, and are aligned with the thread on the cylinder clamping surface.

Chapter 4

Tensile tests

The last stage of the thesis involves the tensile tests that enables to study the performance of the designed system. A tensile test machine of model Zwick & Roell RetroLine 50kN has been allocated for several slots in the LEMSC laboratory. The parameters of the experiments can be set in a specific software paired with the machine, called TestXpert. The data extracted include the elongation and the force over the whole test. During the test, elongation is measured by two extensometers that are initially separated by a reference length. This length varies throughout the test and the ratio is calculated at the end. The data treatment is carried out by the python program to plot the data and to perform statistical tests.

4.1 Fabric samples to validate the model

As seen in the state of the art, the behavior of the tendons varies with different factors. Random differences over the samples can be observed which could prevent a proper validation of the device. Therefore, it is necessary to find a way to test the device with strictly identical samples. One solution of the problem could be the use of fabric. In fact, the homogeneity in terms of density and composition over the whole set can be ensured easily. However, the drawback resides in the loss of the control of the failure location. Indeed, the specimen will break at its weakest point, but if the sample is strictly homogeneous over the whole length, this particular point will be extremely difficult to localize. Nevertheless, this method remains convenient to assess the efficiency of the device. In fact, if a significant number of samples break nearly at the same location between the bits, it could validate the model.

4.1.1 Samples preparation and methods

Two set of fabric samples will be used for the tests with two different materials. The objective is to assess the device at two level of constraints as one of fabric is more solid than the other, and to collect sufficient data to come up with a reliable conclusion. In the first part of the testing step, the cylinder configuration will be used at both bits with free-ended samples. In the second part, the gripper configuration will be tested at the upper extremities.

Free-ended samples

The first set contains 21 polyester ropes (280 Dtex type) with a cross section of 4 mm wide and 0.2 mm thick. They are used to tight transplantation bags (referenced MP9570) provided by the Belgian firm Beldico. The samples are all 40 cm long and the elongation is measured over a section of 17.5 cm long at the middle. A preload of 5N has been applied at a rate of 20 mm/min. Then, the test has

been performed at a rate of 10 mm/s. The samples have been wrapped twice around the cover-semi cylinder complex and all inserted into the left of the bits. The reference length, i.e., the length that separates initially the extensometers, is set to 2.5 cm. The position of the sample on the clamping surface has been controlled for each : the traverse edge was adjacent to the top edge of the semi cylinder (Figure 4.1) and the longitudinal axis was set to lie at the center.

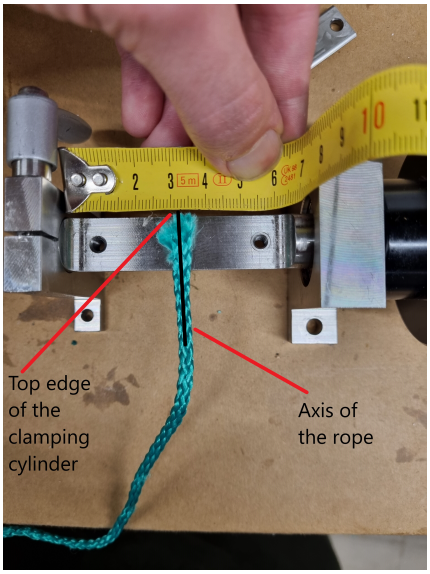
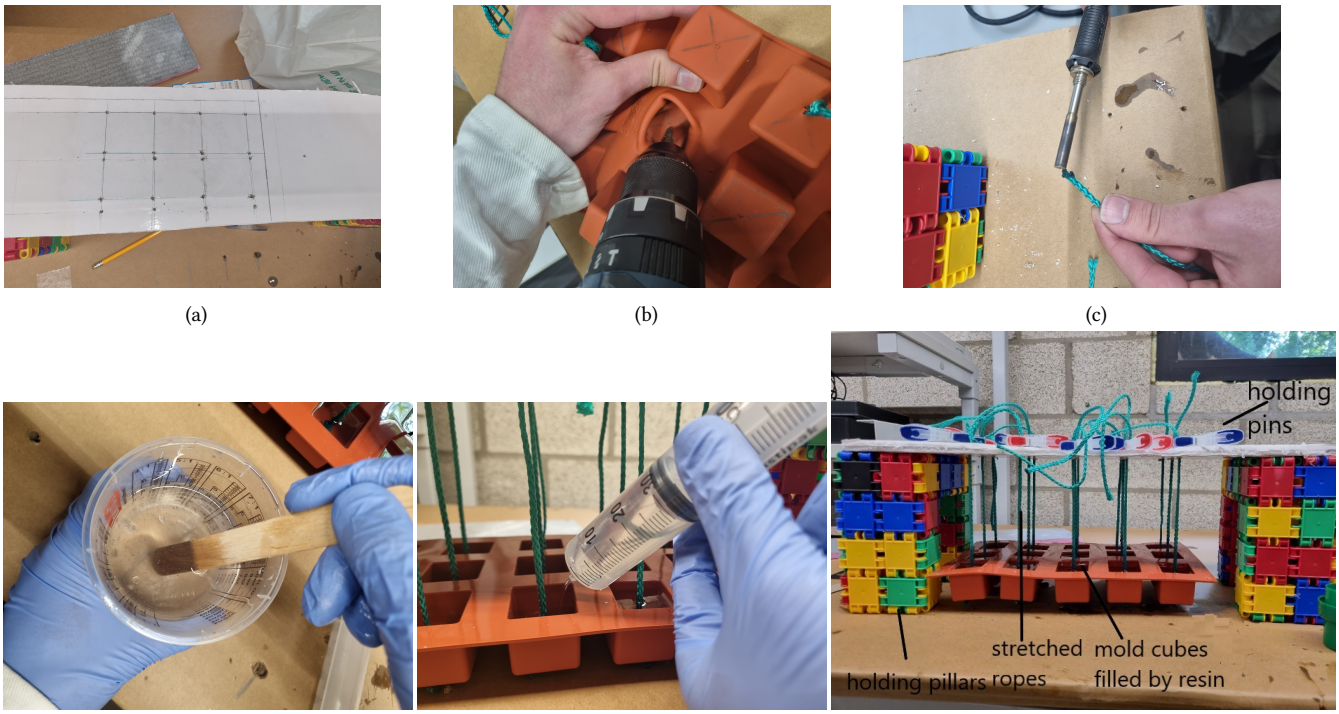


Figure 4.1: Picture of the sample fine positioning on the clamping cylinder. The traversal and longitudinal position was set before clamping

The second set of ropes is more resistant than the first one. It contains 28 samples cut out from a single long rope made of polypropylene of with a circular cross section of diameter 3 mm. The length is set at 30 cm for every samples and the control of the position was the same as previously. The specimen was wrapped around the closed semi cylinder twice at the top bit and once and a half at the bottom. A preload of 10N has been reached at a rate of 20 mm/min to ensure that the sample is completely stretched. The tests have been then performed with a rate of 10 mm/sec and the reference length was set to 15 cm.

Rigid block ended sample

To evaluate the performance of the system with the gripper configuration, synthetic samples with a macroscopic structure close to the tendon are prepared : They are constituted of the same polypropylene rope of 30 cm long attached to a solid bloc of WWA resin epoxy. To constitute the samples, a set of 15 cubic mold has been used to fill in the liquid resin. Figure shows the preparation. A hole has been smoothly drilled at the center of each cubes, which has been reported to a cardboard template also drilled. The holes were aligned and the templates were hold by two pillars on the sides. 28 specimens have been cut out of the source rope that passed through both holes.This ensured a proper vertical positioning of the samples during the preparation. To facilitate the passing, the extremity has been burnt by a soldering iron to hardener the tissue at this end. Under the bottom surface of the cubic molds, a knot has been tightened to make a stop on the other side of the mold. Another knot has been made deep in the cube to ensure that the rope is held in the resin when it dries. On the top surface of the template, the ropes were held by pins to ensure that they were stretched. When the ropes were immobilized, a mixture of 100g resin to 40g WWBA epoxy hardener has been poured to obtain the rigid version. 30ml of the mixture were poured on each cube using a syringe and the samples were dried for 5 days.



(a) (b) (c)

(d) (e) (f)

Figure 4.2: Experimental set up of polypropylene-resin block complex. a: The center of each mold cube has been drawn on the upper template. b : a hole has been drilled at those centers using a soft drilling machine. c : The extremity of the rope has been burnt to pass through the hole. d : the epoxy resin and the hardener has been mixed thoroughly. e : The mixture has been poured using a syringe for fine dosage (30ml). f : The ropes has been stretched and immobilized by pins lying on the top template

Figure 4.3 shows the final product extracted from the molds 5 days later. The epoxy mixture followed well the shape of the mold that is similar to the sample scanned in Figure 3.2. The knot at the bottom of the block has been resin impervious, and the portion beyond the bloc (at the bottom) has been cut off. On the upper part, the rope is rigid next to the bloc and then flexible until the other extremity. This is due to the fact that the resin rose inside the rope by capillarity action. This is faithful with the equivalent biological sample as it represents its enthesis. Regarding the tests, the same strain rate has been applied for the whole set.

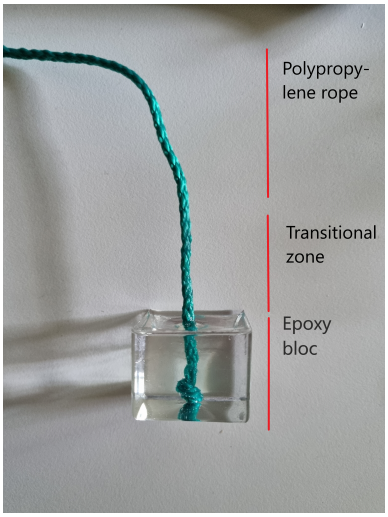
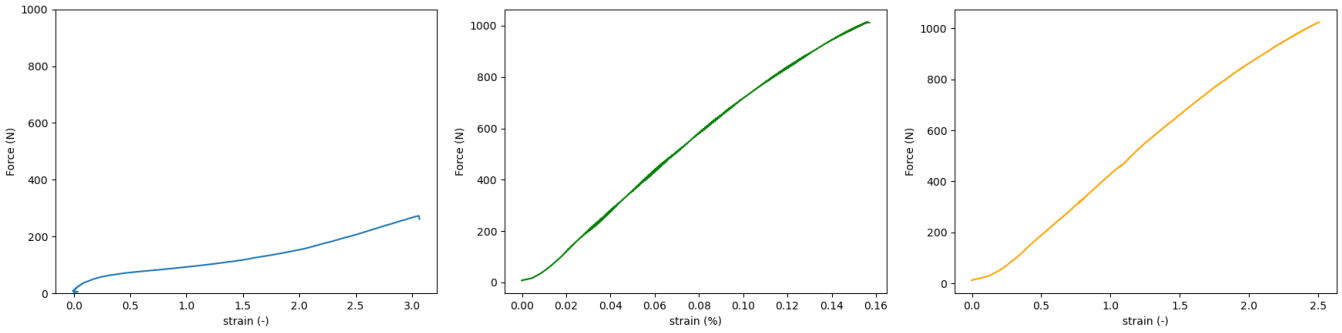


Figure 4.3: Final product of the polypropylene-epoxy sample

4.1.2 Results

Data on force, strain and failure location on the samples will be analyzed in this subsection. Figure 4.4 shows the typical curve of the force-strain relationship for the three samples types. The polyester rope (Figure 4.4a) presents, after a toe region before a force of 75N, an elastic region expands to forces over 250N, directly followed by the rupture. Regarding the polypropylene sample (Figure 4.4b), the overall shape remains similar. The toe region is however tighter probably because the rope is stiffer than the first set type. In addition, the ultimate force load is much higher than the first set, reaching values up to 1000N. The curve is very similar for the epoxy-polypropylene complex sample (Figure 4.4c) as it reaches the same level of maximum loading force.



(a) Load force-strain relationship on the 15^{th} polyester sample

(b) Load force-strain relationship on the 18^{th} polypropylene sample

(c) Load force-strain relationship on the 14^{th} epoxy-rope complex sample

Figure 4.4: Typical load force-strain relationship for each group

In order to validate the model of bits, statistical analysis has been carried out over the rope specimens. The first criteria to assess concerns the failure location. This should never be localised in the bits as it would mean that the model weakens the sample, altering its mechanical behavior. In addition, the reproductibility of the method should ensure that the break occurs significantly at the same region of the sample. The first statistics are obtained in Table 4.1. On average, the polyester samples broke at 28.57 cm from the bottom bit but the dispersion are relatively important as the standard deviation reaches 5.11 cm. This is probably due to the fact that the value range is relatively large (from 9 to 31cm). In contrast, the second set of data shows less variability, with a range size of only 3 cm and a low standard deviation. The location of failure in the second set is slightly less than 9 cm below that of the first set. Regarding the fictive bone-ended samples, the range size is relatively small with short discrepancies as well.

Parameters	Polyester samples	Polypropylene samples	Epoxy-Polyester complex samples
n	19	26	14
Mean (cm)	28.57	20.26	12.96
Standard deviation (cm)	5.11	1.26	2.12
Range (cm)	[9-31]	[19 - 22]	[9 - 16]

Table 4.1: Statistics on the failure location of the polyester ropes

The first set of test has been carried out on the white samples. As seen in the table 4.2, two samples broke under 10 cm from the bottom. One of them broke in the bit. In fact, it has to be noted

that a portion of 7.6 cm is coiled around the cylinder for each bit. Indeed, the coiling length (L_c) can be split as follow : The clamped portion of the sample is as long as the diameter of the main cylinder (1.2 cm). Then, the wrapped portion corresponds to its semi perimeter and the one of the cover. This component has a curvature of 21 cm over a portion equivalent to $\frac{\pi}{5}$ radian. The sum of those contribution can be computed as followed :

$$\left\{ L_c = 2 \times \pi \times (0.6 + \tfrac{2.1}{5}) + 1.2 \quad (cm) \right.$$

Considering this information, it can be noted that two samples broke in the bits (W4 and W9). Although this observation, this first result shows positive insight on the performance of the system, as the failure location seems to be relatively close within the data set. In the subsequent analysis, both specimens that were broken into pieces will be excluded from further examination.

Sample name	Failure location from the bottom (cm)	Sample name	Failure location from the bottom (cm)
W1	29	W12	31
W2	29	W13	9
W3	31	W14	29
W4	7	W15	31
W5	30	W16	31
W6	21	W17	31
W7	29	W18	31
W8	30	W19	31
W9	34	W20	31
W10	29	W21	31
W11	31		

Table 4.2: Location of failure of the polyester ropes

To assess efficiently this criteria, several statistic tests have been considered. The most relevant one remains the linear regression as it study a potential linear relationship between the samples and their failure location. This information has been retrieved from all the samples by measuring this location from their bottom extremity. Figure 4.5 shows the result of the linear regression. The failure location has been plot for every specimens of polyester ropes (Figure 4.5a), polypropylene ropes (Figure 4.5b) and polypropylene-epoxy complex samples (Figure 4.5c). The data are represented by the blue dots and the red lines corresponds to the linear regression. A qualitative analysis of the graphs indicates a weak dependency between the data as the slopes do not exceed 0.25 (in absolute value). This has to be extensively confirmed with statistical tests.

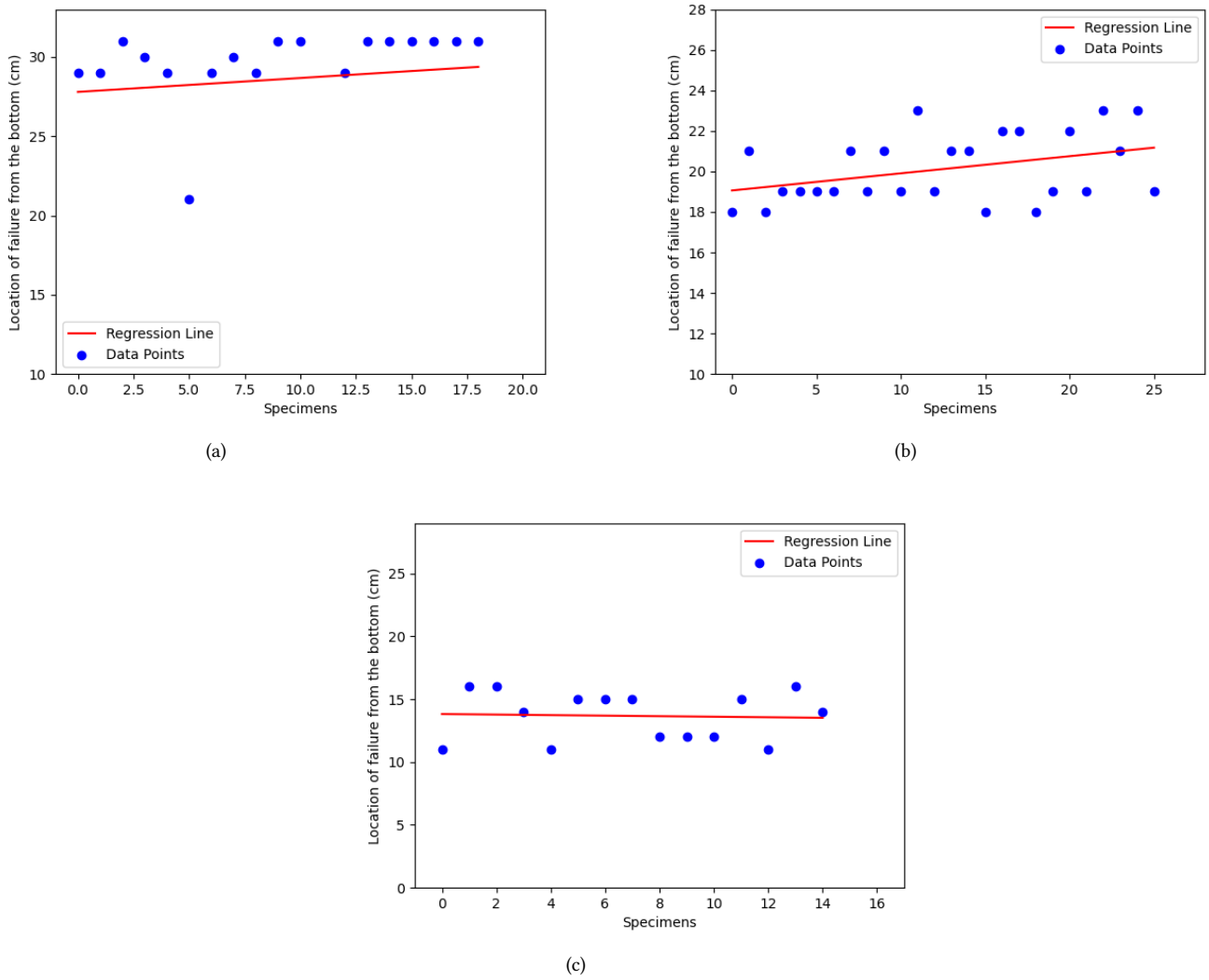


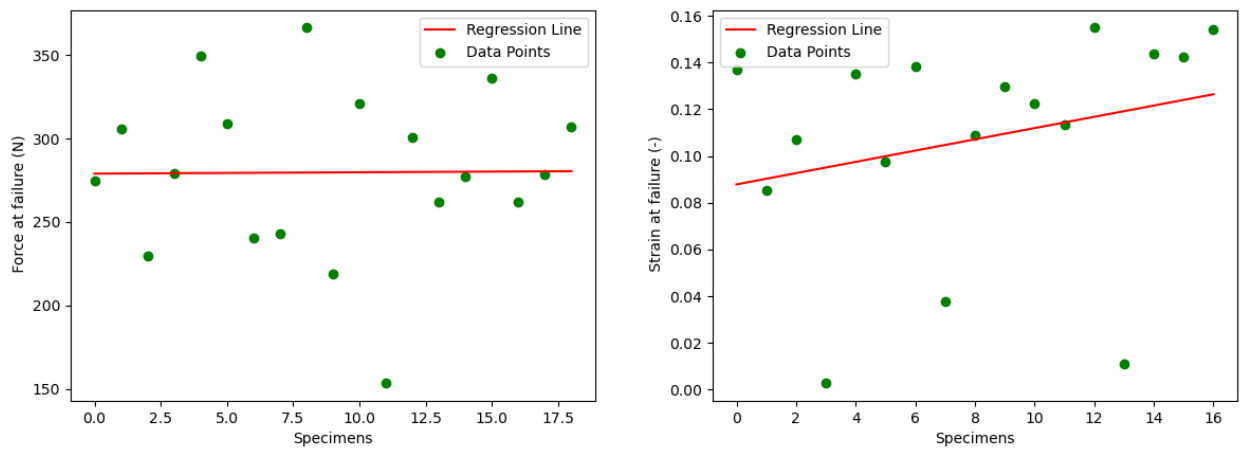
Figure 4.5: Linear regression performed on the polyester (a), polypropylene (b) and polypropylene-epoxy complex samples (c)

To find out if there is a significant difference over the failure location of the samples, a t-test has been carried out on the three sample groups. This consists in examining the probability of observing the given set of data under an initial hypothesis (null hypothesis H_0). In this context, this one argues that there is no relationship between the data, which means here no significant difference between them [94]. By conducting the test, the level of confidence, also known as the p_value, has been determined to be 70,25% for the polyester set. In the literature, a threshold of 95% is normally set to accept the null hypothesis [95]. In that case, the p_value is too low to assert that there is a significant difference between the samples. However, this is not enough to reject this hypothesis. Nevertheless, this analysis gives an understanding about the relationship between the samples. This is also evidenced by the linear regression shown before (Figure 4.5a). In fact, the slope of the curve is equal to 0.08 which indicates a weak relationship. This observation has to be confirmed with the other parameters.

Sample name	Failure force (N)	Strain at failure (-)
W1	274.92	13.67
W2	305.49	8.53
W3	229.64	97.90
W4	278.93	122.67
W5	349.64	10.71
W6	309.08	98
W7	240.78	-2.89
W8	243.13	0.27
W9	366.27	13.52
W10	219.07	9.77
W11	320.67	13.81
W12	84.62	3.78
W13	153.46	10.89
W14	300.54	12.98
W15	261.75	12.26
W16	277.09	11.33
W17	335.98	15.48
W18	47.91	1.09
W19	261.91	14.36
W20	278.77	14.23
W21	307.11	15.39

Table 4.3: Force data during the tensile tests on the polyester samples

The similar analysis on the force data can be carried out. Table 4.3 retrieves the values of force at break and the corresponding strain for the polyester set. On average, the samples broke at 259N and reaches load force up to 366N. Regarding the failure force, it appears that two data points can be identified as outliers since they are below 100N. In fact, during the experiments, those samples were not correctly positioned which caused instability leading to earlier break. This could be due to the fact that those samples were not stable during the test. Therefore, they are rejected for the statistical analysis. Figure 4.6 shows the linear regression on the force data and the distribution along the specimens of this group. The analysis on the failure force is displayed in Figure 4.6a. An observation of the linear regression may indicate a low level of relationship as the slope is equal to 0.08. This is confirm by a p_value equal to 97%. This value exceed the threshold (95%) which means that the null hypothesis can be reliably accepted. Therefore, it leads to the conclusion that there is no significant difference in terms of failure force within the samples. However, some cautions need to be taken in this case. In fact, the data exhibits some variability as indicated by a standard deviation of 48.98N and a range of force from 153 to 366N. Disparities may have affected the data and introduced bias in the t-test. This can be explain by the fact that the compressive force were not controlled as the clamping cover was tightened to the cylinder manually. The samples did not bear the same amount of constraints which can have altered the results. The test should be performed again with a higher amount of data.



(a) (b)

Figure 4.6: Plot of the linear regression performed on the maximum loading force (a) and the strain at failure (b) data for the polypropylene ropes

Regarding the strain at failure retrieved in table 4.3, outliers above 0.9 due to instability of the sample are also observed. Moreover, in the test of W7 specimen, the extensometers were not positioned on the sample, leading to errors on the measurement. Those specimens are thus rejected. The linear regression carried out on the strain sample (4.6b) displays a positive correlation between the specimens and their elongation at strain. However, a statistical test on this variable is not relevant. In fact, the extensometers are initially designed to be attached on a hard material. The fact that the fabric tissues are soft materials does not allow a stable contact between the extensometers and the sample. The point on which the elongation is measured is suspected to change during the test as the tool could slightly move on the sample. In addition, the extensometers are difficult to position perfectly on the samples as they are very tight (4 mm width) and the pair of needle closes after preloading. This makes it difficult to precisely set the position of the sample. Variability could have been introduced due to the lack of precision of the deformation measurements. Therefore, this will not be taken into account for the rest of the study.

Sample name	Failure location from the bottom (cm)	Sample name	Failure location from the bottom (cm)
G1	22	G15	21
G2	21	G16	22
G3	19	G17	22
G4	19	G18	21
G5	19	G19	22
G6	19	G20	19
G7	21	G21	19
G8	19	G22	19
G9	21	G23	22
G10	7	G24	19
G11	21	G25	19
G12	34	G26	22
G13	19	G27	20
G14	21	G28	19

Table 4.4: Location of failure of the polypropylene ropes

The second set of data concerns the polypropylene ropes. The same t-tests will be carried out to determine whether there is a significant difference within the data. Table 4.4 displays the location of failure of those samples. Two samples broke at the bits (G10 and G12) and are also discarded for the rest of the analysis. Prior observation suggests that the data are more consistent than the previous ones with minimal observed disparities. The t-test indicates that the occurrence of these data under the null hypothesis yields a probability of 90%. This is relatively close to the threshold mentioned previously (95%). In this particular framework, it can be argued that the null hypothesis remains true, suggesting no significant difference within the data. However, a particular feature can be retrieved from those data. The location of failure sometimes occurs relatively close to the bits. In fact, it can be easily found that the portion of wrapped sample has a length of 7.6 cm at the top and 5.7 cm at the bottom. As the samples measured 30 cm, it can be inferred that the ones that broke at 22 cm were approximately at the outlet of the device. More specifically, it corresponds to an edge of the clamping cover. The sample is systematically folded at this particular location which could represent a weak points on it. This seems to be consistent as the rope is assumed to be perfectly homogeneous. Hence, when subjected to higher loading forces, it is evident that the sharp edges of the device could lead to the failure of the samples at the contact point. This highlights the importance of addressing the issue by considering modifications to the clamping cover of the device. Specifically, it could be proposed that the sharpness of the edges is reduced in order to prevent any potential weakening of the samples. By implementing this adjustment, it is anticipated that the overall integrity and durability of the samples can be better preserved during testing procedures.

Sample name	Failure force (N)	Strain at failure (-)	Sample name	Failure force (N)	Strain at failure (-)
G1	936.44	0	G15	1016.39	0.13
G2	829.40	0.13	G16	1013.30	0.15
G3	813.57	-0.04	G17	1011.84	0.16
G4	891.55	1.26	G18	1011.84	0.16
G5	947.50	0.46	G19	971.24	-0.03
G6	1049.19	1.25	G20	997.11	0.16
G7	983.92	0.11	G21	1014.24	1.22
G8	997.35	0.12	G22	946.77	0.14
G9	987.61	1.29	G23	274.03	0.99
G10	937.34	0.09	G24	1025.63	0.19
G11	1002.21	1.25	G25	1073.76	0.15
G12	386.91	0.07	G26	1045.32	1.69
G13	712.36	0.05	G27	994.89	0.18
G14	214.70	0.08	G28	803.04	1.08

Table 4.5: Force data during the tensile tests on the polypropylene samples without resin bloc

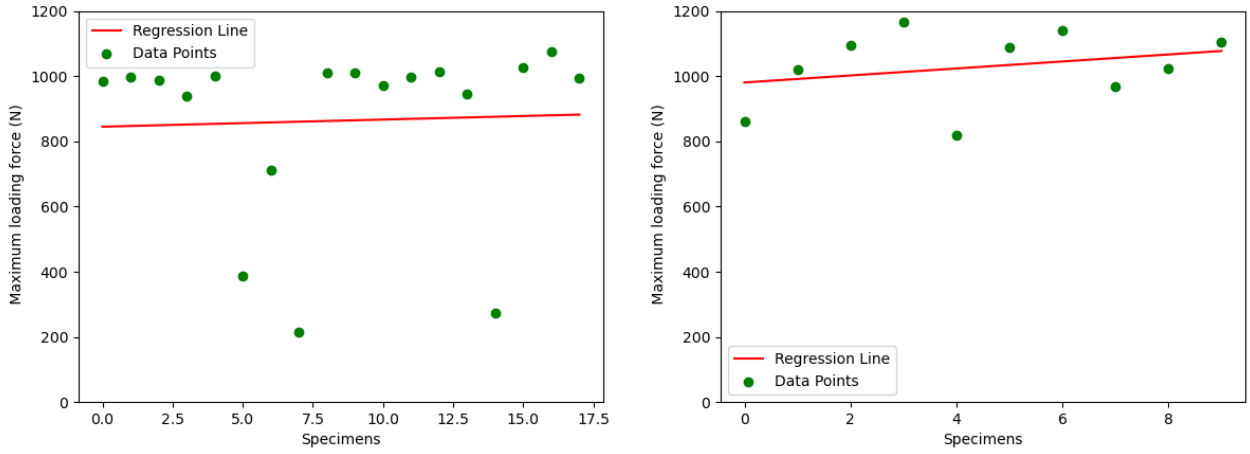
Concerning the failure location on the third set of data, the t-test retrieved a value of 78% for the p_value, indicating that there is no statistically significant evidence to reject the null hypothesis. Although the number of sample is not sufficiently high to provide reliable conclusions, this level of confidence suggests that the gripper variant does not induce significant variability on the properties of the samples. The t-test carried out on the force at failure may supports this assessment.

Sample name	Location of failure from the bottom (cm)	Sample name	Location of failure from the bottom (cm)
GBL1	11	GBL9	12
GBL2	16	GBL10	12
GBL3	16	GBL11	12
GBL4	14	GBL12	15
GBL5	11	GBL13	11
GBL6	15	GBL14	16
GBL7	15	GBL15	14
GBL8	15		

Table 4.6: Location of failure of the resin polypropylene complex samples (from the bottom bit)

Finally, a comprehensive analysis of the failure force can be conducted on both the free-ended and block-ended samples. Figure 4.7 illustrates the results of the linear regression performed on the failure force data displayed in Table 4.5. The corresponding strain at failure is also shown, but for the same reason as before, this is not taken into account. A t-test has been made for each set. It has to be noted that some data have not been considered for this analyses. In fact, the samples on which the elongation could not be retrieved due to the extensometers slipping have been removed. This ensures that the data are treated under similar quality standards making the analysis more consistent. By computing the level of confidence for the null hypothesis on the two sets, a p_value of 86% for the free-ended samples and 43% for the resin-polypropylene complex samples have been

obtained. For the first, this provides solid grounds to argue that there are no statistically significant differences between the data. For the second, however, the p_value is too small to reliably support this hypothesis. This is due to the fact that 15 samples is not enough to constitute a solid analysis.



(a) (b)

Figure 4.7: Linear regression performed on the free-ended samples (a) and bloc-ended samples (b)

The location of rupture did not occur in the resin block or at the stiff zone of the rope. This suggests that the grippers ensured, for this particular type of sample, secure holding and maintained the properties of the samples. However, the location of failure may be different from the real biological tissue that is reproduced. Some studies [16] mentioned in the Chapter 2 argued that the enthesis, i.e. the transitional zone between the tendon and the bone, is the weakest region of the sample. But for this set of test, this does not constitute a critical point as the failure location distribution of the set is the only point of interest of the statistical tests.

4.2 Validation with biological material

4.2.1 Overview of the animal models

The next step of the project is to perform tensile tests on real tendons in order to observe the behavior of the system with biological tissues. The origin of the tissues have to be thoroughly chosen in order to represent closely the human tendons in terms of structure and composition. Some animals such as the rabbit, the sheep or the pig could be the best choice for the first clinical validation tests. Rabbit could provide samples that meet the requirements such as the Flexor Digitorum Profundus (FDP), and present the advantage of having paired tendons [96]. But their size could be limiting for such a device. Compared to pig, sheep is the animal that shares the most similarities with human in terms of size and histology according to some studies [97]. But the availability of the samples and the feasibility of the harvest is more complex. Therefore, the pig will serve as a model for this thesis. As it has also paired tendons, a study of the symmetry between the lower limbs as well as the upper limbs will be performed to assess the performance of the bits. Although the mechanical properties of the tendons cannot be compared to the human model, the pig can still provide some insight on the reliability of the design.

4.2.2 *In vitro* testing with tendons of pigs

The choice of the animal is the pig for relevance and availability reasons. As the animal is expected to have paired tendons from the right and the left limb, a statistical comparison can be made to assess whether there is a significant difference between two homologous tendons. In fact, the animal should not have solicited one limb differently from the other. Therefore, it can be realistically assumed that the homologous tendons should have similar mechanical properties. In this context, if no statistical differences are found within paired tendons, another argument could be provided to validate the model.

4.2.3 Samples preparation and origin

The samples to test were harvested on 4 six-month-old sows. They have been provided to the CHEX laboratory (referenced as LA1230416) in Saint-Luc hospital in the scope of the project 2021/UCL/MD/072 validated by an ethic commission. This did not require the use of the tendons, which is the reason why those tissues were available for the present thesis. The first two animals were put down on April 11^{th} by injection of a potassium-based substance after being anesthetized. The next two ones were sacrificed on April 18^{th} with the same operating mode. The four limbs were cut off immediately after the death were confirmed. Two orthopedic physicians and one biomedical engineer harvested the tendons after removing out the skin of the limb, as shown in figure 4.8. Direct incision were made to spot the tendons that were isolated from the surrounding tissues. The samples longer than 10 cm were conserved at -80°C before the tests. 16 groups were constituted, each group containing the samples from the same limb and animal. On the first day of the tests, the samples from the first two pigs were thawed 4 hours before the tests in a bath containing physiological liquid with 0.9% NaCl. The samples remained in the liquid until the test were performed.

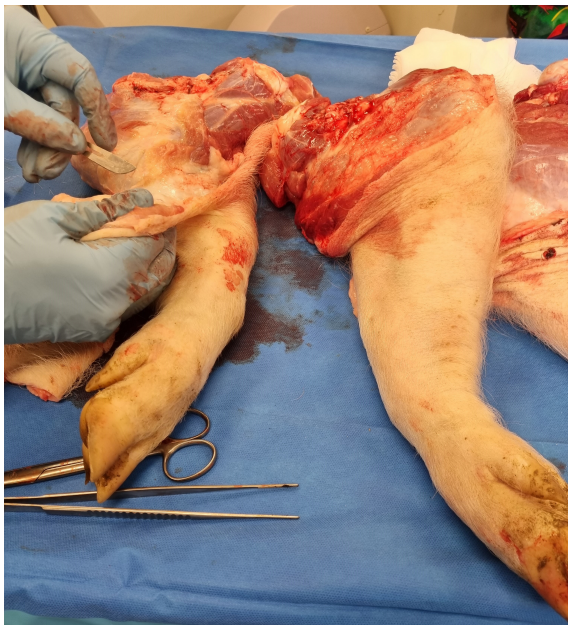


Figure 4.8: Picture of the tendon harvest on one pig.

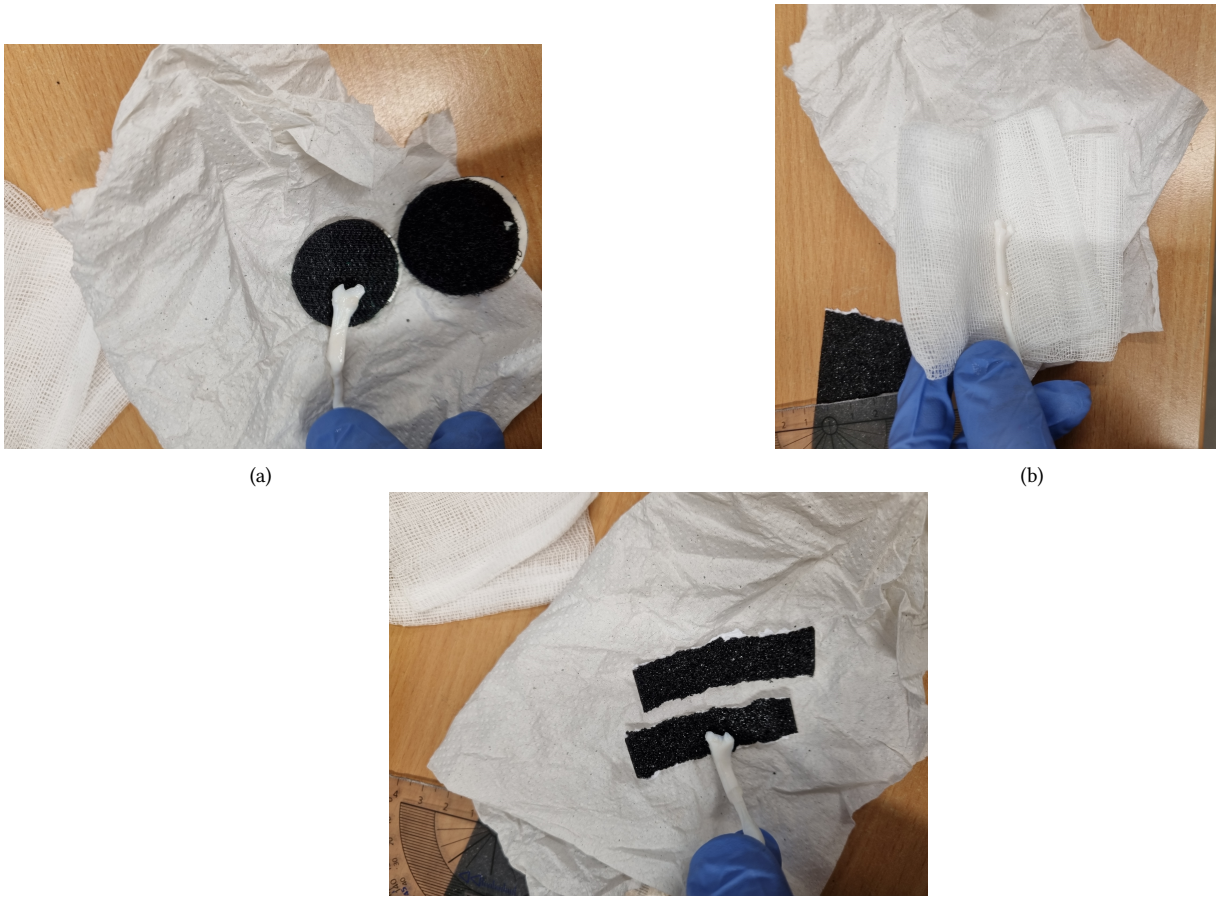
4.2.4 First results : Slipping problem

The first experiments conducted with the samples from two pigs showed some limitations of the model. In fact, slipping inside the clamping cylinder were observed, and some samples were slipped out of the bits. After investigations, this led to the conclusion that the humidity of the samples

degraded the friction coefficient with the stainless steel. In addition, the knurled knobs to screw the cover against the clamping surface relies only on the hand force of the user. This could have been insufficient to tight the sample and immobilize it, which caused this problem.

4.2.5 Alternatives to avoid slipping

To prevent the samples from slipping inside the bits, several options have been considered. Before testing them, the knurled knobs were removed out of the system and classical screws tightened by a wrench were used instead. Regarding the clamping surface, it had to be modified to change the friction coefficient. Increasing the rigidity of the surface has been considered, but it could damage the sample and the extremities. Therefore, three solutions were tested, as shown in figure 4.9. The first one consists in sticking a scratch (4.9a) to the clamping surface. This intermediate component would absorb the excess of humidity and enhance the friction without damaging the sample. The second solution consists in the use of pad (4.9b). The tendon would be wrapped around a piece of pad inside the clamping area of the bit to produce the same effect as the scratch. The last solution involves the use of a grip tape sticker 4.9c. A sticking side is deposited on the clamping surface and the rough side is in contact with the sample. This solution enhance the most friction compared to the others as it is usually used to prevent people from slipping on a sliding floor.



(a) (b) (c)

Figure 4.9: Pictures of the solutions that have been considered to prevent slipping. a : The sample is sandwiched between the two pieces of scratch and they are both clamped. b : The sample is wrapped around a piece of pad and then clamped. c : A piece of grip tape is stick to the clamping surface and is in contact with the clamped tendon

The tendons from two of the pigs served to test the three solutions in a qualitative way. Some tests are performed to detect slipping and to see the effect on the tendon consistency at the extremities.

The first solution that has been discarded is the scratch. In fact, slipping has been observed on the tested pig sample. This is due to the fact that the absorbed humidity has degraded the friction coefficient between the two materials. Therefore, this solution has been set aside. The next solution to be tested involved the grip tape. Five samples of tendon pigs from the lower limbs have been tested and unambiguous results have been generated as shown in figure 4.10a. Every samples broke inside the bits, and the clamped extremities have been damaged. To evidence the excessive roughness of the grip tape, a single sample of Achilles tendon of bull has been tested. The specimen came from the wastes of a slaughter and has been transmitted for the present study. This tendon has been chosen because it is one of the strongest animal tendon that can be found, and damages caused by the grip tape would definitively discard this solution. Figure 4.10b shows the extremity of the tendon after the test. Failure occurred at this particular area and rips off have been found on the surface of the tissue. This leads to the conclusion that the grip tape does not constitute a reliable solution against slipping as the surface is excessively rough.



(a)



(b)

Figure 4.10: Pictures of the damages on the extremities of the tendons using a piece of grip tape. Five samples of pigs (a) and one bull Achilles tendon (b) were tested

4.2.6 Results

At the day of the tests, the remaining samples were transported in a frigolite box filled with dry ice maintaining them at the same temperature as a long distance separates the storage location from the testing laboratory. They were finally thawed 1 hour before the tests. All those samples were tested with a piece of pad and the new screws, which provided better results. Figure 4.11 shows the typical stress-strain curve obtained for a tendon from the lower limb. This specimen had a section of $8mm^2$ and was 14 cm long. The four regions (toe, elastic,plastic and failure) were clearly identified thanks to the proper positioning of the extensometers on the sample. This did not occur systematically for the reason explained before (see Subsection 4.1.2). For this reason, statistical tests will be carried out only on the failure location because the data are not fully reliable. Nevertheless, a qualitative observation can be made on this curve for the tendon of this size. The Young Modulus, which is graphically defined as the slope of the elastic region, is around 17MPa and the yield stress reaches also approximately 17MPa. The failure occurred at 19MPa at 9 cm from the bottom end. This is not

localised in the bits as the samples has been wrapped once around both components, which took a portion of 3.8 cm on each sides.

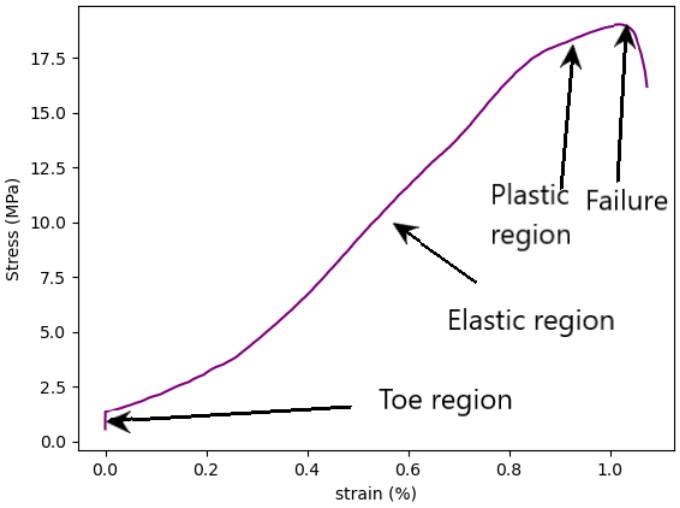


Figure 4.11: Typical Stress-strain relationship of a pig tendon from the upper limb

Similarly as in the first part of the tensile tests, statistical tests will be performed on the failure location on the samples. To assess the performance of the device with biological samples, the data will be paired limb by limb, where samples with the same sizes and corresponding left-right limbs will be associated together. A paired t-test is performed to determine whether there is a significant difference between homologous samples.

In order to check reliably the possible significant differences between the specimens, samples are clustered with respect to their width and thickness, and length whenever possible. Table 4.7 displays the alignment of the samples. Their are designated as the template $CiSj_k$ with i representing the pig specimen (3 or 4), j representing the limb (1 or 2) and k representing the tendon numbering (1 to 6 or 7). Some samples were discarded due to their relative short length (less than 10 cm) or if they presented rips off at the surface.

Paired samples	Length (cm)	Width (mm)	Thickness (mm)	Location of Failure (cm)	Paired samples	Length (cm)	Width (mm)	Thickness (mm)	Location of Failure (cm)
$C3S1_1$	13	6	2	4	$C4S1_1$	17	4	2	0
$C3S2_5$	11	6	2	6	$C4S2_3$	14	4	2	8
$C3S1_2$	12	6	2	11	$C4S1_2$	17	6	2	10
$C3S2_7$	20	6	2	11					
$C3S1_3$	16	4	2	9	$C4S1_3$	16	4	2	12
$C3S2_2$	13	4	2	10	$C4S2_4$	14	4	2	9
$C3S1_4$	14	5	2	7	$C4S1_4$	12	4	2	0
$C3S2_4$	16	5	2	5	$C4S2_2$	17	4	2	16
$C3S1_5$	20	4	2	16	$C4S1_5$	11	5	1	9
$C3S2_6$	17	4	2	17					
$C3S1_6$	17	3	2	8	$C4S1_6$	14	3	2	7
$C3S2_3$	25	3	2	14	$C4S2_1$	17	3	2	12
$C3I1_1$	24	10	4	0	$C4I1_1$	19	10	4	0
$C3I2_1$	17	10	4	0	$C4I2_1$	22	10	4	8
$C3I1_2$	26	4	2	18	$C4I1_2$	22	10	4	0
$C3I2_4$	21	5	2	6	$C4I2_2$	22	10	4	8
$C3I1_3$	30	3	2	5	$C4I1_3$	18	4	2	13
$C3I2_6$	22	3	2	9	$C4I2_3$	20	4	2	6
$C3I1_4$	22	5	2	6	$C4I1_4$	20	4	2	0
$C3I2_4$	21	5	2	6	$C4I2_4$	18	4	2	0
$C3I1_5$	17	5	2	6	$C4I1_5$	10	4	2	14
$C3I2_5$	17	5	2	0	$C4I2_5$	18	4	2	0
$C3I1_6$	20	3	2	6	$C4I1_6$	20	4	2	12
$C3I2_6$	22	3	2	9	$C4I2_6$	14	4	2	5
					$C4I1_7$	14	3	2	6
					$C4I2_7$	14	3	2	8

Table 4.7: Paired samples from limb 1 and limb 2 with pig 3 and 4

Table 4.7 shows the proposed alignment of the data. The 4fourth pig did not provide as much upper limb samples from one to another, which is the reason why there is two data points that do not have an homologous value. It has also to be noted that a value of 0 corresponds to a break at the bottom bit. By performing the t-test, it appears that there is 71% of chance to observe those values if no significant difference is assumed. This is a reliable value in this context for several reasons. First, as said before, the tightening torque was not controlled nor quantified which could introduce variability within the samples. Second, the location of failure is not perfectly determines as the tendon does not systematically rip off transversely. Third, all the samples do not have exactly the same length. This is due to the fact that there were more than one people to harvest the samples, and the incision was not perfectly the same for each paired tendon. Despite those limitations, this provides a positive insight on the performance of the system. Indeed, those tests proved that the coiling system that aims to release the compressive constraints is a good approach to design a tailored model of bit in the context of tendon traction tests.

4.3 Tests with human tendons

Finally, some tests have been carried out on a set of human tendons. This set contains a sample of hamstring and three Achilles tendonS. The Achilles tendons come from the Saint Luc Hospital morgue while the two other samples come from the Tissue bank. There were expected to be destroyed due to the fact that they did not fulfill the criteria for allograft transplantation. Those samples are referenced in Table 4.8.

Achilles 1	5118 15421G
Achilles 2	5118 15421D
Achilles 4	682212327D
Hamstring	BO389200517500 height

Table 4.8: References of the human samples

A strain rate of 10 mm/s has been applied as it is referred to a walking condition [98]. The location of failure is here studied for the gripper configuration as all the samples contain a block bone. One Achilles and the Hamstring broke at the enthesis, while the two others broke at the free-ended extremity. This confirms the fact that the clamping pressure has to be controlled when the cover is tightened on the cylinder, otherwise breaks can occur at a random location. The samples that broke at the enthesis seem to presented a proper compressive constraints as this is theoretically the location of the weakest region.

4.4 Conclusion

The tests performed on the fabric samples displayed good performances in terms of t-test. The location of failure as well as the maximum loading force were significantly the same on the three data sets. However, the compressive constraints need to be properly quantified because it introduced variability that should not appear. Moreover, it could be interested to improve the deformation measurement tool in order to obtain proper values of the elongation. By doing so, t tests can be carried on the Young Modulus as well as the elongation at failure, which could provide significant information on the efficiency of the device.

Some samples broke at the sharp edge of the clamping cover. This is due to the fact that an important folding occurs at this location which could have potentially weakened the specimens. For this reason, two recommendation can be proposed : First, a new cover can be designed to take this feature into account. Second, a proper way of measuring the compressive constraints should be done to further reduce the variability.

Chapter 5

Discussion and conclusion

5.1 Areas of improvement

The assessment of the device efficiency relied mainly on the location of the failure and the failure force. Some parameters such as the Young Modulus could not be studied to see whether there is a significant difference between homologous samples. This was due to the fact that the extensometers did not enable to measure correctly the elongation of the samples throughout the tests. The next stage of this topic consists in improving the way of measurement of the deformation on the samples. Instead of two more accurate extensometers, it could be interested to look at other techniques of measurement. Some studies on biological materials [61] suggests to use some markers attached on the sample, and the elongation is retrieved. A more accurate technique could be the displacement tracking of speckles spread on the sample by Digital Image Correlation. This would also enable to study the elongation of a larger area of the sample as the tendon does not necessarily have a constant section over its length.

The design shows positive insight in reducing the compressive constraints on the clamping area of the sample. To further enhance this effect, the cover and the tightening measurement need to be quantified systematically. In addition to that, it seems that the extensometers do not provide a good way to measure the elongation. The technique of DIC or the application of speakles patters could provide a better solution for this.

5.2 Outlooks

The model elaborated in this project needs fine tuning to be reliable for researches on the mechanical properties of tendons. As soon as the device is validated, it can be tested on a environment close to the one in the body (i.e., at 99% humidity and at 37°C). In fact, it has been evidenced that the testing environment influences significantly the mechanical behavior of the tendons, as seen in chapter 2. To study the impact of treatments, it is important to consider some tests with the conditions of the body. Some laboratories have developed a device that simulates those conditions. Incorporating the model of bits in such devices may be the objective of next projects to validate the model.

Moreover, the development of a more complex machine can be carried out to spread the tensile tests making on tendons. The tests realized in the present scope required the user to be accompanied by trained people to perform the tests. To allow the specialists of the tissues banks to make tensile tests, the ergonomic of the device has to be taken into account to be incorporated in the facilities of the hospitals. As a results, a compact and transportable system easy to use is required, and has to fit strict safety standards to obtain the CE label.

Furthermore, it is relevant to consider the development of non-destructive tests. So far, the tensile tests performed in this project but also in the literature involved solicitation until failure. It can be interesting to assess the strength of the allografts by a relevant mechanical test that ensure with a relatively high level of confidence that the tendon presents low risk of rupture. One approach can be to localize the weakest regions of the tendons and retrieve their mechanical properties. Some thresholds can be then determined to discard the weakest specimens but also to keep some allografts that were expected to be rejected for safety reasons. In fact, the mechanical properties of the grafts are not systematically assessed, and some are discarded because their are suspected to be too tender. The development of a reliable test protocol can contribute to the reduction of allograft wastes.

5.3 Conclusion

The present model of bit enabled to test several types of samples, from fabric to biological tissues. The performance of the system with the given conditions provides positive outlooks for further studies. In fact, no significant differences were found within the samples. However, extensive tests should be performed to further reduce the variability and to overcome the problem of elongation measurement. This would help to provide a reliable model that would enable to extensively study the properties of the tendon for the development of new sterilization treatments. Tests on human samples provided qualitative results, but a better measurement of the mechanical properties should be performed to study properly the behavior of human tendons on such a model. Before that, some modification could be brought to the system, such as another clamping cover and a proper way to measure the constraints on the clamping surface. This thesis showed how mechanics and biology can meet to provide some elements that improve the healthcare system.

Bibliography

[1] Wang JH. Mechanobiology of tendon. J Biomech. 2006;39(9):1563-82. doi: 10.1016/j.jbiomech.2005.05.011. Epub 2005 Jul 5. PMID: 16000201.

[2] Teach me anatomy, "Anatomical planes", last update on September 30, 2022 by Oliver Jones, consulted on April 2023. url : https://teachmeanatomy.info/the-basics/anatomical-terminology/planes/.

[3] Medi Belgium NV, "Tendon d'Achille", url : https://www.medibelgium.be/fr/sante/corps-humain/tendons-ligaments/tendon-dachille/.

[4] Nantes Chirurgie Jenesse et Sport, "LCA techniques opératoires, "url : https://www.nantes-chirurgie-jeunesse-sports.fr/je-me-fais-operer-du-genou/je-dois-me-faire-operer-du-lca/lca-techniques-operatoires/.

[5] Igor Santos, Ultimate Tensile Strength Test. Consulted on May 2023. Url : https://www.researchgate.net/figure/Ultimate-Tensile-Strength-Test_fig4_256194980.

[6] ZhongLi Instrument Technology Co, universal testing machine. Consulted on May 2023. Url : Definitionandsetup.

[7] Davis, J. R.. Tensile Testing, A S M International, 2004. ProQuest Ebook Central, https://ebookcentral.proquest.com/lib/uclouvainbe/detail.action?docID=3002341.

[8] Eurostat, Ageing Europe - statistics on population developments, data extracted in july 2020, consulted in April 2023. Url : https://ec.europa.eu/eurostat/statistics-explained/index.php?title=Ageing_Europe_-_statistics_on_population_developments#Older_people_.E2.80.94_increasingly_old_and_with_growing_dependency.

[9] World Health Organisation, Ageing and health, published in 2023, url = https://www.who.int/news-room/fact-sheets/detail/ageing-and-health#:~:text=By\%202030\%2C\%201\%20in\%206,will\%20double\%20(2.1\%20billion).

[10] Karahan N. Yılmaz B. Kaya, M. Tendon structure and classification., 2019. [cited 2022 Nov 05], doi: 10.5772/intechopen.84622,.

[11] Thiago. publisher= Biochemical Pharmacology, p 240-244 , year : 20, url=.

[12] Varacallo M. Bordoni B. anatomy tendons. [Updated 2022 Jul 18]. In: StatPearls [Internet]. Treasure Island (FL): StatPearls Publishing; 2022 Jan-. url : https://www.ncbi.nlm.nih.gov/books/NBK513237/.

[13] Wang JH, Thampatty BP, Lin JS, Im HJ. Mechanoregulation of gene expression in fibroblasts. Gene. 2007 Apr 15;391(1-2):1-15. doi: 10.1016/j.gene.2007.01.014. Epub 2007 Jan 31. PMID: 17331678; PMCID: PMC2893340.

[14] Almekinders LC, Banes AJ, Ballenger CA. Effects of repetitive motion on human fibroblasts. Med Sci Sports Exerc. 1993 May;25(5):603-7. PMID: 8388071.

[15] Ellen C. Breen. Mechanical strain increases type i collagen expression in pulmonary fibroblasts in vitro. *Journal of Applied Physiology*, 88(1):203–209, 2000. PMID: 10642382, url : https://doi.org/10.1152/jappl.2000.88.1.203, doi : 10.1152/jappl.2000.88.1.203.

[16] Deymier AC, An Y, Boyle JJ, Schwartz AG, Birman V, Genin GM, Thomopoulos S, Barber AH. Micro-mechanical properties of the tendon-to-bone attachment. Acta Biomater. 2017 Jul 1;56:25-35. doi: 10.1016/j.actbio.2017.01.037. Epub 2017 Jan 11. PMID: 28088669; PMCID: PMC5575850.

[17] Gupton M, Imonugo O, Terreberry RR. Anatomy, Bony Pelvis and Lower Limb, Knee. 2022 Nov 15. In: StatPearls [Internet]. Treasure Island (FL): StatPearls Publishing; 2023 Jan–. PMID: 29763193.

[18] O'Brien M. The anatomy of the Achilles tendon. Foot Ankle Clin. 2005 Jun;10(2):225-38. doi: 10.1016/j.fcl.2005.01.011. PMID: 15922915.

[19] Basso, O., Johnson, D. Amis, A. The anatomy of the patellar tendon. Knee Surg Sports Traumatol Art 9, 2–5 (2001). https://doi.org/10.1007/s001670000133, published in 2000.

[20] Basso, O., Johnson, D. Amis, A. The anatomy of the patellar tendon. Knee Surg Sports Traumatol Art 9, 2–5 (2001). https://doi.org/10.1007/s001670000133.

[21] Andrikoula S, Tokis A, Vasiliadis HS, Georgoulis A. The extensor mechanism of the knee joint: an anatomical study. Knee Surg Sports Traumatol Arthrosc. 2006 Mar;14(3):214-20. doi: 10.1007/s00167-005-0680-3. Epub 2005 Nov 10. PMID: 16283173.

[22] Waligora AC, Johanson NA, Hirsch BE. Clinical anatomy of the quadriceps femoris and extensor apparatus of the knee. Clin Orthop Relat Res. 2009 Dec;467(12):3297-306. doi: 10.1007/s11999-009-1052-y. Epub 2009 Aug 19. PMID: 19690926; PMCID: PMC2772911.

[23] Pope JD, El Bitar Y, Mabrouk A, Plexousakis MP. Quadriceps Tendon Rupture. 2022 Dec 17. In: StatPearls [Internet]. Treasure Island (FL): StatPearls Publishing; 2023 Jan–. PMID: 29494011.

[24] Beltran L, Ghazikhanian V, Padron M, Beltran J. The proximal hamstring muscle-tendon-bone unit: a review of the normal anatomy, biomechanics, and pathophysiology. Eur J Radiol. 2012 Dec;81(12):3772-9. doi: 10.1016/j.ejrad.2011.03.099. Epub 2011 Apr 27. PMID: 21524864.

[25] van der Made AD, Wieldraaijer T, Kerkhoffs GM, Kleipool RP, Engebretsen L, van Dijk CN, Golanó P. The hamstring muscle complex. Knee Surg Sports Traumatol Arthrosc. 2015 Jul;23(7):2115-22. doi: 10.1007/s00167-013-2744-0. Epub 2013 Nov 5. PMID: 24190369.

[26] Frank RM, Hamamoto JT, Bernardoni E, Cvetanovich G, Bach BR Jr, Verma NN, Bush-Joseph CA. ACL Reconstruction Basics: Quadruple (4-Strand) Hamstring Autograft Harvest. Arthrosc Tech. 2017 Aug 14;6(4):e1309-e1313. doi: 10.1016/j.eats.2017.05.024. PMID: 29354434; PMCID: PMC5622412.

[27] Briggs AM, Woolf AD, Dreinhöfer K, Homb N, Hoy DG, Kopansky-Giles D, Åkesson K, March L. Reducing the global burden of musculoskeletal conditions. Bull World Health Organ. 2018 May 1;96(5):366-368. doi: 10.2471/BLT.17.204891. Epub 2018 Apr 12. PMID: 29875522; PMCID: PMC5985424.

[28] Lim WL, Liau LL, Ng MH, Chowdhury SR, Law JX. Current Progress in Tendon and Ligament Tissue Engineering. Tissue Eng Regen Med. 2019 Jun 26;16(6):549-571. doi: 10.1007/s13770-019-00196-w. PMID: 31824819; PMCID: PMC6879704.

[29] Geremia JM, Bobbert MF, Casa Nova M, Ott RD, Lemos Fde A, Lupion Rde O, Frasson VB, Vaz MA. The structural and mechanical properties of the Achilles tendon 2 years after surgical repair. Clin Biomech (Bristol, Avon). 2015 Jun;30(5):485-92. doi: 10.1016/j.clinbiomech.2015.03.005. Epub 2015 Mar 11. PMID: 25828432.

[30] Neumayer, F., Crevoisier, X., Assal, M., Diagnostic et traitement de la rupture du tendon d'Achille, Rev Med Suisse, 2012/349 (Vol.-2), p. 1490–1495. URL: https://www.revmed.ch/revue-medicale-suisse/2012/revue-medicale-suisse-349/diagnostic-et-traitement-de-la-rupture-du-tendon-d-achille.

[31] F. Khiami, M. Di Schino, E. Sariali, D. Cao, E. Rolland, Y. Catonné, Traitement de la rupture chronique du tendon d'Achille par une suture raccourcissante et une greffe libre d'aponévrose du triceps sural, Revue de Chirurgie Orthopédique et Traumatologique, Volume 99, Issue 5, 2013, Pages 490-497, ISSN 1877-0517, https://doi.org/10.1016/j.rcot.2013.06.001. url : https://www.sciencedirect.com/science/article/pii/S187705171300169X.

[32] Yu-Jie Song, Ying-Hui Hua, Tendon allograft for treatment of chronic Achilles tendon rupture: A systematic review, Foot and Ankle Surgery, Volume 25, Issue 3, 2019, Pages 252-257, ISSN 1268-7731, https://doi.org/10.1016/j.fas.2018.02.002. found in (https://www.sciencedirect.com/science/article/pii/S1268773118300250).

[33] Song YJ, Hua YH. Tendon allograft for treatment of chronic Achilles tendon rupture: A systematic review. Foot Ankle Surg. 2019 Jun;25(3):252-257. doi: 10.1016/j.fas.2018.02.002. Epub 2018 Feb 10. PMID: 30321974.

[34] Guiraud, K., Silvestre, G., Bastin, C. et al. Higher sensitivity with the lever sign test for diagnosis of anterior cruciate ligament rupture in the emergency department. Arch Orthop Trauma Surg 142, 1979–1983 (2022). https://doi.org/10.1007/s00402-021-04154-x.

[35] van Melick N, van Cingel RE, Brooijmans F, Neeter C, van Tienen T, Hullegie W, Nijhuis-van der Sanden MW. Evidence-based clinical practice update: practice guidelines for anterior cruciate ligament rehabilitation based on a systematic review and multidisciplinary consensus. Br J Sports Med. 2016 Dec;50(24):1506-1515. doi: 10.1136/bjsports-2015-095898. Epub 2016 Aug 18. PMID: 27539507.

[36] American Academy of Orthopaedic Surgeons, "Quadriceps Tendon Tear", Contributed and/or Updated by Michael J. Alaia and Rick Wilkerson, peer-reviewed by Thomas Ward Throckmorton and Stuart J. Fischer, last reviewed in October 2021, consulted in April 2023. url : https://orthoinfo.aaos.org/en/diseases--conditions/quadriceps-tendon-tear/.

[37] American Academy of Orthopaedic Surgeons? "Patellar Tendon Tear", Contributed and/or updated by Jocelyn Ross Wittstein and Rick Wilkerson, peer-reviewed by Thomas Ward Throckmorton and Stuart J. Fischer, last reviewed in October 2021, consulted in April 2023. url : https://orthoinfo.aaos.org/en/diseases--conditions/patellar-tendon-tear/.

[38] Philippe M. Tscholl et al. Comment choisir le type de greffe pour la reconstruction du ligament croisé antérieur ? Rev Med Suisse, 2017/569 (Vol.3), p. 1339–1342. DOI: 10.53738/REVMED.2017.13.569.1339 URL: https://www.revmed.ch/revue-medicale-suisse/2017/revue-medicale-suisse-569/comment-choisir-le-type-de-greffe-pour-la-reconstruction-du-ligam

[39] Thomas Vangsness. *Allografts: Graft Sterilization and Tissue Banking Safety Issues.* publisher= Biochemical Pharmacology, p 240-244 , year : 2009, url= https://reader.elsevier.com/reader/sd/pii/B9781416054740000096?token=119AAC5BA2CD8614463A3AA1E48473578CA448108487DDBAD5A37F2D8C792CDCA originRegion=eu-west-1&originCreation=20230412173921.

[40] OPNT, National Data, U.S. Department of Health Human Services, consulted in April 2023. Url : https://optn.transplant.hrsa.gov/data/.

[41] Christian Delloye Olivier Cornu. *Allogreffes de l'appareil locomoteur et banque de tissus.* Encyclopédie Medico-chirurgicale, 14-015-A-10, year : 1998.

[42] Cartmell JS, Dunn MG. Effect of chemical treatments on tendon cellularity and mechanical properties. J Biomed Mater Res. 2000 Jan;49(1):134-40. doi: 10.1002/(sici)1097-4636(200001)49:1<134::aid-jbm17>3.0.co;2-d. PMID: 10559756.

[43] Zhang, Hao-Ran Xu, Mingyou Zhang, Lei Zhang, Hao Yang, Li Liu, Jie Zhang, Jing[U+2010]yu Hu, Yong[U+2010]cheng. (2022). Effects of Chemical Sterilization and Gamma Irradiation on the Biochemical and Biomechanical Properties of Human Tendon Allografts In Vitro Study. Orthopaedic Surgery. 14. 10.1111/os.13465.

[44] Spire B, Dormont D, Barré-Sinoussi F, Montagnier L, Chermann JC, Inactivation of lymphadenopathy-associated virus by heat, gamma rays and ultraviolet light, Lacet 1985 ; 2 : 188-189.

[45] Fedeler B, Vangness T, Moore T, Li Z, Rasheed S, Effects of gamma irradiation on the human bone-patellar ligament-bone grafts obtained from infected cadavera, J Bone Joint Surg 1994 ; 76A : 1032-1035.

[46] Collagen cross-link anomalies following chemical treatment and gamma irradiation – Dr Julia Vettese Congrès Orthopaedica Belgica, Brussels, 27/04/2023.

[47] Westpharma, "Benefits of Electron-Beam Sterilization", updated on Februar 2018, consulted in May 2023. url : https://www.westpharma.com/blog/2018/february/benefits-of-electron-beam-sterilization#:~:text=Electron%2Dbeam%20irradiation%20(e%2D,through%20the%20articles%20being%20sterilized.

[48] Wei Wei, Yujie Liu, Xu Yang, Shaoqi Tian, Chao Liu, Yang Zhang, Zhaoning Xu, Baiqiang Hu, Zhen Tian, Kang Sun, Fractionation of 50kGy electron beam irradiation: Effects on biomechanics of human flexor digitorum superficialis tendons treated

with ascorbate, Journal of Biomechanics, Volume 46, Issue 4,2013, Pages 658-661, ISSN 0021-9290, https://doi.org/10.1016/j.jbiomech.2012.11.049. found here : https://www.sciencedirect.com/science/article/pii/S0021929012007014.

[49] U.S. Department of Health Human Services, "Ethylene Oxide Gas Sterilization ", Center for Diseases Control and Prevention, url : https://www.cdc.gov/infectioncontrol/guidelines/disinfection/sterilization/ethylene-oxide.html last reviewed on September 18, 2016, Consulted on April 2023.

[50] Bechtold JE, Eastlund DT, Butts MK, Lagerborg DF, Kyle RF. The effects of freeze-drying and ethylene oxide sterilization on the mechanical properties of human patellar tendon. Am J Sports Med. 1994 Jul-Aug;22(4):562-6. doi: 10.1177/036354659402200421. PMID: 7943525.

[51] Lomas, R., Jennings, L., Fisher, J. et al. Effects of a Peracetic Acid Disinfection Protocol on the Biocompatibility and Biomechanical Properties of Human Patellar Tendon Allografts. Cell Tissue Banking 5, 149–160 (2004). https://doi.org/10.1023/B:CATB.0000046071.11459.bd.

[52] Schilaty ND, Nagelli C, Bates NA, Sanders TL, Krych AJ, Stuart MJ, et al. Incidence of second anterior cruciate ligament tears and identification of associated risk factors from 2001 to 2010 using a geographic database. Orthop J Sports Med. 2017;5:2325967117724196.

[53] Instron, "TENSILE TESTING An Introduction", consulted on May 2023, url : https://www.instron.com/en/resources/test-types/tensile-test.

[54] N. Saba, M. Jawaid, M.T.H. Sultan, 1 - An overview of mechanical and physical testing of composite materials, Editor(s): Mohammad Jawaid, Mohamed Thariq, Naheed Saba, In Woodhead Publishing Series in Composites Science and Engineering, Mechanical and Physical Testing of Biocomposites, Fibre-Reinforced Composites and Hybrid Composites, Woodhead Publishing, 2019, Pages 1-12, ISBN 9780081022924, https://doi.org/10.1016/B978-0-08-102292-4.00001-1.

[55] Testtex, Tensile Testing Machine Applications and Classifications: the Complete List, consulted on May 2023. Url : https://www.testextextile.com/tensile-testing-machine-applications-and-classifications-the-comp

[56] Hoeppner, David W., Cyclic Loading and Cyclic Stress, edited by Wang, Q. Jane,Encyclopedia of Tribology 2013, Springer US, Boston, MA, p691–698, 978-0-387-92897-5, doi: 10.1007/978-0-387-92897-5_244.

[57] Lee, Yung-Li, et al. Fatigue Testing and Analysis : Theory and Practice, Elsevier Science Technology, 2004. ProQuest Ebook Central, https://ebookcentral.proquest.com/lib/uclouvainbe/detail.action?docID=226735.

[58] Testtex, What are the Types of Textile Testing?, consulted in May 2023. Url : https://www.testextextile.com/what-are-the-types-of-textile-testing/.

[59] R. Fangueiro, F. Soutinho, 3 - Textile structures, Editor(s): R. Fangueiro, In Woodhead Publishing Series in Textiles, Fibrous and Composite Materials for Civil Engineering Applications, Woodhead Publishing, 2011, Pages 62-91, ISBN 9781845695583, https://doi.org/10.1533/9780857095583.1.62. (https://www.sciencedirect.com/science/article/pii/B978184569558350003X).

[60] Mahmoud El-Sherif, 6 - Integration of fibre optic sensors and sensing networks into textile structures, Editor(s): Xiaoming Tao, In Woodhead Publishing Series in Textiles, Wearable

Electronics and Photonics, Woodhead Publishing, 2005, Pages 105-135, ISBN 9781855736054, https://doi.org/10.1533/9781845690441.105.

[61] Heleen Fehervary, Marija Smoljkić, Jos Vander Sloten, Nele Famaey, Planar biaxial testing of soft biological tissue using rakes: A critical analysis of protocol and fitting process, Journal of the Mechanical Behavior of Biomedical Materials, Volume 61, 2016, Pages 135-151, ISSN 1751-6161, https://doi.org/10.1016/j.jmbbm.2016.01.011.

[62] Andrea Corti, Tariq Shameen, Shivang Sharma, Annalisa De Paolis, Luis Cardoso, Biaxial testing system for characterization of mechanical and rupture properties of small samples, HardwareX, Volume 12, 2022, e00333, ISSN 2468-0672, https://doi.org/10.1016/j.ohx.2022.e00333.

[63] Tishya A.L Wren, Scott A Yerby, Gary S Beaupré, Dennis R Carter, Mechanical properties of the human achilles tendon, Clinical Biomechanics, Volume 16, Issue 3, 2001, Pages 245-251, ISSN 0268-0033, https://doi.org/10.1016/S0268-0033(00)00089-9. (found here : https://www.sciencedirect.com/science/article/pii/S0268003300000899).

[64] Louis-Ugbo J, Leeson B, Hutton WC. Tensile properties of fresh human calcaneal (Achilles) tendons. Clin Anat. 2004 Jan;17(1):30-5. doi: 10.1002/ca.10126. PMID: 14695585.

[65] Nagelli CV, Hooke A, Quirk N, De Padilla CL, Hewett TE, van Griensven M, Coenen M, Berglund L, Evans CH, Müller SA. Mechanical and strain behaviour of human Achilles tendon during in vitro testing to failure. Eur Cell Mater. 2022 Apr 21;43:153-161. doi: 10.22203/eCM.v043a12. PMID: 35446434; PMCID: PMC9286485.

[66] Ashcroft, I.A. (2011). Fatigue Load Conditions. In: da Silva, L.F.M., Öchsner, A., Adams, R.D. (eds) Handbook of Adhesion Technology. Springer, Berlin, Heidelberg. https://doi.org/10.1007/978-3-642-01169-6_33.

[67] Shepherd JH, Screen HR. Fatigue loading of tendon. Int J Exp Pathol. 2013 Aug;94(4):260-70. doi: 10.1111/iep.12037. PMID: 23837793; PMCID: PMC3721457.

[68] Seynnes OR, Bojsen-Møller J, Albracht K, Arndt A, Cronin NJ, Finni T, Magnusson SP. Ultrasound-based testing of tendon mechanical properties: a critical evaluation. J Appl Physiol (1985). 2015 Jan 15;118(2):133-41. doi: 10.1152/japplphysiol.00849.2014. Epub 2014 Nov 20. PMID: 25414247.

[69] Farago D, Kozma B, Kiss RM. Different sterilization and disinfection methods used for human tendons - a systematic review using mechanical properties to evaluate tendon allografts. BMC Musculoskelet Disord. 2021 Apr 30;22(1):404. doi: 10.1186/s12891-021-04296-4. PMID: 33941147; PMCID: PMC8091719.

[70] Ren D, Sun K, Tian S, Yang X, Zhang C, Wang W, Huang H, Zhang J, Deng Y. Effects of gamma irradiation and repetitive freeze-thaw cycles on the biomechanical properties of human flexor digitorum superficialis tendons. J Biomech. 2012 Jan 10;45(2):252-6. doi: 10.1016/j.jbiomech.2011.10.035. Epub 2011 Nov 9. PMID: 22078178.

[71] Balsly, C. R., Cotter, A. T., Williams, L. A., Gaskins, B. D., Moore, M. A., Wolfinbarger, L. (2008). Effect of low dose and moderate dose gamma irradiation on the mechanical properties of bone and soft tissue allografts. Cell and Tissue Banking, 9(4), 289-298. doi:10.1007/s10561-008-9069-0.

[72] Conrad BP, Rappé M, Horodyski M, Farmer KW, Indelicato PA. The effect of sterilization on mechanical properties of soft tissue allografts. Cell Tissue Bank. 2013 Sep;14(3):359-66. doi: 10.1007/s10561-012-9340-2. Epub 2012 Sep 13. PMID: 22972164.

[73] Dziedzic-Goclawska A, Kaminski A, Uhrynowska-Tyszkiewicz I, Stachowicz W. Irradiation as a safety procedure in tissue banking. Cell Tissue Bank. 2005;6(3):201-19. doi: 10.1007/s10561-005-0338-x. PMID: 16151960.

[74] Jeffrey Cartmell. Allografts Following Low-Dose Radiation Exposure Prior to Processing/ Musculoskeletal Transplant Foundation Research Development. September 16, 2013. url : https://www.mtfbiologics.org/docs/default-source/mbot/orthopedics/tendons/mechanical-properties-of-tendon-allografts-following-low-dose-rad pdf.

[75] Pruss A, Baumann B, Seibold M, Kao M, Tintelnot K, von Versen R, Radtke H, Dörner T, Pauli G, Göbel UB. Validation of the sterilization procedure of allogeneic avital bone transplants using peracetic acid-ethanol. Biologicals. 2001 Jun;29(2):59-66. doi: 10.1006/biol.2001.0286. PMID: 11580210.

[76] Eras V, Graffunder J, Ahmed N, Brune JC. Influence of peracetic acid-ethanol sterilisation on the biomechanical properties of human meniscus transplants. J Exp Orthop. 2021 Mar 5;8(1):18. doi: 10.1186/s40634-021-00336-z. PMID: 33674898; PMCID: PMC7936009.

[77] Scheffler SU, Scherler J, Pruss A, von Versen R, Weiler A. Biomechanical comparison of human bone-patellar tendon-bone grafts after sterilization with peracetic acid ethanol. Cell Tissue Bank. 2005;6(2):109-15. doi: 10.1007/s10561-004-6403-z. PMID: 15909098.

[78] Scheffler SU, Gonnermann J, Kamp J, Przybilla D, Pruss A. Remodeling of ACL allografts is inhibited by peracetic acid sterilization. Clin Orthop Relat Res. 2008 Aug;466(8):1810-8. doi: 10.1007/s11999-008-0288-2. Epub 2008 May 20. PMID: 18491201; PMCID: PMC2584264.

[79] Scheffler SU, Schmidt T, Gangéy I, Dustmann M, Unterhauser F, Weiler A. Fresh-frozen free-tendon allografts versus autografts in anterior cruciate ligament reconstruction: delayed remodeling and inferior mechanical function during long-term healing in sheep. Arthroscopy. 2008 Apr;24(4):448-58. doi: 10.1016/j.arthro.2007.10.011. PMID: 18375278.

[80] Ollivier M, Sbihi J, Sbihi A, Pithioux M, Parratte S, Argenson JN. Ropivacaine alters the mechanical properties of hamstring tendons: In vitro controlled mechanical testing of tendons from living donors. Orthop Traumatol Surg Res. 2017 Nov;103(7):1027-1030. doi: 10.1016/j.otsr.2017.05.024. Epub 2017 Jul 29. PMID: 28760374.

[81] Zwirner J, Zhang M, Ondruschka B, Akita K, Hammer N. An ossifying bridge - on the structural continuity between the Achilles tendon and the plantar fascia. Sci Rep. 2020 Sep 3;10(1):14523. doi: 10.1038/s41598-020-71316-z. PMID: 32884015; PMCID: PMC7471908.

[82] Kadlub N, Debelmas A, Dallard J, Picard A, Boisson J. Modeling of the human mandibular periosteum material properties and comparison with the calvarial periosteum. Biomech Model Mechanobiol. 2020 Apr;19(2):461-470. doi: 10.1007/s10237-019-01221-6. Epub 2019 Sep 11. PMID: 31512012.

[83] Sharkey NA, Smith TS, Lundmark DC. Freeze clamping musculo-tendinous junctions for in vitro simulation of joint mechanics. J Biomech. 1995 May;28(5):631-5. doi: 10.1016/0021-9290(94)00100-i. PMID: 7775499.

[84] Maiko Iwaki, Manabu Kanazawa, Toshio Arakida, Shunsuke Minakuchi, Mechanical properties of a polymethyl methacrylate block for CAD/CAM dentures, Journal of Oral Science, 2020, Volume 62, Issue 4, Pages 420-422, Released on J-STAGE September 26, 2020, Advance online publication September 09, 2020, Online ISSN 1880-4926, Print ISSN 1343-4934, https://doi.org/10.2334/josnusd.19-0448, found here : https://www.jstage.jst.go.jp/article/josnusd/62/4/62_19-0448/_article/-char/en.

[85] Yukon government. Prévention et traitement des gelures. Consulted in March 2023. Url : https://yukon.ca/fr/prevention-et-traitement-des-gelures.

[86] anses. Azote liquide utilisé dans les activités d'assistance médicale à la procréation. Consulted in March 2023. Url : https://www.anses.fr/fr/content/azote-liquide-utilis\%C3\%A9-dans-les-activit\%C3\%A9s-d\%E2\%80\%99assistance-m\%C3\%A9dicale-\%C3\%A0-la-procr\%C3\%A9ation#:~:text=L'azote\%20liquide\%20ou\%20gazeux,vaporise\%20\%C3\%A0\%20\%E2\%88\%92\%20196\%C2\%B0C.

[87] INRS. Nitrogen (liquified). Consulted in Mach 2023. Url : https://www.inrs.fr/dms/ficheTox/FicheFicheTox/FICHETOX_{}133-2/FicheTox_{}133.pdf.

[88] Xometry. All about masked stereolithography apparatus (msla) 3d printing. Consulted in April 2023. Url : https://www.xometry.com/resources/3d-printing/msla-3d-printing/#:~:text=MSLA\%2C\%20short\%20for\%20masked\%20stereolithography,form\%20a\%20three\%2Ddimensional\%20object..

[89] 3DMaterials. properties of the superpp resin. consulted in March 2023. Url : https://www.3dmaterials.com/shop/store.php?ptype=view&prdcode=1711080001.

[90] AZO Materials, Finding the Right Metals and Alloys for Medical Device Manufacturing, published in May 2021, consulted in May 2023. Url : https://www.azom.com/article.aspx?ArticleID=20175.

[91] metalstripsolutions, 301 CONTRE 304 ACIER INOXYDABLE: QUEL EST LE MEILLEUR?, consulted in May 20023. Url : https://www.metalstripsolutions.com/fr/301-vs-304-stainless-steel/#History_of_301_Stainless_Steel.

[92] Issam Doghri. *Theory of beams (strength of materials).* 2000. publisher="Springer Berlin Heidelberg", address="Berlin, Heidelberg", pages="49–93", isbn="978-3-662-04168-0", doi="10.1007/978-3-662-04168-0_3", url="https://doi.org/10.1007/978-3-662-04168-0_3".

[93] Del Buono A, Chan O, Maffulli N. Achilles tendon: functional anatomy and novel emerging models of imaging classification. Int Orthop. 2013 Apr;37(4):715-21. doi: 10.1007/s00264-012-1743-y. Epub 2012 Dec 20. PMID: 23254856; PMCID: PMC3609991.

[94] Data Analytics, Linear Regression T-test: Formula, Example. author : Ajitesh Kumar. Published on May 2023, consulted on June 2023. url : https://vitalflux.com/linear-regression-t-test-formula-example/#:~:text=In%20linear%20regression%2C%20the%20t,variable%20and%20different%20predictor%20variables.

[95] University of Southampton, T test Is the difference in mean GCSE scores between boys and girls in Year 11 statistically significant?. consulted on June 2023. Url : https://www.southampton.ac.uk/passs/gcse_scores/bivariate_analysis/t_test.page.

[96] Abrahamsson S Nakama LH, King KB et al. Evidence of tendon microtears due to cyclical loading in an in vivo tendinopathy model. *Journal of Orthopaedic Research*, 23:1199–20, 2005.

[97] Peltz TS, Hoffman SW, Scougall PJ, Gianoutsos MP, Savage R, Oliver RA, Walsh WR. Animal Models for Tendon Repair Experiments: A Comparison of Pig, Sheep and Human Deep Flexor Tendons in Zone II. J Hand Surg Asian Pac Vol. 2017 Sep;22(3):329-336. doi: 10.1142/S0218810417500381. PMID: 28774235.

[98] Wren TA, Yerby SA, Beaupré GS, Carter DR. Mechanical properties of the human achilles tendon. Clin Biomech (Bristol, Avon). 2001 Mar;16(3):245-51. doi: 10.1016/s0268-0033(00)00089-9. PMID: 11240060.

Online tools such as *ChatGPT* [1] and *Deepl* [2] have been employed for the writting of the present thesis. These ressources were used to improve the writting quality and to response to some inquiries.

[1] "ChatGPT." OpenAI, 2021. https://openai.com/

[2] https://www.deepl.com/translator

UNIVERSITÉ CATHOLIQUE DE LOUVAIN
École polytechnique de Louvain
Rue Archimède, 1 bte L6.11.01, 1348 Louvain-la-Neuve, Belgique | **www.uclouvain.be/epl**